

Spring 5-8-2015

Development of a Kinetic Model to Investigate the Effect of Compositional Variation and a Processing Condition on the Solid-State Degradation of Gabapentin

Akshata Nevrekar

Follow this and additional works at: <https://dsc.duq.edu/etd>

Recommended Citation

Nevrekar, A. (2015). Development of a Kinetic Model to Investigate the Effect of Compositional Variation and a Processing Condition on the Solid-State Degradation of Gabapentin (Doctoral dissertation, Duquesne University). Retrieved from <https://dsc.duq.edu/etd/1515>

This One-year Embargo is brought to you for free and open access by Duquesne Scholarship Collection. It has been accepted for inclusion in Electronic Theses and Dissertations by an authorized administrator of Duquesne Scholarship Collection.

DEVELOPMENT OF A KINETIC MODEL TO INVESTIGATE THE EFFECT OF
COMPOSITIONAL VARIATION AND A PROCESSING CONDITION ON THE
SOLID-STATE DEGRADATION OF GABAPENTIN

A Dissertation

Submitted to the Graduate School of Pharmaceutical Sciences

Duquesne University

In partial fulfilment of the requirements for
the degree of Doctor of Philosophy

By

Akshata A. Nevrekar

August 2015

Copyright by

Akshata A. Nevrekar

2015

DEVELOPMENT OF A KINETIC MODEL TO INVESTIGATE THE EFFECT OF
COMPOSITIONAL VARIATION AND A PROCESSING CONDITION ON THE
SOLID-STATE DEGRADATION OF GABAPENTIN

Akshata A Nevrekar

Approved: March 19th 2015

Ira Shea Buckner, Ph.D.
Associate Professor
Department of Pharmaceutics
Graduate School of Pharmaceutical Sciences,
Duquesne University, Pittsburgh, PA
(Committee Chair)

Peter L.D. Wildfong, Ph.D.
Associate Professor
Department of Pharmaceutics
Graduate School of Pharmaceutical Sciences,
Duquesne University, Pittsburgh, PA
(Committee Member)

Wilson Meng, Ph.D.
Associate Professor
Department of pharmaceutics
Graduate School of Pharmaceutical Sciences,
Duquesne University, Pittsburgh, PA
(Committee Member)

Patrick T. Flaherty, Ph.D.
Associate Professor
Department of Medicinal Chemistry
Graduate School of Pharmaceutical Sciences,
Duquesne University, Pittsburgh, PA
(Committee Member)

H.M. (Skip) Kingston, Ph.D.
Professor
Department of Chemistry and Biochemistry,
Bayer School of Natural and Environmental
Sciences
Duquesne University, Pittsburgh, PA
(Committee Member)

James K. Drennen, III, Ph.D.
Associate Dean, Research and Graduate
Programs
Graduate School of Pharmaceutical Sciences,
Duquesne University, Pittsburgh, PA

J. Douglas Bricker, Ph.D.
Dean, Mylan School of pharmacy and
Graduate School of Pharmaceutical Sciences,
Duquesne University, Pittsburgh, PA

ABSTRACT

DEVELOPMENT OF A KINETIC MODEL TO INVESTIGATE THE EFFECT OF
COMPOSITIONAL VARIATION AND A PROCESSING CONDITION ON THE
SOLID-STATE DEGRADATION OF GABAPENTIN

By

Akshata A. Nevrekar

August 2015

Dissertation supervised by Ira S. Buckner, Ph.D.

Gabapentin is used in the treatment of seizures and neuropathic pain. Gabapentin undergoes intra-molecular cyclization to form a γ -lactam. The product lactam is twenty times more toxic than gabapentin, causing seizures in animal models. The United States Pharmacopeia (USP) limits the content of lactam in gabapentin formulations to 0.4% w/w. A number of patents have been issued for solid dosage forms formulated to stabilize gabapentin. Despite these efforts, factors contributing to gabapentin's poor stability in the solid-state have not been explored completely.

It was hypothesized, that physicochemical properties of the excipients and compaction pressure will accelerate the solid-state degradation of gabapentin, increasing the kinetic rate constant for lactam formation. To test the hypotheses, binary mixtures and compacts of gabapentin with different excipients were prepared and stored under accelerated study conditions. The concentration of lactam and gabapentin was measured using a validated analytical method. A concentration dependent catalytic effect by the excipients was determined by mixing different concentrations of the excipient with gabapentin. The effect of excipient particle size was determined by mixing different size fractions of the excipient with gabapentin.

Significant degradation of unprocessed gabapentin in the presence of excipients strongly suggested a catalytic role of the excipients on gabapentin's degradation. The existing model was expanded to account for the observed catalytic effect of excipients. A relationship was developed between the rate constant for lactam formation and physical properties of the excipients (such as particle size, morphology, molecular weight, molecular cross sectional area and specific surface area). Along with the catalytic effect of the excipients, compaction pressure and powder properties of the excipients such as moisture content, particle size and yield pressure appeared to be other potential contributing factors affecting gabapentin's degradation.

DEDICATION

*Dedicated to my parents, it was their dream that prompted me to start this journey and,
dedicated to Shravan and Ayan for their support through this journey*

“It takes a dream to get started, desire to keep going and determination to finish”

Eddie Harris Jr.

ACKNOWLEDGEMENT

I would like to take this opportunity to express my gratitude to all the people who have helped in successful completion of this dissertation. Although, a few names appear on this acknowledgment page, there are many others who have helped me in completing this important chapter of my life.

Dr. Ira Buckner, I have been fortunate to have an advisor who has made me independent and capable of exploring on my own and at the same time guided and supported me, when my steps faltered. He has always challenged me with his scientific curiosity and intriguing ideas. He set up high standards and encouraged me to meet those standards.

Dr. Peter Wildfong, for being an excellent co-advisor, who helped simplify the fundamentals of solid-state chemistry through his numerous discussions. I want to thank him for his scientific stimulation and constructive criticisms at group meetings and committee meetings, helping me become a more confident student.

Dr. Patrick Flaherty, for his numerous discussions on the chemistry aspects of this dissertation and being patient in answering all my doubts and questions related to gabapentin.

Dr. Howard Kingston, for his interest in the project and helping me understand and apply appropriate statistical techniques to the presented data. I thank him for encouraging me to look at the real world applications of my project.

Dr. Wilson Meng, for his insightful comments, thought provoking ideas and constructive criticisms at different stages of my dissertation.

Dr Lee Kirsch at the University of Iowa for his constructive feedback and challenging thoughts to help understand the complex world of gabapentin

I greatly value the support from my lab mates, Rahul, Jeff, Namita and Dipy and thank them for being great friends and providing constant encouragement.

Robert Bondi, Benoit Igne for their help with Matlab[®] coding

Roheeth, Ravi, Kalyan and Sudhir for their help with chemistry and molecular modelling

Tinmanee Radaduen at the University of Iowa for her help with the analytical method development

Faculty, administrative staff and students at the graduate school of pharmaceutical sciences at Duquesne University for their support in completing this dissertation

Adhiraj for cheering me in difficult times and always believing in me

Shravan for his love and encouragement, I want to specially thank him for always being there through the difficult times. This Dissertation would not have been possible without his sacrifices and unconditional support.

Ayan for being an unlimited source of inspiration, happiness and relaxation

Aai and Bappa for their love, patience and supporting all my dreams through the last 6 years, my parents for being a constant source of love, support, encouragement, I thank them for always believing in me and praying for me. This dissertation is the results of their blessings and efforts to keep me motivated throughout this journey.

Table of Contents

Abstract	iv
Acknowledgement	vii
List of Tables	xii
List of Figures	xiv
Chapter 1	1
Introduction.....	1
1.1 Statement of Problem	2
1.2. Hypothesis and Specific Aims	4
1.3. Literature Review	5
1.3.1. Model Compound Gabapentin.....	5
1.3.2. Previous studies on gabapentin.....	6
1.3.3. Commonly Used Pharmaceutical Excipients.....	15
1.3.4. Models and Complexities in Solid-State Kinetics	21
1.3.5. Solving Ordinary Differential Equation and Non-Linear Regression	25
1.3.6. Compaction as a Processing Condition.....	31
1.3.7. Conclusion	35
Chapter 2. 37Optimization and Validation of the Analytical Method for Determination of Gabapentin and Its Degradation Product Lactam	37
2.1. Introduction	37
2.2. Materials and Methods.....	38
2.2.1. Materials	38
2.2.2. Instrumentation and chromatographic condition.....	39
2.2.3. Analytical Method Validation	40
2.2.4. Method Optimization.....	43
2.2.5. Stability of gabapentin and lactam.....	44
2.3. Results and Discussion.....	45
2.3.1. Analytical Method Validation	45
2.3.2. Method Optimization.....	52
2.3.3. Stability of Gabapentin and Lactam	54

2.4. Conclusion.....	55
Chapter 3. Investigating the Effect of Excipients on the Solid-State Degradation of Gabapentin	56
3.1. Introduction	56
3.2. Materials and Methods.....	57
3.2.1. Materials	57
3.2.2. Material Pretreatment	57
3.2.3. Determination of Moisture Content.....	58
3.2.4. Physical Mixture Preparation and Study Conditions.....	58
3.3. Results and Discussion.....	63
3.4. Conclusion.....	86
Chapter 4. Expansion of the Kinetic Model of Gabapentin Degradation to Account for the Physicochemical Properties of Excipients	88
4.1. Introduction	88
4.2. Materials and Methods.....	89
4.2.1. Materials	89
4.2.2. Study Designs	89
4.2.3. Particle Size and Shape Determination.....	91
4.2.4. Determination of Molecular Cross-Sectional Area.....	92
4.2.5. Specific Surface Area Measurements	93
4.2.6. True Density Measurement.....	94
4.2.7. Theoretical Estimation of the Fraction Surface Area of the Excipient Particle in Contact with Gabapentin Particle	94
4.3. Results and Discussion.....	98
4.4. Conclusion.....	109
Chapter 5. Effect of Compaction and Powder Properties of Excipients on the Solid-State Degradation of Gabapentin	111
5.1. Introduction	111
5.2. Materials and Methods.....	112
5.2.1. Materials	112
5.2.2. Material Pretreatment.....	112
5.2.3. Determination of Moisture Content.....	112
5.2.4. True Density Determination	113

5.2.5. Study Protocol.....	113
5.3. Results and Discussion.....	116
5.4. Conclusion.....	128
Chapter 6. Conclusion.....	130
Bibliography	137
Appendix 1. Supporting data Chapter 1.....	144
Appendix 2. Supporting documentation for chapter 4.....	149
Specific surface area measurements	149
Molecular Cross-Sectional area measurements	156

List of Tables

Table 1: Structural information of the excipients used in the study	16
Table 2: Calibration curve using gabapentin reference standard (USP).....	47
Table 3: Determination of purity of bulk gabapentin	48
Table 4: Linearity of calibration curves for gabapentin.....	48
Table 5: Linearity of calibration curves for lactam.	49
Table 6: Determination of accuracy of the analytical method for gabapentin.....	51
Table 7: Determination of precision of the analytical method for gabapentin..	51
Table 8: Determination of accuracy of the analytical method for lactam.....	51
Table 9: Determination of precision of the analytical method for lactam.	51
Table 10: The effect of the filter membrane on the recovery of gabapentin and lactam.	53
Table 11: Results for the recovery of gabapentin and lactam in the presence of excipients..	53
Table 12: Application of a central composite design (CCD) to generate different systematic combinations of input parameter values..	62
Table 13: Moisture content of the excipients before physical mixing.....	64
Table 14: The model-estimated parameter values for gabapentin and gabapentin-Tri-Tab [®] physical mixture.....	77
Table 15: The model-estimated parameter values for unprocessed gabapentin relative to the previously published parameter values.....	78
Table 16: The model-estimated parameter values for the gabapentin-Tri-Tab [®] physical mixture, post-fixing for different values of k_{ga0}^*	79
Table 17: Summary of the optimized rate constants for the degradation of gabapentin in the presence of excipients.....	82

Table 18: Cumulative List for the Various Physical Properties of Excipients	104
Table 19: Estimation of surface molar concentration on the excipient particle available for catalyzing lactam formation.....	106

List of Figures

Figure 1: Intramolecular cyclization reaction for the conversion of gabapentin to lactam	2
Figure 2: Solution state degradation of gabapentin under different pH conditions.....	9
Figure 3: Mechanism for the degradation of gabapentin in solution.....	10
Figure 4: Kinetic scheme describing solid-state degradation of milled gabapentin stored under accelerated storage conditions.	13
Figure 5: Degradation profile for milled gabapentin under accelerated storage conditions.....	14
Figure 6: Sample chromatogram for gabapentin.	45
Figure 7: Sample chromatogram for lactam	46
Figure 8: Calibration curves for gabapentin reference standard.	47
Figure 9: Calibration curves for gabapentin (Method Validation)..	49
Figure 10: Calibration curves for lactam (Method Validation)..	50
Figure 11: Chromatogram depicting the stability of gabapentin in solution.	54
Figure 12: Image representing the morphology of a gabapentin particle	65
Figure 13: Images representing the morphology of A. starch particles, and B. the physical mixture of gabapentin and starch particles	65
Figure 14: Images representing the morphology of A. HPMC particles, and B. the physical mixture of gabapentin and HPMC particles.....	65
Figure 15: Images representing the morphology of A. Emcompress [®] particles, and B. the physical mixture of gabapentin and Emcompress [®] particles.....	66
Figure 16: Images representing the morphology of A. HPC particles, and B. the physical mixture of gabapentin and HPC particles.....	66

Figure 17: Images representing the morphology of A. talc particles, and B. the physical mixture of gabapentin and talc particles.....	66
Figure 18: Images representing the morphology of Mono-Tab particles, and B. the physical mixture of gabapentin and Mono-Tab particles.....	67
Figure 19: Images representing the morphology of A-Tab [®] particles, and B. the physical mixture of gabapentin and A-Tab [®] particles.....	67
Figure 20: Images representing the morphology of Tri-Tab [®] particles, and B. the physical mixture of gabapentin and Tri-Tab [®] particles.	67
Figure 21: Effect of the excipients (Set 1) on the solid-state degradation of gabapentin.....	69
Figure 22: Effect of the excipients (set 2) on the solid-state degradation of gabapentin.....	70
Figure 23: Effect of the mixing procedure on the solid-state degradation of gabapentin.....	71
Figure 24: Effect of varying moisture content in Mono-Tab on the solid-state degradation of gabapentin.	72
Figure 25: The effect of varying moisture content in HPMC on the solid-state degradation of gabapentin.	73
Figure 26: Comparison of approximated lactam content (% mole) using the Runge-Kutta method on Excel [®] and Matlab [®]	74
Figure 27: Optimization of the parameters in gabapentin and the gabapentin-Tri-Tab [®] physical mixture.....	76
Figure 28: Comparison of simulated and predicted lactam concentration-time profiles for gabapentin.	77
Figure 29: A comparison between observed and model predicted lactam formation in gabapentin and its physical mixture with excipients.....	80

Figure 30: Estimated value for the rate constant k_2 across the gabapentin-excipient physical mixtures.....	83
Figure 31: Estimated values for the rate constant k_1 across the gabapentin-excipient physical mixtures.....	85
Figure 32: Estimated values for the rate constant k_3 for the gabapentin-Excipient physical mixtures.....	85
Figure 33: Graphical representation of the physical mixture of gabapentin particles with excipient particles of different shapes.....	96
Figure 34: Effect of excipient concentration on the degradation of gabapentin.....	98
Figure 35: Effect of excipient particle size on the degradation of gabapentin.	99
Figure 36: Expanded kinetic model for the solid-state degradation of gabapentin in the presence of excipients.....	100
Figure 37: Estimated catalytic rate constant k_4 ($\text{h}^{-1}\text{mol}^{-1}$) for lactam formation in the presence of excipients.	107
Figure 38: Effect of compaction and the presence of excipients on the solid-state degradation of gabapentin.....	117
Figure 39: Effect of compaction on gabapentin's degradation.....	118
Figure 40: Comparison of the initial lactamization rate ($k_2^* \text{ gaba}_0^*$) between the gabapentin-excipient physical mixtures and compacts.....	119
Figure 41: Effect of compaction on gabapentin's degradation in the presence of Emcompress [®]	120
Figure 42: Effect of compaction on gabapentin's degradation in the presence of HPMC.....	121

Figure 43: A plot suggesting the relationship between the initial lactam formation rate and the yield pressure of gabapentin-excipient physical mixtures.	122
Figure 44: Effect of compaction on gabapentin's degradation in the presence of talc.	123
Figure 45: Effect of compaction on gabapentin's degradation in the presence of starch.	124
Figure 46: A relationship plot of the initial rate for lactam formation and moisture content of the excipients.	125
Figure 47: Effect of compaction on gabapentin's degradation in the presence of HPC.	126
Figure 48: Comparative plot for porosity of the compacts of gabapentin with excipients.	126
Figure 49: A relationship plot for the initial rate of lactam formation and the work of compression for compacts of gabapentin with excipients.	127
Figure 50: Effect of excipients on the rate constant k_3 in gabapentin's degradation kinetics	128
Figure 51: The chromatogram for HPC.	144
Figure 52: The chromatogram for HPMC.	145
Figure 53: The chromatogram for starch.	145
Figure 54: The chromatogram for talc.	146
Figure 55: The chromatogram for Emcompress [®]	146
Figure 56: The chromatogram for Tri-Tab [®]	147
Figure 57: The chromatogram for A-Tab [®]	147
Figure 58: The chromatogram for Mono-Tab.	148
Figure 59: A multi-point BET measurement for Kaolinite reference standard.	149
Figure 60: A multi-point BET measurement for Alumina reference standard.	150
Figure 61: A multi-point BET measurement for Tri-Tab [®]	150
Figure 62: A multi-point BET measurement for A-Tab [®] 75-125 μ m.	151

Figure 63: A multi-point BET measurement for A-Tab [®] 125-250 μ m	151
Figure 64: A multi-point BET measurement for A-Tab [®] 250-500 μ m	152
Figure 65: A multi-point BET measurement for Mono-Tab [®]	152
Figure 66: A multi-point BET measurement for Emcompress [®]	153
Figure 67: A multi-point BET measurement for starch	153
Figure 68: A multi-point BET measurement for HPMC	154
Figure 69: A multi-point BET measurement for HPC	154
Figure 70: A multi-point BET measurement for talc	155
Figure 71: Computation of molecular cross-sectional area for A-tab [®]	157
Figure 72: Computation of molecular cross-sectional area for Emcompress [®]	158
Figure 73: Computation of molecular cross-sectional area for HPC	159
Figure 74: Computation of molecular cross-sectional area for HPMC	160
Figure 75: Computation of molecular cross-sectional area for Mono-Tab	161
Figure 76: Computation of molecular cross-sectional area for starch	162
Figure 77: Computation of molecular cross-sectional area for talc	163
Figure 78: Computation of molecular cross-sectional area for Tri-Tab [®]	164

Chapter 1

Introduction

Solid-state degradation reactions occur commonly in drug substances and their formulations. These reactions occur due to a drug being intrinsically active or unstable.^{1,2} The degradation of drug molecules is typically accelerated by compositional factors, such as the presence of excipients, environmental conditions and exposure of drug molecules to processing conditions.²

Excipients can potentially accelerate the degradation reaction by interacting chemically with drug molecules. An example of such an interaction would be acid-base reaction between an acidic drug and a basic excipient. Amorphous excipients, or excipients with greater non-crystalline content, possess enhanced molecular mobility and ability to interact with water, resulting in accelerated drug degradation.^{2,3} Environmental conditions such as temperature and humidity can accelerate drug degradation by increasing kinetic energy and molecular mobility of the system.^{2,4} Environmental moisture can stabilize drug degradation by facilitating “self-healing” of crystal defects induced during processing.⁵ Processing conditions involve energy input which induces changes in particle size, crystallinity, surface area and crystal form, resulting in modification of physical and chemical properties of a drug molecule.⁶⁻¹¹ Application of stress on a drug crystal during processing creates lattice defects, which act as sites to initiate degradation reactions. These lattice defects can also contribute to lattice disorder, leading to different packing arrangements and conformations within a crystal, making conditions favorable for interaction.^{2,12-14} Hence, compositional, environmental and processing factors are critical in

determining the solid-state degradation of a drug and its dosage forms. Establishing drug stability and reactivity by taking the above factors into consideration becomes an important criterion for designing a stable formulation, ascertaining shelf life, patient safety, storage conditions and optimizing manufacturing processes.¹⁵ The present research explores the underlying effects of compositional and processing factors affecting the solid-state degradation of the model drug gabapentin.

1.1 Statement of Problem

Gabapentin, [1-(amino methyl) cyclohexane acetic acid] is a γ -aminobutyric acid (GABA) analogue used in the treatment of epilepsy and neuropathic pain.^{16,17} It is also used in treatment of bipolar disorder and is effective in reducing spasticity associated with multiple sclerosis.¹⁵ The primary reason for its extensive commercial usage is milder side effects relative to older generation anti-epileptic agents.¹⁸

Gabapentin undergoes degradation by nucleophilic attack of the alkyl amine on the carboxylate carbon to form γ -lactam [3, 3-petamethylene-4-butyrolactam] as shown in Figure 1.¹⁵

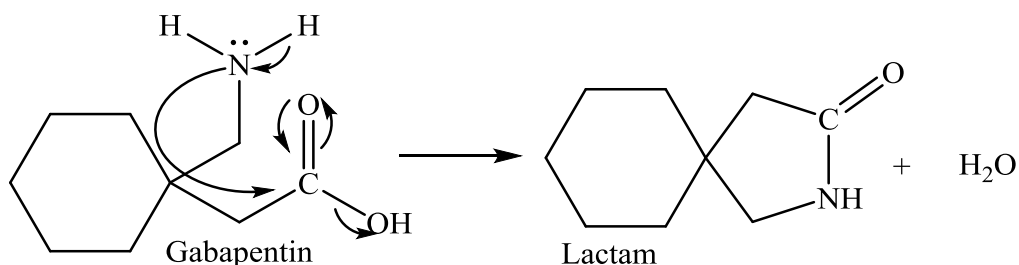


Figure 1: Intramolecular cyclization reaction for the conversion of gabapentin to lactam

The degradation product, “lactam”, is known to be 20-times more toxic than gabapentin itself and has been reported to cause seizures in animal models.¹⁹ The United States Pharmacopeia

(USP) has recommended that the concentration of lactam in any gabapentin formulation should not exceed 0.4% w/w.⁵ Gabapentin is available commercially as either a tablet or a capsule dosage form each of which includes a number of different excipients. Hard gelatin capsules are available for a single dose, containing between 100-400 mg gabapentin, while elliptical film coated tablets are available for a single dose of 600-800 mg gabapentin.²⁰

In 2007, a voluntary recall of 73 million gabapentin tablets was announced by Ranbaxy Pharmaceuticals for exceeding the lactam impurity specifications of gabapentin formulations.²¹ Thereafter, a number of patents have been filed to formulate a more stable dosage form containing gabapentin.²²⁻²⁷

Literature findings^{7,34} have indicated that excipient type, pH conditions and buffering salt concentration may effect the degradation kinetics of gabapentin in solution. The possibility of a similar catalytic reaction (due to excipients, pH, salt concentration) in the solid-state, mediated by common excipients used to formulate gabapentin, requires further exploration. Hence, providing evidence for the role of excipient properties affecting the degradation of gabapentin needs to be attempted.

Considering the commercial availability of gabapentin as tablets along with the excipients, the effect of compression pressure on the degradation kinetics needed investigation. Compaction as a processing condition could potentially increase the concentration of reactive molecules within gabapentin crystals, accelerating lactam formation. Therefore, the present reaserch will help

investigate the effect of excipient properties and compaction conditions affecting the solid-state degradation of gabapentin.

1.2. Hypothesis and Specific Aims

Stemming from the previous research conducted on the solid-state degradation of gabapentin, the objective of this work was to **develop an understanding of the role of excipients and compaction as a processing condition on the solid-state degradation of gabapentin**. The research primarily focuses on determining the role of excipient concentration and their physical-chemical properties on gabapentin's degradation. The research will also help to identify other potential factors associated with powder properties of excipients and compaction conditions impacting gabapentin's degradation.

The experiments were designed to test the central hypothesis, that **physicochemical properties (such as specific surface area, molecular weight, particle size, particle shape and, acidic or basic strength) of the excipients will accelerate the solid-state degradation of gabapentin, increasing the rate constant (k_2) for lactam formation**. The degradation kinetics, **predominantly the initial rate of lactam formation, will be further accelerated by compaction of the gabapentin-excipient physical mixtures**.

The overarching objective of the project is to use the research findings to develop a risk assessment tool, which would have the ability to predict the amount of lactam generated over a predetermined time frame in gabapentin formulations, in the presence of varying excipient properties and compaction conditions.

1.3. Literature Review

1.3.1. Model Compound Gabapentin

Gabapentin is an achiral γ -amino acid, which has the propensity to undergo intramolecular cyclization to form a lactam molecule. The ability to undergo cyclization has been attributed to the close proximity between the amine and the carboxylic group in the gabapentin molecule.²⁸

Gabapentin was derived by adding a cyclohexyl group to the γ -amino butyric acid backbone.¹⁹ Gabapentin is a white to off-white colored crystalline solid with a melting point of 165°C. It is freely soluble in water (~150 mg/ml at pH 7.4) under both acidic and basic conditions. It is a BCS class III drug with a log partition coefficient (n-octanol/0.05 M phosphate buffer pH 7.4) of -1.25.²⁰ Gabapentin has a molecular weight of 171.24 g/mole, and pK_{a1} of 3.7 and pK_{a2} of 10.7 respectively.⁵ It is a low potency drug and is typically dosed at high concentrations to provide the necessary pharmacological effect.²⁹ The absorption of gabapentin in the brain is delayed because of its inability to passively diffuse the blood brain barrier (BBB).¹⁹ It is transported to the brain by saturable transporters.¹⁹ Gabapentin is toxic at concentrations of 8000 mg/kg. In the solid-state, gabapentin exists in its zwitterionic form, while in solution, it exists as cationic, anionic, zwitterionic and neutral species depending on the pH of the solution.³⁰ The lactam degradation product is a white crystalline solid with a melting point of 85°C.⁸³ Lactam is toxic at a concentration of 300 mg/kg.²³

Pharmacology: Gabapentin is a GABA analogue that does not bind to GABA receptors or alter the metabolism of GABA in the brain. The binding sites for gabapentin are located on neurons in the brain that are rich in glutaminergic synapses. Gabapentin is also a weak inhibitor of the

branched chain aminotransferase enzyme involved in glutamic acid synthesis in the brain.¹⁹ The therapeutic action of the drug is thought to involve voltage gated calcium ion channels.¹⁵ Less than 3% of the administered drug is bound to the plasma proteins, and approximately 20% of the drug concentration is available for cerebrospinal fluid (CSF) circulation.²⁰ Elimination of gabapentin from the systemic circulation occurs via renal excretion and the half-life in the body is between 5-7 h.²⁰

1.3.2. Previous studies on gabapentin

Physical Stability of gabapentin

Four solid forms of gabapentin have been reported in the literature.³¹ The commercially available Form II is anhydrous, and is the most thermodynamically stable. Form I (monohydrate) is the most stable form in aqueous conditions, while Form III has a unique intramolecular hydrogen bond between the amine and the carboxylic groups. Form IV is hypothesized to be the last transformed polymorph of gabapentin before its intramolecular cyclization to the lactam molecule.^{30,32,33}

Progressive polymorphic transformation was observed upon heating gabapentin from ambient temperature to its melting temperature. It was observed that as gabapentin Form I is heated above its melting temperature it dehydrates and transforms to Form III followed by Form IV. In contrast, heating Form II and Form III under similar conditions, results in direct transformation to both Form IV with some degradation to lactam.³²

Commercially available Form II is physically stable in up to 50% RH conditions while Form III and Form IV transform to Form II under similar humidity conditions. At 100% RH conditions all the anhydrous Forms (Form II, III, and IV) of gabapentin transform to the monohydrate.

Grinding and kneading results in polymorphic conversion of gabapentin Form III and Form IV to Form II, however gabapentin Form II remains physically stable under these conditions. Form I, on the other hand, undergoes transformation to Form III at elevated temperatures (50°C) and Form IV under desiccated conditions.²¹ The above results indicate the physical stability of gabapentin Form II (used in the presented research) under the accelerated environmental conditions (50°C / 5% RH) and the physical mixing used in the presented research.

Inter-conversion between polymorphic forms of gabapentin has been observed when it is exposed to processing conditions such as milling (ball mill), and accelerated temperature conditions (50°C) in the presence of excipients. It was observed that co-milling gabapentin for 120 min along with excipients, (such as calcium phosphate dihydrate, magnesium stearate, cyclodextrins, mannitol and corn starch), did not cause any polymorphic transformation of the stable Form II, while co-milling with excipients, (such as microcrystalline cellulose, hydroxypropylmethylcellulose (HPMC) and Kollidon[®] K-30), demonstrated polymorphic transformation from Form II to Form IV. Co-milling gabapentin with fumed silicon dioxide and talc resulted in conversion of Form II to Form IV and a significant amount of lactam. The polymorphic conversion of gabapentin was thought to be induced by co-processing gabapentin with excipients.⁷ The type of excipient processed with gabapentin seemed to affect the transformation. The energy used in co-milling the materials increased the mobility of gabapentin

molecules to facilitate form change. Additionally, the nature (hard/soft) of excipients co-milled with gabapentin contributed to the increased molecular mobility and accelerated form conversion. It is important to note the potential role of excipient type in driving the polymorphic conversion of processed gabapentin. The findings of the above study are especially important when determining the effect of excipient type especially its nature on the solid-state degradation of compacted gabapentin in the presented research.

Chemical Instability of Gabapentin in Solution State

Gabapentin was found to be unstable in aqueous solution and capable of undergoing cyclization to form the lactam degradant.^{7,34} Heating a buffered solution (0.025-0.1M) of gabapentin at 80°C resulted in accelerated lactam formation (Figure 2). A plateau of maximum reaction rate for lactam formation was reached when the amine was present as a free base (nucleophile). A 27-fold decrease in the reaction rate was observed after increasing the amount of protonated amine. The pH-rate profile for the reaction showed a minimum degradation rate at neutral pH conditions (pH 6-7) and significant reactivity at both acidic pH (pH 2.2) and basic pH conditions (pH >10)^{7,34}.

A scheme for lactam formation in solution under different pH conditions was proposed in Figure 3. In this scheme, the neutral amino group acts as a nucleophile, attacking the deprotonated carboxyl carbon, to drive lactam formation. The zwitterionic and the cationic forms of gabapentin on the other hand are relatively less reactive.³⁴ The observed reactivity at low pH was thought to be due to the attack of the free amino group on the protonated carboxyl group, leading to formation of a neutral tetrahedral intermediate (T^0) as seen in Figure 3. General acid

catalysis resulted in breakdown of the intermediate form by addition of a proton provided by the buffering species to the leaving hydroxyl group.

The kinetics for lactam formation were observed to be dependent on buffer concentration (general base catalysis), buffer type (sulfate, acetate, phosphate, and borate) and pH conditions. The lactam formation was catalyzed (specific base catalysis) under both acidic and basic pH conditions.¹⁵ This solution state degradation of gabapentin catalyzed by the above mentioned factors was further accelerated by increasing temperature conditions.^{32,35,36}

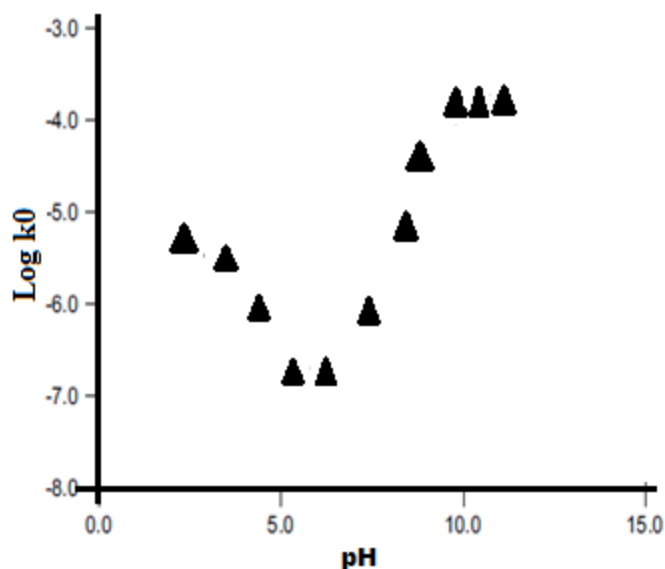


Figure 2: Solution state degradation of gabapentin under different pH conditions.¹⁵ An accelerated lactam formation was observed under both acidic and basic pH conditions. “Reprinted from Tetrahedron, volume 64, issue 28, Zambon Elena, Giovanetti Roberto, Cotarca Livius, Pasquato Lucia. Mechanistic investigation on 2-aza-spiro[4,5]decan-3-one formation from 1-(aminomethyl)cyclohexylacetic acid (gabapentin), pp 6739-6743, Copyright (2008), with permission from Elsevier.”

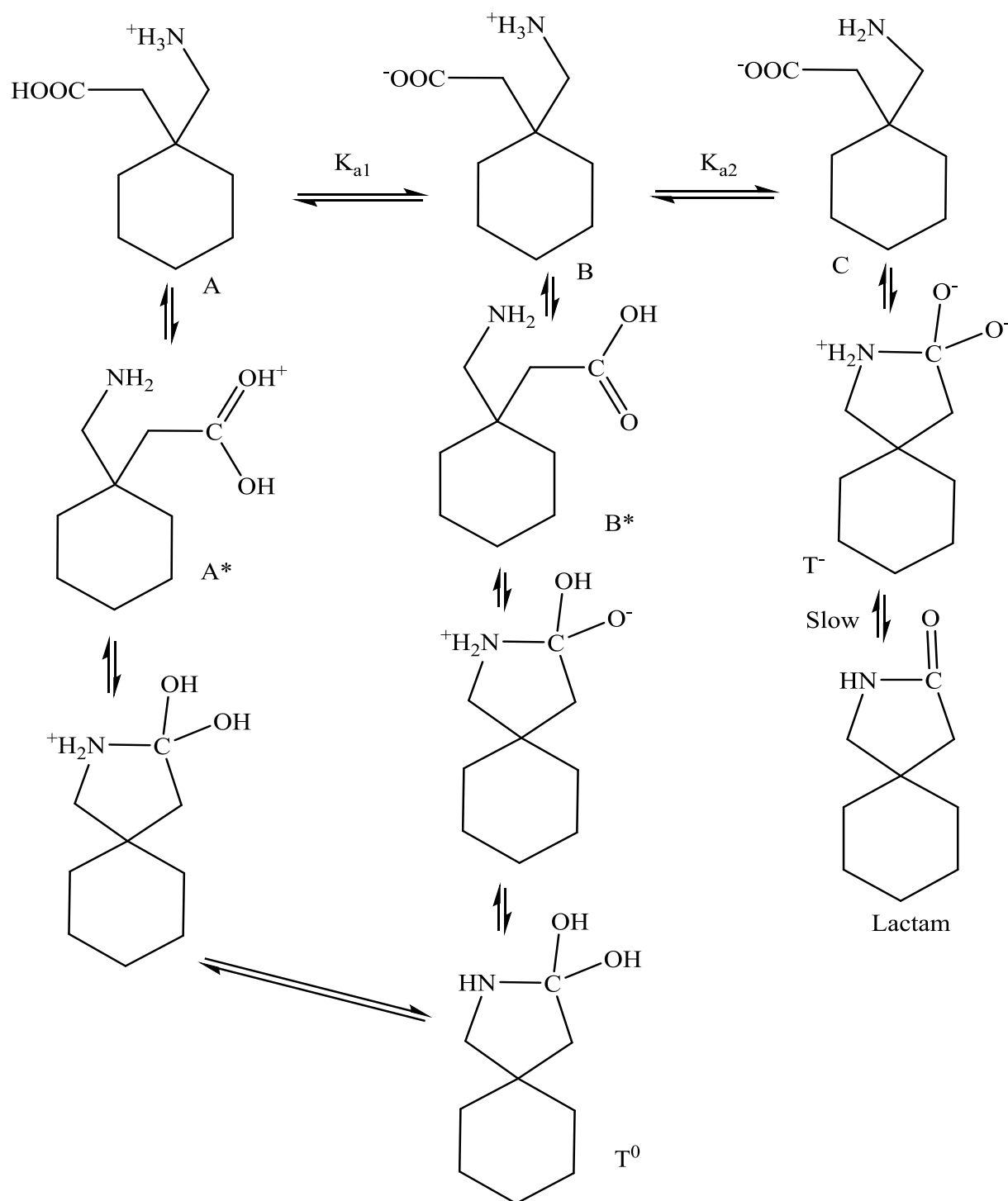


Figure 3: Mechanism for the degradation of gabapentin in solution.¹⁵ The zwitterionic form (B) and the protonated form (A) are less reactive than the unprotonated form (C). “Reprinted from Tetrahedron, volume 64, issue 28, Zamboni Elena, Giovanetti Roberto, Cotarca Livius, Pasquato Lucia. Mechanistic investigation on 2-aza-spiro[4,5]decan-3-one formation from 1-(aminomethyl)cyclohexylacetic acid (gabapentin). pp 6739-6743, Copyright (2008), with permission from Elsevier.”

Chemical Instability of Gabapentin in the Solid-State

Gabapentin was found to be susceptible to milling-induced chemical instability. This instability was attributed mainly to the formation of crystal defects, which increased the concentration of reactive gabapentin molecules. These reactive molecules, primarily comprising of the surface molecules and other damaged molecules in the bulk of the crystal, were capable of spontaneously converting to lactam at a faster rate compared to the less reactive molecules (stable) in the bulk of the crystal.⁵ The increased rate (500-fold) of lactam formation on milling was credited to the combined effects of enlarged surface area, duration of milling and in-process lactam levels.^{1,5}

The presence of environmental moisture was seen to stabilize milled gabapentin by enabling healing of crystal defects incorporated during milling.⁵ Healing of crystal defects was further expedited by surface adsorbed moisture.⁵ Milled gabapentin particles demonstrated higher stability when stored under relative humidity conditions greater than 31%.

Conversion of lactam back to gabapentin, was found to be irreversible under varying conditions of humidity (31-81% RH), temperature (50°C, and 80°C) and in buffered solutions (pH 2.2, 7.0, 8.5).⁵ These results highlighted that conversion of lactam back to gabapentin only occurs under harsh conditions and is less likely to occur under the accelerated study conditions used in our research to test gabapentin's stability. However, the role of excipient moisture on the degradation of gabapentin needs to be further studied considering, the ability of moisture to either stabilize gabapentin or potentially accelerate the catalytic effect of the excipients.

Solid-State Stability of Gabapentin Co-Processed with Excipients

A study investigated lactam formation in lyophilized blends of gabapentin with cyclodextrins, lactose, polyvinyl pyrrolidone (Kollidon[®] K-30), mannitol, trehalose and D-raffinose.³⁷ The mixtures were maintained at 50°C and variable humidity conditions (0, 45, 75% RH). Accelerated lactam formation was not observed when gabapentin in its freeze dried form was maintained under accelerated temperature and humidity conditions in the absence of excipients. Amongst the excipients lyophilized with gabapentin, highest lactam formation was observed in mixtures of gabapentin with cyclodextrins, especially HP- β -cyclodextrin. The accelerated lactamization was attributed to the restricted conformational freedom between the reacting functional groups of gabapentin as a result of inclusion complexation. Increasing humidity was seen to further accelerate lactam formation, due to moisture facilitating inclusion of gabapentin in the cavity of cyclodextrin. Accelerated lactam formation was observed in case of lyophilized blends of gabapentin with Kollidon[®] K-30 and lactose. A possible explanation for the effect of lactose was thought to involve Maillard reaction and successive Amadori rearrangement between lactose and the primary amino group of gabapentin. However, lyophilized mixtures of gabapentin and sugars did not show accelerated lactam formation. The study however speculated reasons for the effect of excipient type but was not able to clearly separate the effect of excipient properties from other convoluting effects of lyophilization.³⁷ The presented research will further explore the effect of excipient properties affecting the kinetics of lactam formation in the absence of any processing conditions.

Kinetic Model for Solid-State Degradation of Gabapentin

A quantitative solid-state kinetic model (Figure 4) has been developed, that accounts for the mechanistic effects of environmental conditions and processing conditions (milling) on the degradation of gabapentin.¹ The degradation was successfully described by rate constants k_1 ($\text{h}^{-1}\text{mol}^{-1}$) for autocatalytic branching, k_2 (h^{-1}) for spontaneous dehydration, k_3 ($\text{h}^{-1}\text{mol}^{-1}$) for moisture induced recovery or branching termination and gaba_0^* (% mole), which represented chemically intact gabapentin molecules with greater reactivity or mobility present inherently in the crystal. The kinetic model assumes formation of lactam by spontaneous conversion of gaba^* .¹ Equations 1-3 describe the kinetics for the solid-state degradation of gabapentin.¹

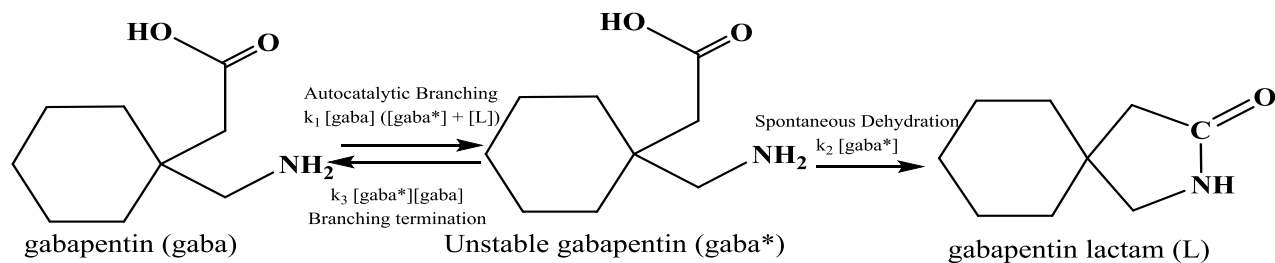


Figure 4: Kinetic scheme describing solid-state degradation of milled gabapentin stored under accelerated temperature and humidity conditions.¹ “(Kinetic Model for Solid-State Degradation of Gabapentin. J. Pharm. Sci., Vol. 101, pp 2123-2133), by Zong. Z., Qui. J., Tinmanee. R., Kirsch. L.E. Copyright (2012) by Wiley periodicals, Inc.. Reproduced with permission from Wiley periodicals, Inc. via Copyright Clearance Center.”

$$\frac{d[\text{gaba}]}{dt} = -k_1 [\text{gaba}][\text{gaba}^* + \text{L}] + k_3 [\text{gaba}][\text{gaba}^*] \quad \text{Equation 1}$$

$$\frac{d[\text{gaba}^*]}{dt} = k_1 [\text{gaba}][\text{gaba}^* + \text{L}] - k_3 [\text{gaba}][\text{gaba}^*] - k_2 [\text{gaba}^*] \quad \text{Equation 2}$$

$$\frac{d[\text{L}]}{dt} = k_2 [\text{gaba}^*] \quad \text{Equation 3}$$

A typical degradation profile for milled gabapentin under accelerated environmental conditions (40°C / 5% RH) was described by two predominant phases (Figure 5). The first phase ((1) Figure 5) primarily involved the initial lactam formation due to rapid conversion of the reactive gabapentin molecules inherently present in the sample (gaba_0^*). This was followed by the second phase ((2) Figure 5), described by a combination of disorder propagation, moisture induced termination and chemical conversion of gabapentin to lactam.¹ The model involved consecutive processes of crystal defect propagation and spontaneous conversion of gabapentin to lactam. The kinetics for gaba^* formation were described as an autocatalytic process with the rate being catalyzed by the concentration of gaba^* and lactam.

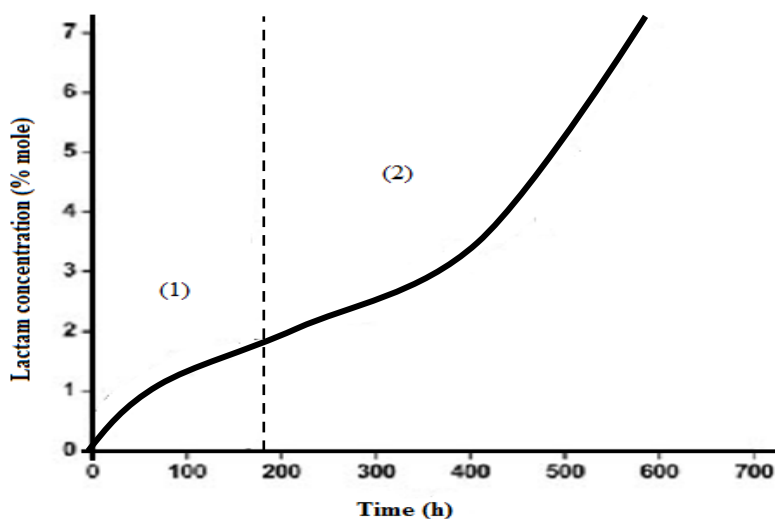


Figure 5: Degradation profile for milled gabapentin under accelerated storage conditions. The degradation profile on the left of the dotted line (1) denotes the initial rate of lactam formation predominantly described by rate constant k_2 and gaba_0^* . The degradation profile on the right of the dotted line (2) is predominantly described by rate constants k_1 and k_3 . This phase represents the autocatalytic branching or moisture induced termination phase in the degradation kinetics. “(Kinetic Model for Solid-State Degradation of Gabapentin. J. Pharm. Sci., Vol. 101, pp 2123-2133), by Zong. Z., Qui. J., Tinmanee. R., Kirsch. L.E. Copyright (2012) by Wiley periodicals, Inc.. Reproduced with permission from Wiley periodicals, Inc. via Copyright Clearance Center.”

In summary, the cyclization reaction is believed to initiate at imperfection sites within the crystal lattice. As the concentration of reactive gabapentin molecules is consumed, the reaction propagates due to the generation of new nuclei at lactam and gabapentin molecular interfaces.

Environmental temperature conditions impact rate constants k_1 , k_2 , k_3 , while moisture conditions have a predominant effect on rate constant k_3 . Extended Arrhenius equation (Equation 4-6)¹ was used to estimate the rate constants for gabapentin's degradation after milling as a function of environmental conditions in the absence of excipients.¹

$$k_1 = 1.48 \times 10^{10} \times \exp\left(-\frac{10707}{T}\right) \quad \text{Equation 4}$$

$$k_2 = 2.40 \times 10^9 \times \exp\left(-\frac{8295}{T}\right) \quad \text{Equation 5}$$

$$k_3 = 2.15 \times 10^6 \times \exp\left(-\frac{8163}{T}\right) \times \exp(0.0923 \times \% RH) \quad \text{Equation 6}$$

Milling duration impacted the value of gaba_0^* , which was estimated to vary between 0.46-1.04% mole for gabapentin samples milled between 15-60 min.¹ The study clearly demonstrated that the processing increased the concentration of reactive gabapentin molecules.

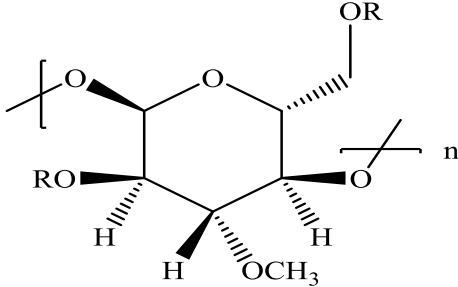
The above equations can be used to estimate the value of rate constants and the concentration of reactive gabapentin molecules after processing and varying the environmental conditions. In the presented research, the estimates would be used to establish a range for the initial parameter values during parameterization of the data, using non-linear regression.

1.3.3. Commonly Used Pharmaceutical Excipients

The chemical structures or formulae for all the excipients procured in the study are provided in Table 1.

Table 1: Structural Information for the Excipients used in the Study³⁸

Excipient chemical name	Common name	Structure / chemical formula
Dibasic calcium phosphate dihydrate	Emcompress [®]	$\text{Ca}(\text{HPO}_4) \cdot 2\text{H}_2\text{O}$
Dibasic calcium phosphate anhydrous	A-Tab [®]	$\text{Ca}(\text{HPO}_4)$
Tribasic calcium phosphate	Tri-Tab [®]	$\text{Ca}_5\text{OH}(\text{PO}_4)_3/10\text{CaO}_3\text{P}_2\text{O}_5 \cdot \text{H}_2\text{O}$
Monobasic calcium phosphate	Mono-Tab	$\text{Ca}(\text{H}_2\text{PO}_4)_2$
Starch	Unipure [®] DW	<p>Amylose unit</p>
		<p>Amylopectin unit</p>
HPC	Klucel [®] EF	<p>R = $\text{CH}_2(\text{OH})\text{CH}_3$</p>

HPMC	Methocel[®]	 <p style="text-align: center;">R = CH₂(OH)CH₃</p>
Magnesium silicate	Talc	$Mg_3Si_4O_{10}(OH)_2$

Dibasic calcium phosphate anhydrous (A-Tab[®]) and Dibasic calcium phosphate dihydrate (Emcompress[®])

The major pharmaceutical application of dicalcium phosphate is that of a diluent in tablet and capsule formulation due to its good compaction and flow properties. Its predominant deformation mechanism is by brittle fracture. The molecular weight of A-Tab[®] is 136.06 g/mole and that of Emcompress[®] is 172.09 g/mole. Dicalcium phosphate is non-hygroscopic and is stable at room temperature. The anhydrous grade does not transform to the dihydrate form. However, the dihydrate form can lose its water of crystallization under high temperature and low humidity conditions. The true density of the anhydrous grade of dicalcium phosphate is around 2.89 g/cm³, while bulk and tap densities are 0.78 g/cm³ and 0.82 g/cm³ respectively. The true density of the dihydrate form is 2.38 g/cm³ and bulk and tap densities are 0.91 g/cm³ and 1.17 g/cm³ respectively. The average particle size diameter is around 180 μm for both the anhydrous and the dihydrate form. The specific surface area (20-30 m²/g) for the anhydrous form is greater relative to the specific surface area (0.44-0.46 m²/g) for the dihydrate form. The excipient is known to be incompatible with tetracycline antibiotics and drugs such as indomethacin, aspirin, aspartame, ampicillin, cephalexin, and erythromycin.³⁸

Tribasic Calcium Phosphate (Tri-Tab[®])

Tri-Tab[®] is used in the pharmaceutical industry as an anti-caking agent, glidant, diluent and binder in case of direct compression or wet granulated formulations. In some cases, the excipient is also used as a tablet disintegrant and as a major source of calcium and phosphorus. Its primary bonding mechanism is by plastic deformation.³⁸

Tribasic calcium phosphate is available in two forms 1. $\text{Ca}(\text{PO}_4)_2$ with a molecular weight of 310.20 g/mole and 2. $\text{Ca}_5(\text{OH})(\text{PO}_4)_3$ with a molecular weight of 1004.70 g/mole. In the dissertation studies, the second form of Tri-Tab[®] was used. The true density of the material is 3.14 g/cm³ while, bulk and tap density values are 0.3-0.8 g/cm³ (powder form-granular form) and 0.95 g/cm³ respectively. The melting point is 1670°C, providing stability to the material under high temperature conditions. Specific surface area of the material is 70-80 m²/g. The material is slightly hygroscopic (2% moisture content, under 15-65% RH conditions) as the surface moisture is picked up and contained within small pores in the crystal structure. The excipient is available with an average particle diameter of 350 μm and is known to be incompatible with tetracycline antibiotics and tocopheryl acetate.³⁸

Hydroxypropyl Cellulose (HPC/Klucel[®])

Hydroxypropyl cellulose (HPC/Klucel[®]) is partially substituted poly (hydroxypropyl) ether of cellulose, containing not more than 0.6% silica or other anticaking agent. The excipient is used in the pharmaceutical industry as a coating agent for extended release formulations, binding agent, stabilizing agent, emulsifying agent and viscosity enhancing agent.

The molecular weight is dependent on the chain length and varies between 50,000-12, 50,000 g/mole. The material has a bulk density of 0.5 g/cm³ and a glass transition

temperature of 130 °C. The material decomposes between 260-275°C. The material is slightly hygroscopic adsorbing about 4% w/w moisture at 50% RH conditions and 12% w/w moisture at 84% RH conditions. The material is known to be incompatible with substituted phenol derivatives, methyl and propyl paraben.³⁸

Hydroxypropyl Methyl Cellulose (HPMC, Methocel[®])

Hydroxypropyl methyl cellulose is used in the pharmaceutical industry as a bio-adhesive material, coating agent in controlled release formulations, dissolution enhancing agent, emulsifying agent, dispersing agent, film forming agent and in extended and modified release formulations. It is available as several grades varying in their molecular weight between 10,000-15,00,000 g/mole and one to two degrees of substitution. The degree of substitution denotes the amount of substituent groups on the anhydroglucose units of cellulose. True density of the material is 1.32 g/cm³ and bulk and tap density are 0.34 g/cm³ and 0.55 g/cm³ respectively. Glass transition temperature of HPMC is between 170-180°C, and it decomposes at approximately 230 °C. It is slightly hygroscopic and absorbs ~10% moisture at relative humidity conditions of 70%. HPMC is known to be incompatible with oxidizing agents, and is known to form a complex with metallic salts or ionic organics to form insoluble precipitates.³⁸

Pregelatinized Starch

Pregelatinized starch (Unipure[®]) is chemically or mechanically processed to rupture all or parts of the starch granules. Partial gelatinization renders starch flowable and directly compressible, while full gelatinization produces cold water soluble starch which is mainly used as a wet granulating agent. Pregelatinized starch, is known to contain 5% free amylose, 15% free amylopectin and 80% unmodified starch. It is used in the pharmaceutical industry as tablet or

capsule diluent, disintegrant and tablet binder. In comparison to starch, pre-gelatinized starch possesses enhanced flow properties and compression characteristics. The material deforms predominantly by plastic flow accompanied by substantial elastic deformation.³⁸ The true density of pre-gelatinized starch is 1.51 g/cm³ and bulk and tap densities are approximately 0.58 g/cm³ and 0.87 g/cm³ respectively. Pre-gelatinized starch is hygroscopic and absorbs approximately 15% w/w moisture at 70% RH conditions. Mean particle diameter is around 52 µm and specific surface area varies between 0.18-0.28 m²/g.³⁸

Talc

Talc is purified, hydrated magnesium silicate with a molecular formula of Mg(Si₂O₅)₄(OH)₄. It may contain variable amounts of iron and aluminium silicate as impurities. It is used in the pharmaceutical industry as an anticaking agent, glidant, tablet and capsule diluent, lubricant and dissolution retardant in controlled release formulations. Talc adsorbs insignificant amounts of moisture at 90% RH conditions and ambient temperature conditions. Almost 99% of talc particles pass through sieve number 44 (355 µm) and have a specific surface area of 2.41-2.42 m²/g. Talc is known to be incompatible with quaternary ammonium compounds.³⁸

Monobasic Calcium Phosphate

Monobasic calcium phosphate is used in the food industry as a leavening agent and in the pharmaceutical industry for tablet production, due to its desirable flowability and good compaction properties. The material is of anhydrous grade, white in color, granular and free flowing. It is non-hygroscopic with true density of 2.23 g/cm³ and has poor water solubility (18 g/l). Monobasic calcium phosphate is a considerably strong acid with a pH value of 2 for its 25% w/v slurry. The majority (95% w/w) of its particles pass through sieve of mesh size 90 µm.

The acidic nature of the excipient limits its usage with drugs prone to acid catalyzed degradation.^{38,39}

Based on the above information, all excipients used in the presented research are likely to be both physically and chemically stable under the accelerated study conditions employed. Most of the excipients are also not likely to absorb large quantities of water under the low humidity conditions (5%) of the study. Thus the confounding effect of moisture on gabapentin's stability during the accelerated storage period is less likely.

1.3.4. Models and Complexities in Solid-State Kinetics

The kinetic model for gabapentin reported in the literature included critical mechanisms such as nucleation of lactam molecules in gabapentin crystals and autocatalysis of the conversion of stable gabapentin molecules to reactive gabapentin molecules. The kinetic model designed to predict solid-state stability of gabapentin has a combination of nucleation model theory and Prout-Tompkins autocatalytic theory. Therefore it is important to understand the mechanisms and principles underlying the existing solid-state models reported in the literature.

Solid-state kinetics differs from a typical solution state reaction due to the inhomogeneity associated with the solid sample. The reactivity is different across different regions in the solid, depending on the molecular degrees of freedom across the solid sample. In solids, reactions are typically initiated at defect sites in the crystal lattice or at crystal surfaces, edges and corners. Ideally, a perfect crystal has minimal reactivity due to the absence of any imperfections. However, perfect crystals are rare and most crystal lattices contain imperfections. The lattice imperfections are predominantly in the form of point defects and dislocations. The imperfection

sites are energized sites due to molecules possessing higher free energy, resulting in lower activation energy required to initiate and drive the reaction.⁴⁰

A kinetic model is a theoretical and/or a mathematical description of a kinetic event that occurs experimentally. In solid-state, a model can describe a particular reaction type and translate that mathematically into a rate equation. Based on the mechanistic assumptions of the model and the shape of the isothermal plot of concentration vs. time, they can be classified as sigmoidal, acceleratory, linear or deceleratory.^{40, 41}

Nucleation Model Theory: The kinetics of many solid-state reactions are described by nucleation models typically the Avrami model. The rate limiting step in the model is assumed to be the formation and growth of nuclei, which are finite quantities of products in the reactant lattice. Nucleation models account for both nucleation and growth rates. However, the energy barrier for nuclei generation would be larger relative to that for growth. The contribution of nucleation may decrease as the reaction progresses, leading to an effective activation energy that varies with the progress of the reaction. Nucleation rates are derived based on the assumption that nucleation is either single step or involves multiple steps. Single step nucleation assumes that nucleation and growth both take place in a single step, while in multi-step nucleation, several steps are required to generate a growth nucleus.^{40,42-44} In the presented research, the spontaneous conversion of reactive gabapentin to lactam is assumed to follow a single step nucleation reaction.

Reaction Order Based Model Theory: The rate law is based on the reaction order. These models are simple models similar to those used in homogenous kinetics. In these models, the reaction rate is proportional to the concentration, the amount or fraction, of remaining reactant raised to a particular power. This is the reaction order.^{40-42, 45}

Autocatalytic Model Theory: In homogenous kinetics, autocatalysis will occur when the products catalyze the reaction. This occurs when the reactants are regenerated in the process known as branching. In autocatalytic models, the reaction rate increases as the products are formed. The reactants will be consumed over time and the reaction will enter the termination stage where it will cease. The reaction rate vs. time profile shows a bell shaped plot with both an acceleration and a decay period. The model was first derived by Prout and Tompkins for thermal decomposition of potassium permanganate which produced considerable crystal cracking during decomposition. The mechanistic model of nucleus branching was used to formulate the Prout-Tompkins model.⁴⁶⁻⁴⁸ In the presented research, the generation of reactive gabapentin molecules within a particle of gabapentin is expected to be autocatalyzed by the concentration of lactam and inherent reactive molecules.

The Prout –Tompkins equation involves three assumptions:

1. Linear dependence of the termination rate constant (k_T) on the concentration of the reactant species.
2. If the first assumption holds valid then $k_T = k_b/2a_i$ where $a = a_i$ at inflection point on the curve and k_b is the branching rate constant.
3. Value of $a_i = 0.5$ requires a sigmoidal curve function. The derivative form of the Prout-Tompkins model is provided in Equation 7.

$$\frac{d_x}{d_t} = k' (1 - x)(x)$$

Equation 7

In the above equation, x denotes the mole fraction of the product measured at time t , and k' ($\text{mol}^{-1}\text{h}^{-1}$) is the rate constant for the transformation.⁴⁶

Major complexities in solid-state kinetics of drug molecules

Solid-state kinetics typically involves major complexities, which need to be understood in order to define the model assumptions. Some of the complexities relevant to the presented research have been discussed below.

Distribution of reactive molecules: different samples of a material can possess different concentrations of defect sites, defect types, and concentration of reactive molecules. Since the above molecules are more reactive than ordered bulk molecules, they undergo a reaction at different rates creating a complex kinetic scheme for drug degradation. This complexity exists in the case of gabapentin's degradation, wherein reactive molecules are likely to have different rates of degradation and varying degrees of freedom. When describing degradation using a kinetic scheme, it is important to describe it with simplicity in order to be able to accurately estimate rate constants involved in the degradation. In the presented research, it is assumed that no major differences are present between the degradation rates of disordered molecules due to differences in their defect type (either on the surface or in the bulk of the crystal). In summary, all the disordered molecules in the gabapentin crystal are assumed to have similar reactivity irrespective of their defect type.

Particle size variations in the sample: for reactions initiating at imperfection sites or crystal surfaces, larger particles with lower specific surface area will likely have a lower overall rate of degradation relative to smaller particles. Samples with variable particle sizes have a potential to show complex reaction behavior. To eliminate the issue associated with varying particle size distribution in the sample, gabapentin and the excipients selected for the presented research were controlled for their particle size fractions.

Powder packing: sample packing could affect solid reaction kinetics, wherein loosely packed powders, containing air pockets can have variable reaction kinetics compared to a tightly packed sample. This is due to the reduced thermal conductivity of the air pockets in loose powder or their ability to trap evolved gases.^{40,41} This could be one of the complexities especially seen in the case of compacts of physical mixtures of gabapentin with the excipients. The presented research, will explore the relationship between compact porosity of gabapentin-excipient physical mixture and the initial rate for lactam formation.

All the above complexities need to be considered when analyzing the kinetic data and selecting a model for the solid-state drug degradation. Therefore understanding the mechanism of degradation is critical when defining solid-state kinetics of drug molecules.

1.3.5. Solving Ordinary Differential Equation and Non-Linear Regression

On application of the desired model, the differential equations associated with the model need to be numerically treated for approximation of a solution and estimation of the kinetic parameters. The initial value problem for a differential equation involves finding a function $y(t)$

that satisfies the initial condition $y(t_0) = y_0$. A numerical solution based on equation 8 generates a sequence of values for every independent variable, t_0, t_1, \dots, t_n , and a corresponding sequence of values for the dependent variable y_0, y_1, \dots , such that each y_n approximates the solution at t_n . Determination of step size (h_n) is important when approximating a solution using numerical methods (Equation 9).

$$\frac{dy}{dt} = f(t, y(t)) \tag{Equation 8}$$

$$h_n = t_{n+1} - t_n \tag{Equation 9}$$

The simplest numerical method for solution of an initial value problem is Euler’s method. It uses a fixed step size h and generates an approximate solution by using Equation 10 and Equation 11

$$y_{n+1} = y_n + hf(t_n, y_n) \tag{Equation 10}$$

$$t_{n+1} = t_n + h \tag{Equation 11}$$

The biggest defect of the Euler’s method is that it does not provide an error estimate.

Single step methods are often called Runge-Kutta methods, after the two German mathematicians. The classical Runge-Kutta was used for hand computations before the invention of digital computers. It uses four function evaluations per step as shown in a series of equations (Equation 12-16).^{49,50}

$$s_1 = f(t_n, y_n) \tag{Equation 12}$$

$$s_2 = f\left(t_n + \frac{h}{2}, y_n + \frac{h}{2} s_1\right) \tag{Equation 13}$$

$$s_3 = f\left(t_n + \frac{h}{2}, y_n + \frac{h}{2} s_2\right) \tag{Equation 14}$$

$$s_4 = f(t_n + h y_n + h s_3) \quad \text{Equation 15}$$

$$y_{n+1} = y_n + \frac{h}{6} (s_1 + 2s_2 + 3s_3 + s_4) \quad \text{Equation 16}$$

After numerically estimating the solution to the differential equations using initial value estimates for the parameters, the next step is to use non-linear regression to optimize parameter estimations, which will provide a predicted curve that best fit the data.

Non-Linear Regression

A number of data sets are analyzed by fitting a curve using non-linear regression. Curve-fitting standardizes data interpretation into a uniformly recognized form. Curve-fitting describes experimental data as a mathematical equation in the form $y = f(x)$, where x is the independent variable and y is the dependent variable, and f is the function including the parameters that describe the data.⁵¹

The non-linear regression is a powerful tool for fitting an equation to a set of data in order to acquire values of unknown parameters. Similar to linear regression, non-linear regression procedures determine parameter estimates by reducing the sum of squares of the distances of the data points to the curve (least squares approach). If the 'y' value of each observed data point is called y_{data} and the y predicted value of the curve is called y_{curve} , the goal is to minimize the residual sum of squares (SS) as calculated in Equation 17. These methods are appropriate when the experimental uncertainty is Gaussian and unrelated to the values of x and y .⁵²

$$SS = \text{sum} [(y_{\text{data}} - y_{\text{curve}})^2] \quad \text{Equation 17}$$

The non-linear regression problems are solved iteratively. An initial estimate of the value for each parameter is provided; the non-linear regression procedure then adjusts these values to improve the fit of the curve to the data. The iterations (value adjustments) continue until negligible improvement of the fit is observed. All iterative techniques are given a starting point or initial estimate of parameter values by calculation or intelligent guessing. Several methods can be chosen to perform the iterations. One of the commonly used techniques is the Marquardt method. This method involves a combination of two algorithms namely, the method of steepest descent and Gauss-Newton.⁵²

The method of steepest descent works by providing an arbitrary step length to move along the direction of steepest descent. This procedure is then repeated until the lowest value for the sum of squares is obtained. Essentially, a minimum sum of squares is obtained by moving downhill from the initial estimates provided for the parameters.⁵²

The Gauss-Newton algorithm alters the value of parameters to directly reach the minimum. The Gauss-Newton method works poorly with initial iterations, and may result in a poor fit or a wrong solution. This method works well when the sum of square error (SSE) is close to the minimum.

Another iterative method is the simplex method, where the values for the initial estimate and the initial increment value for each parameter needs to be provided. This method starts with three starting values, and after several iterations the algorithm rejects the worst of the solutions generated. The advantages of this method over other non-linear regression algorithms include its

fast speed and its rare convergence to a local minimum. Hence, it can be used with non-continuous functions. The disadvantages are that it does not estimate standard error for each parameter and is more difficult to use since the starting increments for each parameter need to be provided.^{52,53}

The Marquardt method has several advantages, the most important being that it combines the strengths of the methods, steepest descent and Gauss-Newton. Due to these advantages it has been used to optimize the rate constants in case of the presented studies with gabapentin.⁵²

Non-linear regression cannot find the best curve through a set of data points but can optimize the parameters in a specified equation that calculates 'y' as a function of 'x' and one or more parameters. The function is selected to describe a hypothetical physical or molecular model. All non-linear regression procedures calculate the derivative of 'y' with respect to all parameters. Some programs require the derivatives to be determined and entered as an equation, while other programs such as Excel Solver[®] (used in this research), and calculate the derivatives numerically by evaluating the equations before and after altering the value of the parameter by a small amount. Initial estimates for each parameter in the equation need to be specified based on previous experience, preliminary analysis based on linear transformation, or on a hunch. It is not difficult to estimate parameters if one understands both the physical model that the equation represents and the meaning of each parameter. Poor selection of initial values results in longer processing times and may lead to the program going in a wrong direction and not converging to a solution. It is also possible that poorly selected values can cause the program to converge on a wrong solution.⁵²

Another important parameter in non-linear regression is the convergence criterion, especially when calculations occur iteratively and the computer needs to be told when to stop. Too loose a criterion can cause the program to stop before it has reached the best fit. On the other hand too tight a criterion can result in consumption of the computer time. Considering the time limitation, a tight convergence criterion (10^{-10}) was attempted across all the parameter estimates for gabapentin's degradation in order to avoid convergence to a wrong solution.^{52,54}

When assessing goodness of fit, it is important to examine the graph of the curve superimposed to the data points. In addition to viewing the graph, two statistical methods can be used to quantitate goodness of fit:

1. Root mean square (RMS) this takes into account the average deviation of the curve from the points. When considering the residuals plot (residual vs. 'x' value), the 'y' value of each point is replaced by the distance of that point from the curve. The residual value should be randomly distributed across the plot. If the equation is inappropriate, the residuals tend to cluster. This indicates systematic deviations of the data points from the predictions of the curve.
2. The value of the square of correlation coefficient (R^2) is important for non-linear regression when represented as a fraction of the variance in the 'y' value, reduced by the curve.^{52,54}

In non-linear regression, it is possible that the final fit is not the best possible fit. To guard against this issue one can repeat non-linear regression several times using different starting values, this provides a more intuitive grasp of the equations used.

In research studies with gabapentin the initial starting values were altered randomly as well as systematically using a central composite experiment design in a 4 (parameters) x 3 (levels) matrix. The range for altering the starting values was selected to be two orders of magnitude higher and lower than the parameter estimates published in previous studies with gabapentin.¹

1.3.6. Compaction as a Processing Condition

One of the research studies presented in this document involved understanding the impact of compression pressure and powder properties of excipients on solid-state degradation of gabapentin. This study was designed to test the hypothesis that exposure of gabapentin to compaction pressure will increase lattice defects in gabapentin crystal and reduce its particle size resulting in an increase in the initial rate for lactam formation. To understand the impact of compaction pressure and powder properties of excipients, it is important to understand the theory behind tablet formation.⁵⁵

A tablet is formed by reducing the volume of particles consolidated into a single body. This process can be divided as a series of different phases. At the beginning, the volume starts to reduce and the particles are arranged into a closer packing structure. At a certain point, the packing properties and friction between particles will prevent any further particle rearrangement. At this point, further reduction in volume will result in an elastic, viscoelastic or plastic deformation of the particles. Additionally, fragmentation will result in generation of smaller particles, which will also undergo deformation resulting in volume reduction. Amongst the excipients used in the presented research, microcrystalline cellulose, HPC and HPMC

undergo plastic deformation, while talc, Emcompress[®] and the drug gabapentin deform by brittle fragmentation.⁵⁶⁻⁶⁷

The process of compaction will result in the particle surfaces being brought in close proximity with each other, leading to formation of inter-particulate bonds. Predominant bonding mechanisms include, mechanical interlocking between irregularly shaped particles, inter-particulate attraction forces and creation of solid bridges due to melting of particles. The process of compaction will therefore result in increased particle contact and reduced particle size, both of which will affect the solid-state degradation of drugs.^{61,63-65,68}

A number of factors affect deformation mechanism. One such factor is material crystallinity. Amorphous materials undergo plastic deformation while most crystalline materials undergo brittle fragmentation.^{69,70} Particle size and shape are amongst other important determinants of deformation behavior. It has been observed that increasing the irregularity and roughness of granules changes the compression behavior from plastic deformation towards that of particle fragmentation and attrition.^{71,72}

Addition of glidants such as talc to the formulation results in decreased surface roughness of the drug particles by formation of a uniform coating of the glidant particle around the drug particle. This reduces the frictional drag between particles. Glidants also act as physical barriers between particles reducing the attractive forces between them and removing any surface adsorbed moisture to improve their flow properties.^{73,74}

Moisture absorbed by amorphous regions in the materials have a significant effect on physical and mechanical properties of formulations such as flow, compression, hardness, surface energy, die-wall friction and Young's elastic modulus.⁷⁵ Moisture is responsible for plasticization of the material during the compression phase, thus affecting the bond formation processes.^{76,75,77} This highlights the need to understand the relationship between moisture content of the excipients and the rate of lactam formation in the compacts of gabapentin with excipients.

Analysis of Powder Compaction Data

Studying compaction mechanism for powders has become an important part in the development of solid oral dosage forms. Measurements related to the compaction of powders are facilitated by the availability of instrumented tablet presses, commonly known as compaction simulators. These instruments help measure punch force, upper and lower punch displacement, axial and radial load transmission and temperature changes.

The Heckel Equation is amongst the most popular methods used in pharmaceutical research to determine the volume reduction mechanism during compression.^{59,71,78,79} It is based on the assumption that powder compression follows first order kinetics, with the inter-particulate voids as the reactant and the powder densification as the product. According to the Heckel relationship, the degree of compact densification with increasing compaction pressure is directly proportional to porosity (Equation 18).

$$\frac{d\rho_r}{dP} = k\varepsilon \quad \text{Equation 18}$$

In the above equation, ρ_r is the relative density at pressure P and ε is the porosity.

The relative density is defined as a ratio of density of the compact at pressure P , to the density of the compact at zero porosity (true density).

Equation 19 is used in the calculation of porosity for gabapentin-excipient compacts to understand the effect of compact porosity on the initial rate for lactam formation.

$$\varepsilon = \left(\frac{V_p - V_0}{V_p} \right) = 1 - \rho_r \quad \text{Equation 19}$$

In the above equation, V_p and V_0 are the volume at any applied pressure and volume at theoretical zero porosity respectively. Equation 18 and equation 19 can be used to derive equation 20.

$$\frac{d\rho_r}{dP} = k(1 - \rho_r) \quad \text{Equation 20}$$

The differential equation in equation 20 can be solved to generate equation 21.

$$\ln \left[\frac{1}{(1 - \rho_r)} \right] = kP + A \quad \text{Equation 21}$$

The plot of equation 21 yields a graph with a linear portion having slope k and intercept A .

The reciprocal of k gives a material dependent constant known as yield pressure (P_y), which is inversely related to the ability of the material to deform plastically under pressure.⁷⁹⁻⁸¹ The intercept of the extrapolated linear region A is a function of the original compact volume.

The main utility of Heckel plots arises from their ability to identify predominant deformation behavior of a material. The Heckel relationship is explored in the presented research to

understand the predominant deformation mechanism of the excipients in the physical mixture with gabapentin, and for establishing any connection of this material property with accelerated lactam formation.

1.3.7. Conclusion

Gabapentin is used in the treatment of many neurological disorders with a major application being in the treatment of epilepsy. Gabapentin has a potential to undergo intramolecular cyclization to form its degradation product lactam. Lactam is 20-fold more toxic than gabapentin and has been reported to cause seizures in animal models. The concentration of lactam has been regulated to 0.4% by USP. A number of recalls worth millions of dollars have been issued in the last couple of years (2010-2013) due to the exceedingly high lactam content in gabapentin formulations.

Literature findings have indicated an effect of pH, salt concentration and excipients on the solution state stability of gabapentin. In solid state gabapentin is known to undergo accelerated degradation under accelerated temperature conditions and application of processing conditions such as milling and lyophilization. One study has highlighted potential effect of excipient type on its degradation kinetics.

The main objective of this project was to test for the effect of excipient properties on gabapentin's degradation profile. In order to test the role of excipients a robust and accurate analytical method was developed and validated for the quantification of gabapentin and lactam. The overlying objective was to develop a relationship between the rate constant for lactam

formation and properties of excipients affecting the degradation kinetics. The final objective was to identify the effect of compaction as a processing condition on gabapentin's degradation profile considering its commercial availability as a solid oral dosage form.

Chapter 2

Optimization and Validation of the Analytical Method for Determination of Gabapentin and Its Degradation Product Lactam

2.1. Introduction

The objective of this dissertation is to identify various factors related to formulation composition and compaction, which affect the solid-state stability of gabapentin. An important step toward fulfilment of this objective is the accurate quantification of gabapentin and lactam in their binary mixtures and in their compacts with excipients. Thus, selecting an analytical method, optimizing and validating the same as per established guidelines, are a key aspects of the project.

Literature studies indicate a number of analytical methods using different instrumental techniques for the separation and quantification of gabapentin and lactam. When selecting a method, it is important to note that gabapentin is a highly polar compound which is poorly retained on most reverse-phase high performance liquid chromatography (RP-HPLC) columns. On the other hand, its degradation product, lactam, is strongly retained on RP-HPLC columns. Due to gabapentin's poor column retention, most analytical methods involve extraction and derivatization steps before quantitative determination.³⁶ The quantification of gabapentin in human plasma and serum has been reported using gas chromatography, capillary electrophoresis and HPLC techniques.^{52, 82-86} Analytical techniques developed for bioanalysis of gabapentin also include mass spectrometry in combination with gas or liquid chromatography.^{52,85,86}

An analytical method using HPLC instrumentation along with UV detection and without derivatization has been developed for the successful determination of potency for gabapentin in its marketed formulations.^{5,36} The separation is achieved using a cyano column with an isocratic elution method. The cyano column is selected due to the higher retention time of gabapentin relative to the retention time on other C₁₈ columns for organic molecules. The other reason stated for column selection has been to exploit the combination of hydrophilic and hydrophobic interactions of the cyano groups with compounds possessing amine or amide functional groups, which are found in both gabapentin and lactam. The method used a higher volume (95% v/v) of the aqueous phase relative to the organic phase to increase the retention time (71 min) for lactam. The buffered aqueous phase had a neutral pH (6-7), since low pH conditions resulted in poor resolution between gabapentin and lactam in addition to poor stability of gabapentin.^{5,36}

The above method offered several advantages. Thus, it was selected, optimized (to improve its specificity), and validated as per ICHQ2A guidelines. Along with the method validation, preliminary studies to test the interference of excipients and filter membrane on the extraction efficiency of gabapentin and lactam were performed. The stability of gabapentin and lactam in the mobile phase and in the sample solvent was studied to negate the effect of solution state kinetics confounding the observed degradation of gabapentin in its solid-state.

2.2. Materials and Methods

2.2.1. Materials

Gabapentin was obtained from Hangzhou Starshine Pharmaceutical Co. Ltd. (Hangzhou, China). Gabapentin reference standard was purchased from the United States Pharmacopeia (USP)

(Rockville, Maryland). Lactam standards were purchased from USP for the validation studies and Sigma-Aldrich (St. Louis, Missouri) for all other preliminary studies. The excipients used in the study included calcium phosphate dibasic dihydrate (Emcompress[®], E. Mendell. Co. Inc, New York), monobasic calcium phosphate (V-90 grade, Innophos, New Jersey), dibasic calcium phosphate anhydrous (A-Tab[®], Innophos, New Jersey), tribasic calcium phosphate anhydrous (Tri-Tab[®], Innophos, New Jersey), modified corn starch (Uni-pure[™] DW, National starch LLC, New Jersey), hydroxypropyl cellulose (HPC, Klucel EF[®], Ashland Inc., Kentucky), hydroxypropyl methyl cellulose (HPMC, Methocel[™] E50 Prem LV, Dow Chemical Co., Michigan) and talcum (Talc, Fisher Scientific, Massachusetts). HPLC grade monobasic potassium phosphate and dibasic potassium phosphate were purchased from Sigma-Aldrich (St. Louis, Missouri) for mobile phase preparation. HPLC grade acetonitrile was purchased from VWR International (Radnor, Pennsylvania). Deionized water filtered through a 0.45 micron filter was obtained from an in-house Milli-Q water purification system (Millipore Corporation, Billerica, Massachusetts). Nylon syringe filters (0.4 μm) for sample filtration and nylon filters (0.2 μm) for mobile phase filtration were purchased from VWR International (Radnor, Pennsylvania).

2.2.2. Instrumentation and chromatographic condition

The method used a reverse phase HPLC system (Waters[®] 2890 separation module) equipped with an ultra-violet (UV) photodiode array detector. The column selected was a μ-Bondapack cyano column (3.9 mm x 390 mm) (Waters Co. Op. Massachusetts).⁸⁷ The mobile phase was composed of 95 parts phosphate buffer pH 6.8-7.0 (10 mM KH₂PO₄/ 10 mM K₂HPO₄) and 5 parts of acetonitrile. The mobile phase pH was adjusted to 6.8 to ascertain maximal stability of

gabapentin in solution. The mobile phase pH was measured using pH meter H12210 (Hanna Instruments, Carrollton, Texas). The mobile phase was filtered using a nylon filter (0.2 μm) and degassed 1 h prior to analysis. Flow rate of the mobile phase was adjusted at 1.0 ml/min and the injection volume of 20 μl was selected. Detection of gabapentin and lactam was performed at a single wavelength of 210 nm with the column maintained under ambient temperature conditions (20-22°C).

2.2.3. Analytical Method Validation

The analytical method was validated for specificity, assay, linearity, range, accuracy, precision, limit of detection, and limit of quantification. The protocol for all designed studies and the data reporting was as per ICH Q2A guidelines.

Specificity

Specificity of the method was determined by analyzing all single components, namely gabapentin (2 mg/ml), lactam (40 $\mu\text{g/ml}$), and excipients (2 mg/ml) such as Emcompress[®], A-Tab[®], Tri-Tab[®], Mono-Tab, HPMC, HPC, starch and talc used in the stability studies. All chromatograms were evaluated to confirm the absence of similar elution times for gabapentin, lactam, or any other confounding peaks from the excipients to be used in the study subsequently.

Assay (Determination of Purity) for Bulk Gabapentin

Gabapentin stock solution I (5 mg/ml) was prepared using the USP reference standard for gabapentin in deionized filtered water as a medium for standard preparation. For complete solubilization of gabapentin, the standard solution was sonicated for a minute. The stock solution I was then used to prepare calibration standards ($n = 3$) at 5 different concentration levels by

using a serial dilution technique. The five concentrations ranged from 0.5 mg/ml to 5 mg/ml. The calibration was repeated on 3 separate days to determine the inter-day precision. The calibration standards were then used to determine the purity of the bulk gabapentin procured for the degradation studies.

Another stock solution II (5 mg/ml) of gabapentin was prepared using bulk gabapentin, which was diluted with filtered deionized water to prepare sample solutions (n = 6) of low (0.5 mg/ml), medium (2 mg/ml) and high (5 mg/ml) concentrations. The purity of gabapentin was determined based on the linear equation of the calibration curve for gabapentin using calibration standards. The purity of bulk gabapentin is reported as average percent purity (n = 6) relative to the reference standard and precision has also been reported as percent relative standard deviation (% RSD) amongst the replicates and confidence interval (95%) (n = 6).

Linearity and Range

Standard calibration curves were prepared using six calibrators (3 concentrations x 2 inj.) for gabapentin over a range of 0.4–10 mg/ml and six calibrators (3 concentrations x 2 inj.) for lactam over a range of 8–240 µg/ml on three separate days. The data of peak area versus drug concentration was treated by linear least square regression analysis. The standard curves were evaluated for inter-day and intra-day linearity.

Preparation of Standard Solutions for Calibration

A gabapentin stock solution III (20 mg/ml) was prepared using bulk gabapentin. Calibration standards were prepared at 6 different concentration levels ranging between 0.4 mg/ml and

10 mg/ml. A concentration range was selected, keeping in mind the larger mass of gabapentin (200 mg) to be used for the accelerated stability studies. A lactam stock solution I (5 mg/ml) was prepared using the USP reference standard. Since lactam is the degradation product measured, the ability to detect and quantitate smaller concentrations was important. Keeping this in mind, calibration standards were prepared for concentrations ranging between 8 µg/ml-240 µg/ml.

A gabapentin stock solution IV (20 mg/ml) was used to prepare quality control solutions at low (0.4 mg/ml), medium (4 mg/ml), and high (10 mg/ml) concentrations. Similarly, a lactam stock solution II (5 mg/ml) was used to prepare quality control solutions at low (8 µg/ml), medium (40 µg/ml) and high (240 µg/ml) concentrations.

All of the above quality control and calibration standards were prepared using filtered deionized water as a diluting medium. The above solutions were prepared in triplicates, on three different days as part of the method validation.

Accuracy and Precision

The accuracy and precision of three different concentrations of gabapentin and lactam were determined in triplicates. The analysis was performed on quality control solutions across the calibration range on three separate days. The method accuracy was established by evaluating the amount of gabapentin and lactam in the quality control solutions using the calibration standards. The accuracy results are expressed as percent recovery ($n = 3$) of gabapentin and lactam from the

quality control solutions. Precision, both inter-day and intra-day, is expressed as %RSD (n = 3) for peak areas of gabapentin and lactam.

Limit of Detection and Limit of Quantitation

Limit of detection (LOD) and limit of quantitation (LOQ) for gabapentin and lactam were calculated based on standard deviation of response (σ) and slope (s) of the calibration curves. LOD is calculated as $3.3 \times (\sigma/s)$ and LOQ is calculated as $10 \times (\sigma/s)$. The response (σ) is the standard deviation of intercepts and (s) is the average value of slope from the linear regression equation of the calibration curves (n = 3). The calibration curves were developed in the concentration range of 0.4 mg/ml–10 mg/ml for gabapentin and 8 mg/ml and 240 mg/ml for lactam.

2.2.4. Method Optimization

Effect of Filter Membrane

The possibility of drug-filter membrane (nylon) interaction was determined by studying the recovery of gabapentin and lactam from solutions of known concentrations and volume (2.5 ml). The protocol involved passing the solutions twice through the syringe filter of a known pore size (0.45 μm).

Quality control solutions (n = 2) of gabapentin at low (0.5 mg/ml) and high (5 mg/ml) concentrations, and those of lactam at low (8 $\mu\text{g/ml}$) and high (240 $\mu\text{g/ml}$) concentrations were filtered twice using a nylon syringe filter (0.45 μm / 25 mm). Both the filtrates (F1 and F2) were quantified for the concentration of gabapentin and lactam. The data is reported as the average

(n = 2) percent recovery of gabapentin and lactam and average precision (%RSD, n = 2) for the recovery of gabapentin and lactam from the filtrates.

Effect of Excipients

The analytical method was used to determine the extraction efficiency for gabapentin and lactam in the presence of excipients, namely, Emcompress[®], HPMC, starch, talc, and HPC. These excipients were used in the stability studies with gabapentin. Physical mixtures (n = 2) of gabapentin and excipient in a 1:1 proportion were prepared manually. The extraction efficiency of lactam was determined by spiking its known concentration (200 µg) in the physical mixture. The solutions prepared in deionized filtered water were sonicated for 10 min, filtered using a nylon syringe filter (0.45 µm) and analyzed for the concentrations of gabapentin and lactam.

2.2.5. Stability of gabapentin and lactam

The stability of the aqueous solutions of gabapentin and lactam in the medium (deionized filtered water) for sample preparation and in the mobile phase was determined. Samples of gabapentin (10 mg/ml) and lactam (160 µg/ml) were prepared in deionized filtered water and stored under room temperature conditions (20-22°C) in the dark for 24 h. The samples were analyzed for the recovery of lactam and gabapentin, as well as for identification of any new products generated.

2.3. Results and Discussion

2.3.1. Analytical Method Validation

Specificity

The sample chromatogram for gabapentin (2 mg/ml) is shown in Figure 6 and that for lactam (40 µg/ml) is shown in Figure 7. Retention time ($n = 18$) for gabapentin was 3.75 min (± 0.009 min) and that for lactam is 7.61 min (± 0.056 min). The peaks of both gabapentin and lactam were well separated from each other and could be analyzed accurately. The study to test the matrix effect confirmed absence of any co-eluting peaks, related to the excipients, at the retention times of lactam and gabapentin (appendix 1).

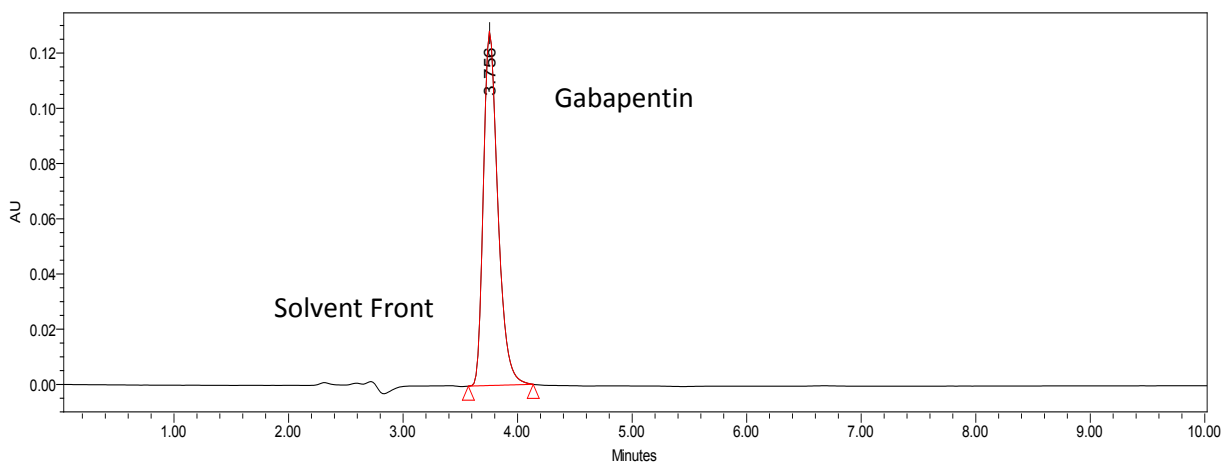


Figure 6: Sample chromatogram for gabapentin (2 mg/ml). The retention time is 3.75 min (± 0.009 min, $n = 18$). The solvent front is seen eluting at 2.5 min.

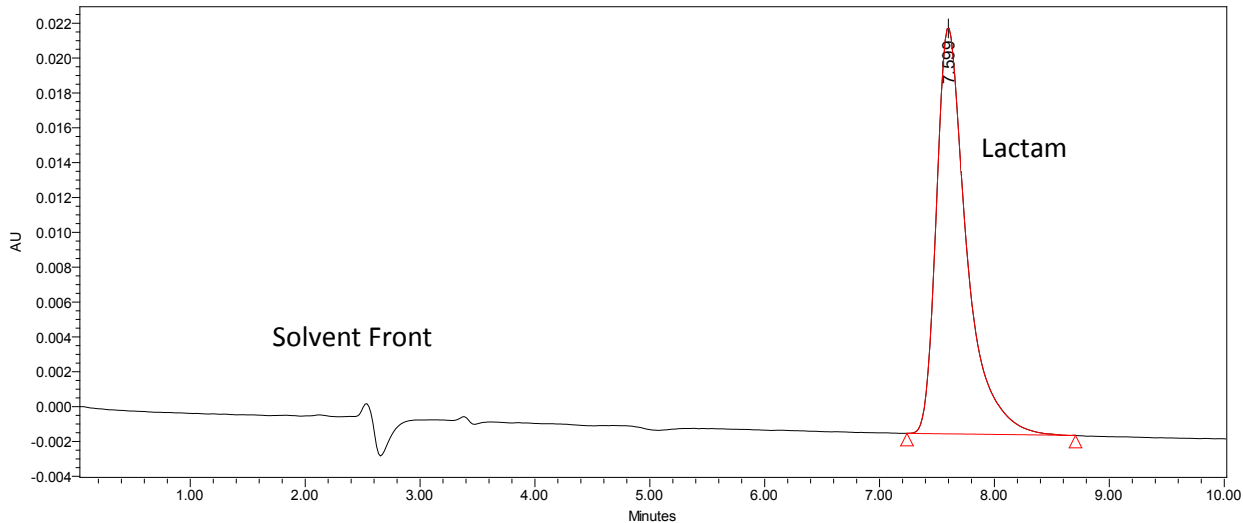


Figure 7: Sample chromatogram for lactam (40 µg/ml). The retention time is 7.61 min (± 0.056 min, n = 18).

Assay for Purity Determination of Bulk Gabapentin

Bulk gabapentin was evaluated for its purity relative to its reference standard (USP). This step was initiated to approve the use of bulk gabapentin in subsequent stability studies and analytical method validation. Results for the calibration curve using the gabapentin reference standard are reported in Table 2 and depicted in Figure 8. The results showed good correlation ($R^2 \geq 0.999$) between peak area and gabapentin concentration. The results for percent recovery and precision among replicates are reported in Table 3. The results suggested bulk gabapentin to possess purity comparable to that of the reference standard. The percent purity and precision (% RSD) of bulk gabapentin was 97.64% and 2.42% at low concentration (0.5 mg/ml), 102.44% and 0.75% at medium concentration (2 mg/ml), and 100.49% and 0.28% at high concentration (5 mg/ml) respectively. Hence, for subsequent studies involving gabapentin, the use of bulk gabapentin was considered appropriate.

Table 2: Calibration curve data using the gabapentin reference standard (USP). The calibration was performed as per ICH Q2A guidelines on three separate days.

Linearity and Range for Calibration Curves Using Gabapentin Reference Standard (USP)					
Standard Curve	Analytical Range (mg/ml)	Calibrators	Slope	y-intercept	R ² Value
validation Day 1	0.5-5	5	509910	20062	0.9995
validation Day 2	0.5-5	5	504610	21739	0.9998
validation Day 3	0.5-5	5	504710	26862	0.9994

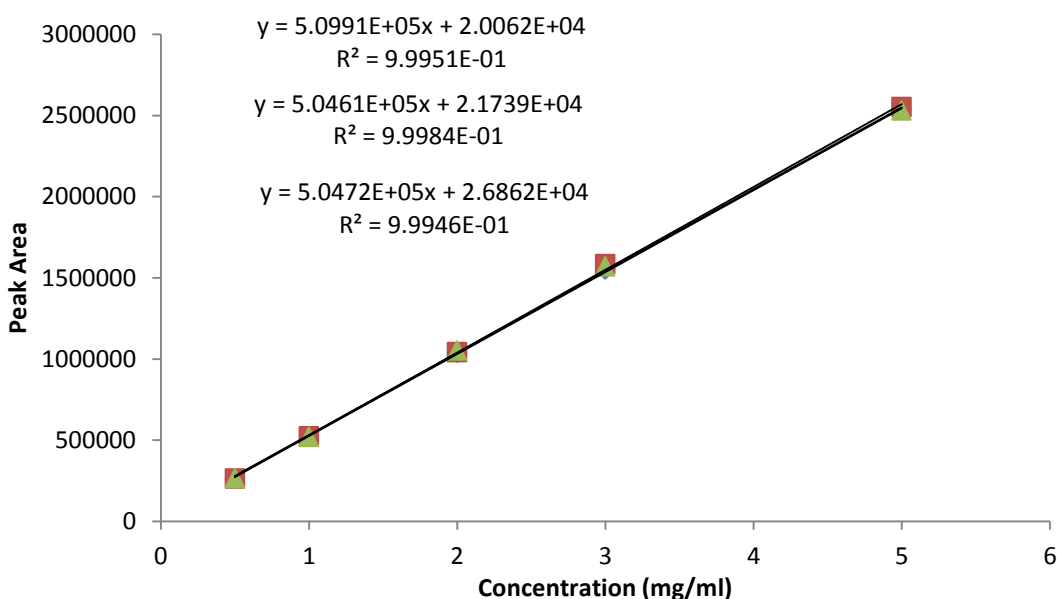


Figure 8: Calibration curves for gabapentin reference standard (USP) solutions. Calibration was performed as per ICH Q2A guidelines on three separate days. The equations represent linear correlation of the peak area for gabapentin and its concentration on the three days of calibration.

Table 3: Purity of bulk gabapentin for the analysis performed at three different concentrations.

Gabapentin Purity: Bulk Drug Substance n = 6 (3 Rep. x 2 inj.)			
Solution Concentration			
	0.5 mg/ml	2 mg/ml	5 mg/ml
% Purity	97.64	102.44	100.49
%RSD (Precision)	2.42	0.75	0.28
Confidence Interval (95%)	2.48	0.81	0.29

Linearity and Range

The linearity for standard calibration curves was established in the analytical range 0.4-10 mg/ml for gabapentin and 8-240 µg/ml for lactam. The results for linearity are summarized in Table 4 for gabapentin and in Table 5 for lactam. The results indicate good correlation ($R^2 \geq 0.999$) between peak area and concentration for gabapentin and lactam in the analytical range selected, as seen in Figure 9 and Figure 10.

Table 4: Linearity of calibration curves for gabapentin. Calibration was performed as per ICH Q2A guidelines on three separate days. Slope, intercept, and the correlation coefficient for the peak area and concentration plot have been reported.

Linearity of Calibration Curves for Gabapentin					
Standard Curve	Analytical Range (mg/ml)	Calibrators	Slope	y-intercept	R ² Value
Validation Day 1	0.4-10	6	549805	790.12	0.9995
Validation Day 2	0.4-10	6	539610	- 15428	0.9994
Validation Day 3	0.4-10	6	549788	18649	0.9999

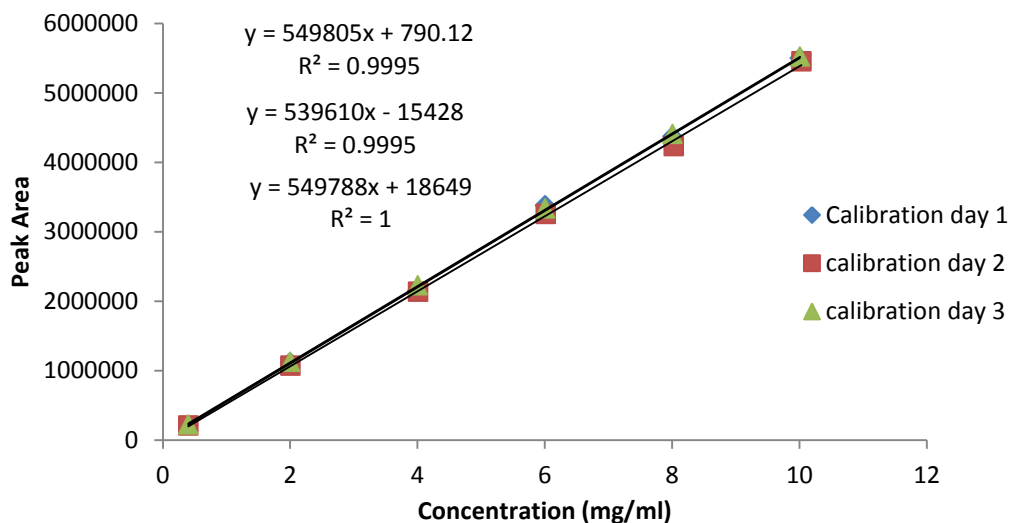


Figure 9: Calibration curves for gabapentin (Method Validation). Calibration was performed as per ICH Q2A guidelines on three separate days. The equations represent the linear correlation between the peak area for gabapentin and its concentration on the three days of calibration.

Table 5: Linearity of calibration curves for lactam. Calibration was performed as per ICH Q2A guidelines on three separate days. Slope, intercept and the correlation coefficient for the peak area and concentration plot have been reported.

Linearity Data of Calibration Curves for Lactam					
Standard Curve	Analytical Range (mg/ml)	Calibrators	Slope	y-intercept	R ² Value
Validation Day 1	8-240	6	10382	-326.55	0.9999
Validation Day 2	8-240	6	10392	579.55	0.9999
Validation Day 3	8-240	6	10577	1016.3	0.9999

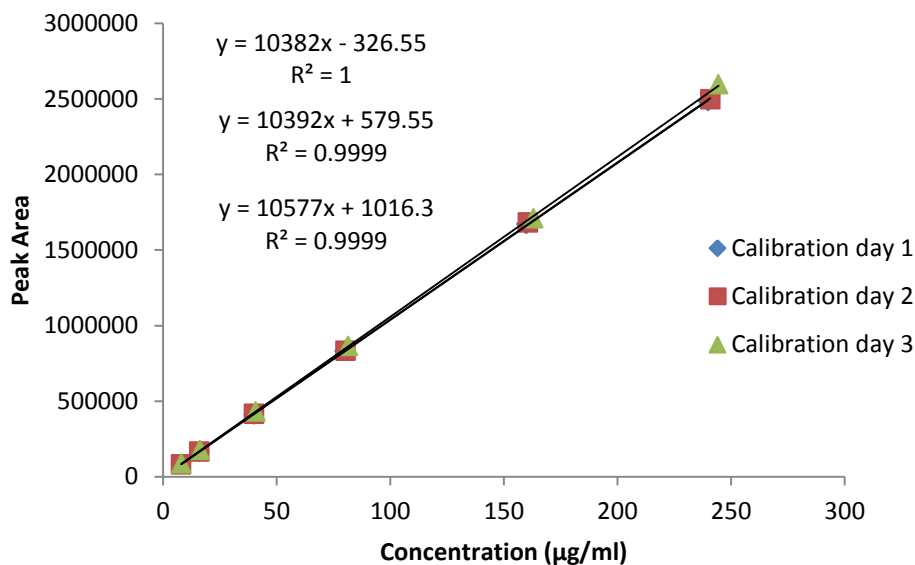


Figure 10: Calibration curves for lactam (Method Validation). Calibration was performed as per ICH Q2A guidelines on three separate days. The equations represent linear correlation between the peak area for gabapentin and its concentration on the three days of calibration.

Accuracy and Precision

The results for the accuracy and precision of analytical quality control samples are summarized in Table 6 and Table 7 for gabapentin and in Table 8 and Table 9 for lactam. Method accuracy was recorded to be greater than 97% at all concentration levels on all three days for gabapentin. Method accuracy was also seen to be greater than 98% at all concentration levels on all three days for lactam. Method precision (n = 3), represented as %RSD was seen to be lower than 2.5% for both gabapentin and lactam. Inter-day and intra-day precisions were recorded to be lower than 2% RSD as well.

Table 6: Determination of accuracy for the analytical method using gabapentin. The method accuracy was determined at three separate concentration levels on three separate days.

Gabapentin Accuracy: Drug Substance (% Recovery n = 3)			
Solution Concentration			
	0.4 mg/ml	4 mg/ml	10 mg/ml
Validation Set 1	98.48	97.46	98.11
Validation Set 2	100.27	97.79	100.09
Validation Set 3	99.41	100.29	101.82

Table 7: Determination of precision for the analytical method using gabapentin. Method precision was determined at three separate concentration levels on three separate days.

Gabapentin Precision: Drug Substance (%RSD n = 3)			
Solution Concentration			
	0.4 mg/ml	4 mg/ml	10 mg/ml
Validation Set 1	0.39	1.29	1.68
Validation Set 2	0.26	0.07	1.64
Validation Set 3	2.2	0.15	0.51
Inter-day	0.9	1.57	1.85

Table 8: Determination of accuracy for the analytical method using lactam. Method accuracy was determined at three separate concentration levels on three separate days.

Lactam Accuracy: Drug Substance (% Recovery n = 3)			
Solution Concentration			
	8 µg/ml	40 µg/ml	160 µg/ml
Validation Set 1	99.02	99.31	99.95
Validation Set 2	99.05	100.05	99.74
Validation Set 3	101.63	99.36	98.23

Table 9: Determination of precision for the analytical method using lactam. Method precision was determined at three separate concentration levels on three separate days.

Lactam Precision: Drug Substance (%RSD n = 3)			
Solution Concentration			
	8 µg/ml	40 µg/ml	160 µg/ml
Validation Set 1	0.57	0.44	0.3
Validation Set 2	0.56	0.25	0.12
Validation Set 3	2.22	0.22	0.98
Inter-day	1.49	0.41	0.94

Limit of Detection and Limit of Quantitation

The limit of detection and the limit of quantitation for gabapentin were 57 µg and 174 µg, respectively, while the limit of detection and the limit of quantitation for lactam were 0.15 µg and 0.47 µg, respectively. Greater sensitivity for the detection of lactam relative to gabapentin is due to its higher ultraviolet absorptivity, which is known to be almost one order magnitude greater than that for gabapentin.

2.3.2. Method Optimization

Effect of Filter Membrane

The propensity of gabapentin and lactam to adsorb on the surface of the filter membrane used in the stability studies was tested. The results of the study are reported in Table 10. The results suggested complete recovery (100% ±3% w/w) of both gabapentin and lactam at high as well as low concentrations, for both the filtrates. The recovery for gabapentin at low concentration (0.5 mg/ml) was 99.46% for the first filtrate and 97.93% for the second filtrate. At a higher concentration (5 mg/ml) the recovery of gabapentin was 100.15% and 100.46% for the two filtrates tested. In the case of lactam, the recovery at a low concentration (8 µg/ml) was 103.6% and 103.3% for the two filtrates, and at a higher concentration (240 µg/ml) the recovery was 99.4% and 100.1% for the two filtrates. Precision (%RSD, n = 3) for the recovery of gabapentin and lactam post-filtration was seen to be below 2%.

Table 10: The effect of the filter membrane on the recovery of gabapentin and lactam. The recovery was analyzed for solutions of gabapentin and lactam at two different concentrations, passed through the filter twice.

Recovery of Compounds Post Filtration Using Syringe Filter (Nylon, 0.45 μm)			
Compound	Concentration / Filtrate	%Recovery (n = 3)	%RSD (n = 3)
Gabapentin	Low 0.5 mg/ml / F1	99.46	0.92
	Low 0.5 mg/ml / F2	97.93	1.14
	High 5 mg/ml / F1	100.15	0.22
	High 5 mg/ml / F2	100.46	0.21
Compound	Concentration / Filtrate	%Recovery (n = 2)	%RSD (n = 2)
Lactam	Low 8 $\mu\text{g/ml}$ / F1	103.3	0.23
	Low 8 $\mu\text{g/ml}$ / F2	103.66	1.7
	High 240 $\mu\text{g/ml}$ / F1	99.4	0.26
	High 240 $\mu\text{g/ml}$ / F2	100.18	0.06

* F1 = First Filtrate, F2 = second Filtrate

Effect of Excipients

The results for the recovery of gabapentin and lactam in the presence of excipients are reported in Table 11. The recovery was seen to be greater than 97% for both gabapentin and lactam in the presence of most excipients. The precision (%RSD, n = 2) for the recovery was seen to be less than 3%.

Table 11: Results for the recovery of gabapentin and lactam in the presence of excipients. Physical mixtures of gabapentin and lactam with the excipients were analyzed to determine the effect of excipients on the extraction of either gabapentin or lactam in solution.

Recovery of Compounds in the Presence of Excipients			
Compound	Excipients	%Recovery (n = 2)	%RSD (n = 2)
Gabapentin	Emcompress®	98.62	0.57
	talc	97.99	0.6
	HPMC	97.73	0.09
	starch	97.54	2.23
Lactam	Emcompress®	99.22	0.88
	talc	98.56	0.11
	HPMC	105.24	1.02
	starch	97.67	2.47

2.3.3. Stability of Gabapentin and Lactam

Lactam was found to be stable in an aqueous medium and under ambient temperature (22°C) and humidity (30% RH) conditions for 24 h. Complete recovery (100% w/w) was observed for lactam, while greater than 99% w/w recovery was observed for gabapentin. A small peak for lactam (2 µg/ml) was seen eluting post 24 h from the gabapentin solution (10 mg/ml) (Figure 11). The degradation rate of gabapentin to lactam in solution was analyzed to be as low as 0.0008% mole/h. The total time gabapentin would be maintained in its solution state before analysis was controlled to be less than 2 h. The preparation of samples prior to analysis confirmed minimal (<0.0016% mole) lactam formation in the gabapentin solution at the time of analysis.

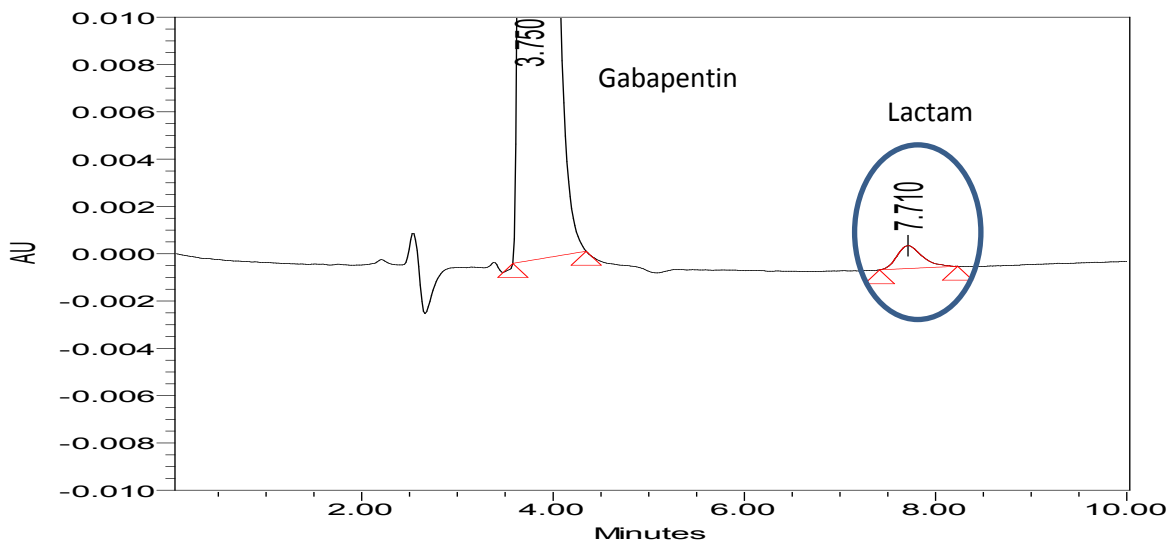


Figure 11: Chromatogram depicting the stability of gabapentin in the solution. A small peak of lactam is seen eluting from the gabapentin sample stored for 24 h in dark under ambient temperature and humidity conditions. The degradation rate for gabapentin in solution was calculated to be <0.0008% mol/h.

2.4. Conclusion

The gabapentin (bulk) procured for the dissertation work was determined to be of purity comparable to its reference standard. The HPLC method was successfully validated for accuracy, precision, linearity, specificity, LOD and LOQ for gabapentin and lactam as per ICH Q2A guidelines.

The method demonstrated specificity for gabapentin and lactam in the presence of excipients, mobile phase medium, and water. The filters and the excipients in the study did not affect the recovery of either gabapentin or lactam. Lactam was found to be stable in the solution medium and mobile phase throughout the study duration. On the other hand, gabapentin was found to convert at a very low rate in the solution under controlled pH conditions.

The method was therefore, considered suitable for the assessment of the solid-state stability of gabapentin and for quantifying its degradation product, lactam, in the presence of excipients.

Chapter 3

Investigating the Effect of Excipients on the Solid-State Degradation of Gabapentin

3.1. Introduction

As discussed in chapter 1, the degradation of drug molecules is accelerated by the presence of excipients. This effect is either due to the chemical interactions between excipients and drug molecules or due to the physical properties of the excipients.²

Commercially available solid dosage forms of gabapentin include film-coated tablets and hard-shelled capsules. Formulating a strong and non-friable solid dosage form of gabapentin requires the addition of excipients to improve its poor compressibility and poor flow properties. Typical excipients used in gabapentin formulations include tablet diluents such as dibasic calcium phosphate, binders such as HPC and corn starch, film coating polymers such as HPMC, flow enhancers such as talc and lubricants such as magnesium stearate.

An important aspect of this research is to provide evidence for the accelerating effect of excipients on the solid-state degradation of unprocessed gabapentin. The identification of excipient properties that contribute to this effect will be explored in the next chapter.

3.2. Materials and Methods

3.2.1. Materials

The model drug gabapentin (Hangzhou Starshine Pharmaceutical Co. Ltd., Hangzhou, China, Batch 0803023) was procured for the stability studies. The excipients to be used in the stability studies were selected based on commercially used excipients in gabapentin formulations and other commonly used tableting excipients. The excipients selected include calcium phosphate dibasic dihydrate (Emcompress[®], E. Mendell. Co. Inc, New York), monobasic calcium phosphate anhydrous (Mono-Tab, V-90 grade, Innophos, New Jersey), dibasic calcium phosphate anhydrous (A-Tab[®], Innophos, New Jersey), tribasic calcium phosphate anhydrous (Tri-Tab[®], Innophos, New Jersey), modified corn starch (Uni-pure[™] DW, National Starch LLC, New Jersey), hydroxypropyl cellulose (HPC, Klucel EF[®], Ashland Aqualon Functional Ingredients., Delaware), hydroxypropyl methyl cellulose (HPMC, Methocel[™] E50 Prem LV, The Dow Chemical Co., Michigan) and talcum (Talc, Fisher Scientific, Massachusetts). All other reagents and solvents procured for analytical quantitation were of HPLC grade.

3.2.2 Material Pretreatment

Specific sieve fractions of the drug and the excipients were obtained by sieve classification using a set of standard sieves (Gilson Company, Inc.) and a sieve shaker (Performer III Model SS-3, Gilson Company, Inc.). The fractions retained on the sieves were weighed at intervals ranging from 20-25 min, until the measured weight change between sieving was less than 0.5% w/w. Specific particle size fraction between 125-250 μm was used for gabapentin and excipients (such as Emcompress[®], Modified corn starch, HPC and HPMC). However, a different particle size fraction (75-125 μm) of the phosphate salts, (such as Tri-Tab[®], A-Tab[®] and monobasic calcium

phosphate (Mono-Tab) was used, due to the limited quantity of the larger particle size fraction ($\geq 125 \mu\text{m}$) for Mono-Tab on sieving. Talc was used as supplied in all experimentation, due to its smaller particle size (100% $< 75 \mu\text{m}$), which precluded classification by sieving.

Gabapentin, due to its reportedly poor stability under low humidity conditions, was equilibrated under controlled conditions of temperature ($20^\circ\text{C} \pm 2^\circ\text{C}$) and humidity (33% RH, magnesium chloride) for one week prior to the study.⁵ However, to prevent any confounding effects of moisture from the excipients, they were equilibrated under controlled conditions of high temperature (50°C) and low humidity (5% RH, Drierite[®]) for at least one week prior to the study.

3.2.3. Determination of Moisture Content

The moisture content (% w/w) of the excipients was determined using thermogravimetric analysis (TGA Q-500, TA Instruments, Delaware). The materials (25-50 mg) were heated from ambient temperatures ($25\text{-}30^\circ\text{C}$) to 110°C and maintained isothermally until the observed change in the sample weight was less than 0.2% w/w per minute. Average value and standard deviation of two replicate measurements is reported.

3.2.4. Physical Mixture Preparation and Study Conditions

To understand the effect of excipients on gabapentin's stability profile, binary mixtures ($n = 3$) of gabapentin and excipients, namely, Emcompress[®], A-Tab[®], Tri-Tab[®], HPMC, HPC, starch, Mono-Tab, and talc were prepared in a 1:1 proportion by weight. Binary mixtures were prepared manually using the geometric dilution technique with the help of a spatula.

All of the physical mixtures were observed under an optical microscope (Model BX-51, Olympus, Pennsylvania) to determine the role of excipient morphology, and size of the excipient particle on their distribution around gabapentin particles. Samples (n = 4) from different areas of the physical mixture were collected and observed under low magnification (4x). Morphology of the individual components was observed under higher (10x) magnification using the microscope.

To understand the effect of the mixing procedure on gabapentin's degradation, gabapentin samples (n = 3), controlled for their particle size (125-250 μm) were analyzed for lactam formation, with and without application of the mixing procedure (manual mixing in a geometric proportion using a stainless steel spatula).

Previous research has indicated the stabilizing effect of environmental moisture on gabapentin's degradation profile. The possibility of a similar stabilizing effect due to excipient moisture content cannot be refuted. Even though the excipients used in the study had low moisture content (<3% w/w), ascertaining a negligible impact of the excipient moisture content on the degradation of gabapentin was important. The study to determine the effect of excipient moisture was performed using Mono-Tab, which inherently possessed low moisture content (0.01% w/w). Mono-Tab was mixed with water to account for a total of 1% moisture. Physical mixtures of gabapentin and Mono-Tab with variable moisture content (0.01% w/w and 1% w/w) were prepared, stored under accelerated conditions of temperature and humidity (50°C, 5% RH) and analyzed using the HPLC technique. The effect of excipient moisture on the kinetics degradation kinetics of gabapentin was further studied using HPMC equilibrated under different relative

humidity conditions (33% RH, 85% RH). The moisture content of the HPMC samples prior to physical mixing was recorded using thermo-gravimetric analysis (TGA).

All of the degradation studies were performed in scintillation vials (20 ml) under accelerated conditions of temperature (50°C) and humidity (5% RH) for the entire duration (697 h) of the study. Samples (n = 3) were withdrawn periodically for quantitation of gabapentin and its degradation product lactam. Deionized and filtered (0.45 µm) water was used to prepare the sample solutions. The sample solutions were filtered using a 0.45 µm nylon syringe filter prior to the HPLC analysis. Data is reported as mean lactam concentration (% mole) over time (h) and error bars represent the confidence interval (95%) for three replicates at every time point.

The existing kinetic model¹ (Figure 4, pg. 13) for solid-state degradation of gabapentin was used to understand the effect of excipients on gabapentin's degradation profile.¹ The Runge - Kutta 4th order numerical approximation method was used to solve the series of differential equations defining the kinetic model using Excel[®] (2010, Microsoft[®], Redmond, Washington).¹ Matlab[®] (R-2013, MathWorks[®], Natick, Massachusetts), with its ode45 function handle (based on the Runge-Kutta algorithm), was used to validate the results of the numerical approximations calculated on Microsoft Excel[®].

The parameters of the differential equations (Equation 1-3, pg. 13), especially rate constants k_1 (autocatalytic branching), k_2 (spontaneous dehydration), k_3 (branching termination), and gaba_0^* (initial concentration of reactive gabapentin molecules) were optimized using the least square approach by the Solver function (Excel Solver[®], Microsoft Office[®] 2010). A generalized reduced

gradient (GRG) method based on the Levenberg-Marquardt algorithm with a forward derivative was selected, a convergence criterion was set at 10^{-10} , and a maximum of 1000 iterations were allowed when parameterizing the model. Constraints were established in order to obtain physically meaningful parameter estimates. One major constraint applied did not allow the values of k_1 and k_3 to be lower than 10^{-8} in order to prevent the estimation of zero valued parameters.

A common issue encountered when optimizing parameters using non-linear regression is ensuring that the solution obtained is not a local minimum. To confirm that a global solution was reached, a central composite design of experiments (CCD) (Table 12) was used to generate a systematic combination of initial values over a broad range. The range for input values was established based on the reported literature parameter estimates ($k_1 = 7.10 \times 10^{-5}$, $k_2 = 0.020$, and $k_3 = 3.60 \times 10^{-5}$) under similar experimental conditions (50°C, 5% RH).¹ A total of 25 different combinations of input values were used during the optimization process. Input values for the parameters k_1 and k_3 were varied in the range 0.000001 - $0.0001 \text{ mol}^{-1}\text{h}^{-1}$, while the value of k_2 was varied between 0.1 - 0.00001 h^{-1} , and the value of gaba_0^* were varied between 0.1 - 5% mole respectively.

Table 12: Application of a central composite design (CCD) approach to generate different systematic combinations of input parameter values. Range for the parameter values is selected based on previously published estimates.

CCD Input Values for Parameter Optimization				k ₁ ,k ₃	Range
k ₁ (mol ⁻¹ h ⁻¹)	k ₂ (h ⁻¹)	k ₃ (mol ⁻¹ h ⁻¹)	gaba ₀ * (% mole)	High	1x10 ⁻⁴
1x10 ⁻⁶	1x10 ⁻⁶	1x10 ⁻⁶	0.1	Low	1x10 ⁻⁶
1x10 ⁻⁶	1x10 ⁻⁶	1x10 ⁻⁶	5	Medium	5x10 ⁻⁵
1x10 ⁻⁶	1x10 ⁻⁶	1x10 ⁻⁴	0.1		
1x10 ⁻⁶	1x10 ⁻⁶	1x10 ⁻⁴	5	k ₂	Range
1x10 ⁻⁶	0.1	1x10 ⁻⁶	0.1	High	0.1
1x10 ⁻⁶	0.1	1x10 ⁻⁶	5	Low	1x10 ⁻⁶
1x10 ⁻⁶	0.1	1x10 ⁻⁴	0.1	Medium	0.05
1x10 ⁻⁶	0.1	1x10 ⁻⁴	5		
1x10 ⁻⁴	1x10 ⁻⁶	1x10 ⁻⁶	0.1	gaba ₀ *	Range
1x10 ⁻⁴	1x10 ⁻⁶	1x10 ⁻⁶	5	High	5
1x10 ⁻⁴	1x10 ⁻⁶	1x10 ⁻⁴	0.1	Low	0.1
1x10 ⁻⁴	1x10 ⁻⁶	1x10 ⁻⁴	5	Medium	2.55
1x10 ⁻⁴	0.1	1x10 ⁻⁶	0.1		
1x10 ⁻⁴	0.1	1x10 ⁻⁶	5		
1x10 ⁻⁴	0.1	1x10 ⁻⁴	0.1		
1x10 ⁻⁴	0.1	1x10 ⁻⁴	5		
1x10 ⁻⁶	0.05	5x10 ⁻⁵	2.55		
1x10 ⁻⁴	0.05	5x10 ⁻⁵	2.55		
5x10 ⁻⁵	1x10 ⁻⁶	5x10 ⁻⁵	2.55		
5x10 ⁻⁵	0.1	5x10 ⁻⁵	2.55		
5x10 ⁻⁵	0.05	1x10 ⁻⁶	2.55		
5x10 ⁻⁵	0.05	1x10 ⁻⁴	2.55		
5x10 ⁻⁵	0.05	5x10 ⁻⁵	0.1		
5x10 ⁻⁵	0.05	5x10 ⁻⁵	5		
5x10 ⁻⁵	0.05	5x10 ⁻⁵	2.55		

Uncertainty (standard error) for the estimated parameters was calculated using a macro (Solveraid[®], Robert De Levie, Washington DC) on Excel[®] (2010, Microsoft[®]), with the code written in visual basic developer (VBA).⁸⁸ Parameter uncertainties were calculated based on the partial differentials and matrix inversion method.⁸⁸ The approach for uncertainty estimation is

based on an assumption that the uncertainties in data pairs (x , y_{exp}) are found in the dependent variable (y_{exp}) and that the uncertainties follow a Gaussian distribution.⁸⁸ Uncertainties in parameter estimates were calculated using Equation 22 through Equation 24. In the equations below, N is the number of data pairs, P is the number of estimated parameters, and m_{ii}^{-1} denotes the i^{th} diagonal term of the inverse of a $P \times P$ matrix, the partial differentials of the fitting function $\frac{dF_n}{da_i}$, where, $F_n = y_{calc}$ and a is denoting the parameter to be estimated.

$$\sigma_i = \sqrt{\frac{m_{ii}^{-1} \times (y_{exp} - y_{calc})^2}{N - P}} \quad \text{Equation 22}$$

$$m_{ij} = \sum_{n=1}^N \frac{dF_n}{da_i} \times \frac{dF_n}{da_j} \quad \text{Equation 23}$$

$$\frac{dF_n}{da_i} = \lim_{\Delta a_i \rightarrow 0} \frac{dF_n}{da_i} = \frac{F_n(x_n a_i(1+\delta), d_{j \neq i}) - F_n(x_n a_i, d_{j \neq i})}{a_i(1+\delta) - a_i}, \delta \ll 1 \quad \text{Equation 24}$$

3.3. Results and Discussion

The moisture content (% w/w) of the excipients equilibrated under low humidity (5% RH) conditions is reported in Table 13. The moisture content of the excipients was recorded to be less than 1% w/w in most cases except starch, which had a moisture content value of $2.69 \pm 0.28\%$ w/w and HPC with a moisture content value of $1.97 \pm 0.38\%$ w/w. The relatively higher moisture content of the two excipients is due to their inherently high water absorption capacities.

Table 13: Mean moisture content (\pm Standard Deviation) of the excipients before physical mixing.

No.	Excipient	Moisture Content (% w/w) (n = 2)
1	Mono-Tab	0.01 \pm 0.0007
2	talc	0.04 \pm 0.0007
3	Emcompress [®]	0.22 \pm 0.0141
4	A-Tab [®]	0.25 \pm 0.0353
5	HPMC	0.44 \pm 0.2899
6	Tri-Tab [®]	0.95 \pm 0.1272
7	HPC	1.97 \pm 0.3818
8	starch	2.69 \pm 0.2828

Optical images of the physical mixtures helped identify the effect of excipient particle size on the distribution of excipient particles around the gabapentin particles. Images of the single component particles (13A-20A) helped in their identification in the binary mixture. Optical images for the physical mixtures of gabapentin and the excipients controlled for their particle size (125-250 μ m) are visualized in Figures 13B-16B. In the case of physical mixtures of gabapentin with excipients of smaller particle size (75-125 μ m) (Figure 18B-20B), a greater number of excipient particles relative to gabapentin particles were observed. This observation indicated, greater number of contact points between gabapentin and the excipient relative to the contact points between gabapentin and larger sized excipient particles. In the case of talc particles (Figure 17B) with the lowest particle size (<3 μ m) amongst the excipients, the adherence of fine talc particles on the surface of gabapentin was seen, indicating a likelihood of greater surface contact between the two components. These observations suggested a need to

account for the particle size of gabapentin and the excipients when understanding the effect of the excipients on the degradation of gabapentin.

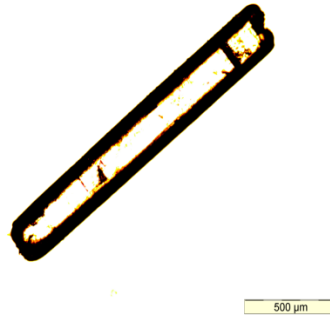


Figure 12: Image representing the morphology of a gabapentin particle under 10x magnification.

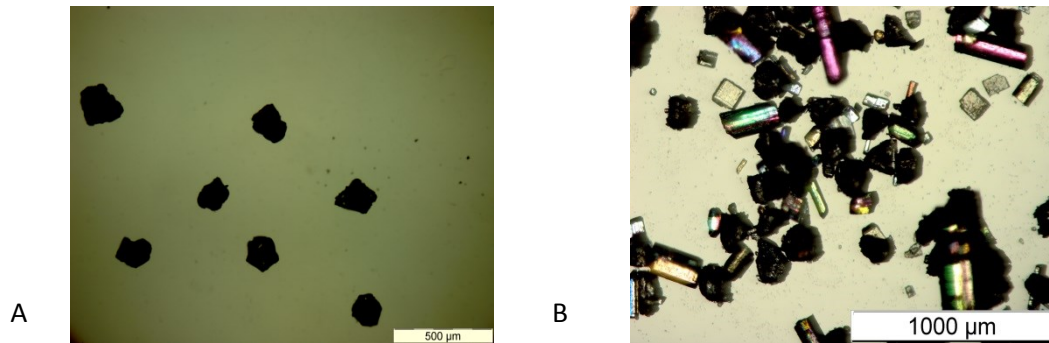


Figure 13: Images representing the morphology of A. starch particles under 10x magnification, and B. the physical mixture of gabapentin and starch particles under 4x magnification.

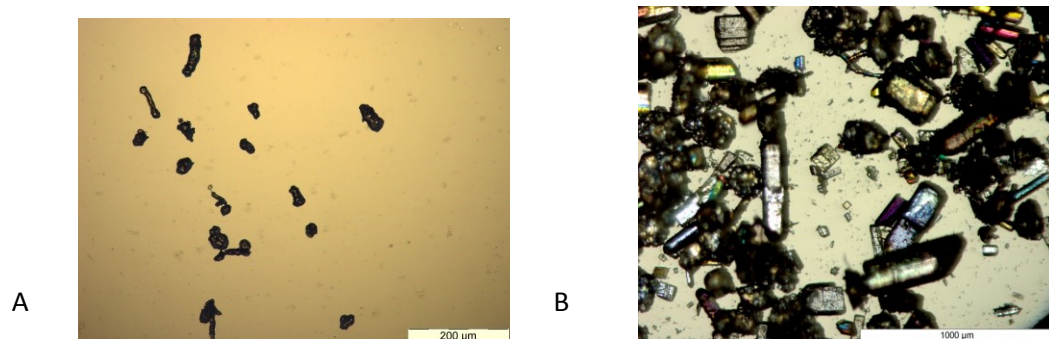


Figure 14: Images representing the morphology of A. HPMC particles under 10x magnification, and B. the physical mixture of gabapentin and HPMC particles under 4x magnification.

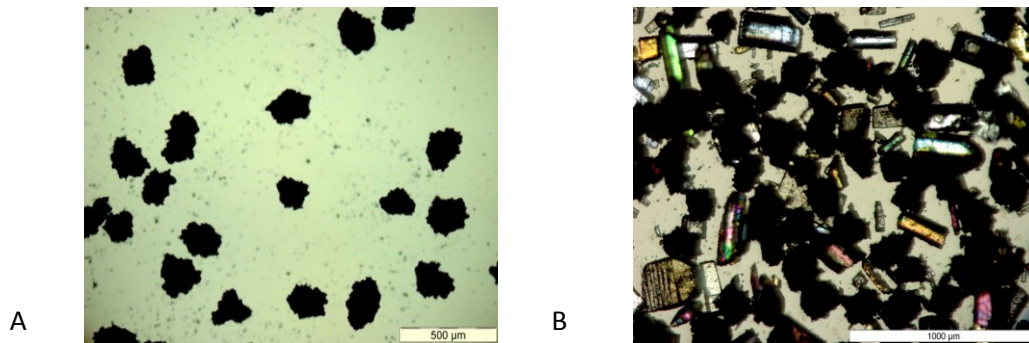


Figure 15: Images representing the morphology of A. Emcompress[®] particles under 10x magnification, and B. the physical mixture of gabapentin and Emcompress[®] particles under 4x magnification.

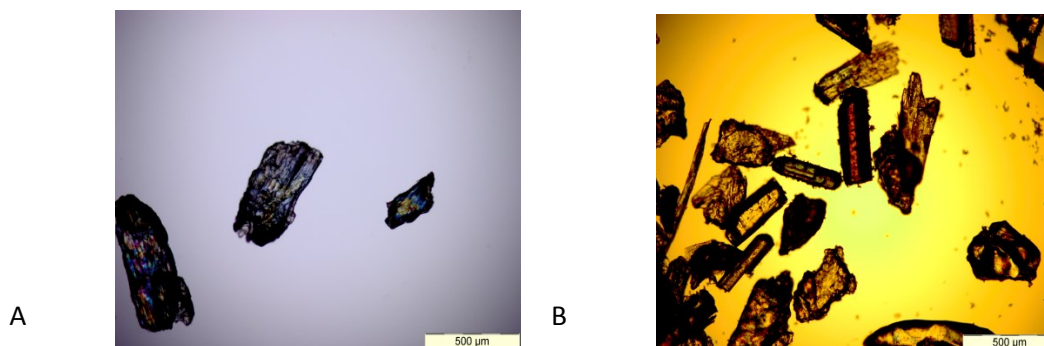


Figure 16: Images representing the morphology of A. HPC particles under 4x magnification, and B. the physical mixture of gabapentin and HPC particles under 4x magnification.

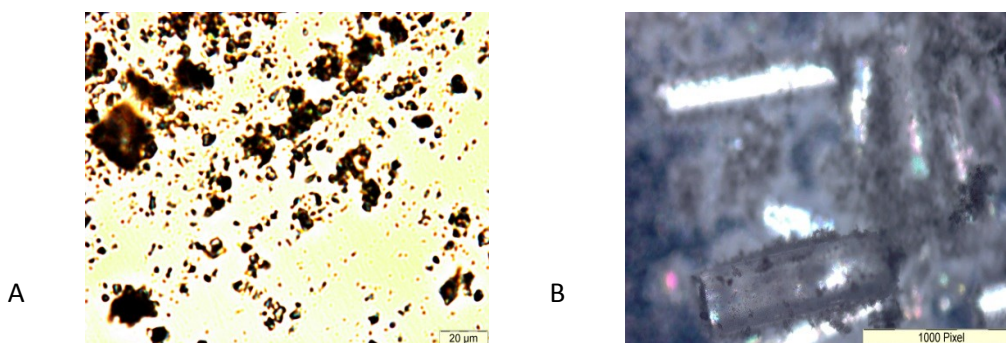


Figure 17: Images representing the morphology of A. talc particles under 500x magnification, and B. the physical mixture of gabapentin and talc particles under 4x magnification. The adherence of fine talc particles on the surface of rectangular gabapentin particles is observed.

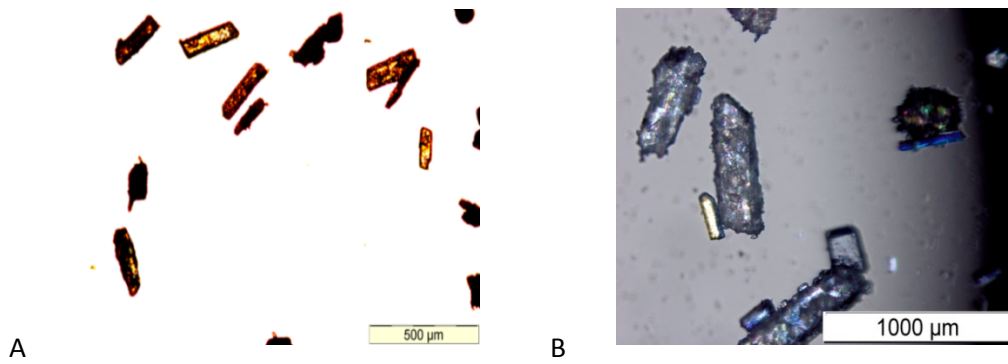


Figure 18: Images representing the morphology of Mono-Tab particles under 10x magnification, and B. the physical mixture of gabapentin and Mono-Tab particles under 4x magnification.

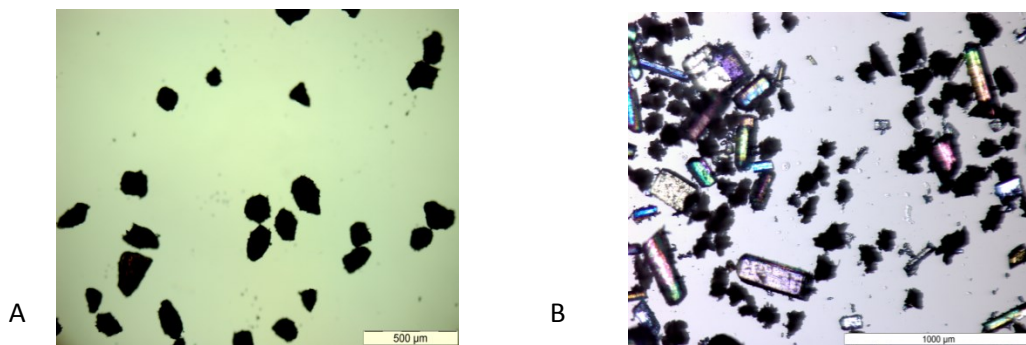


Figure 19: Images representing the morphology of A-Tab[®] particles under 10x magnification, and B. the physical mixture of gabapentin and A-Tab[®] particles under 4x magnification.

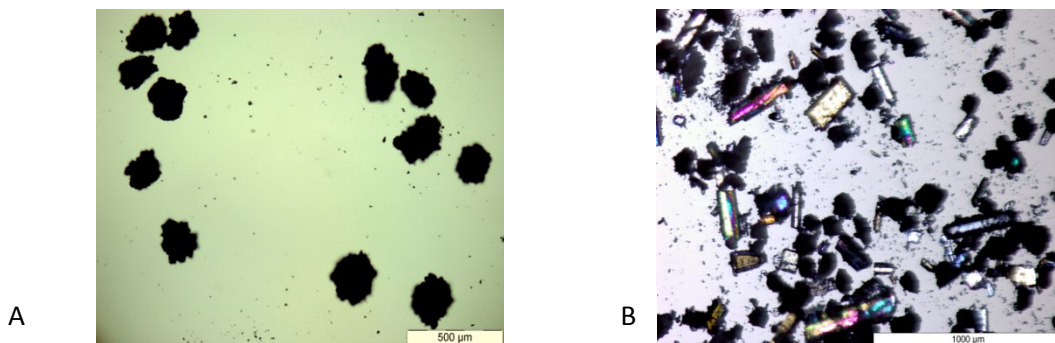


Figure 20: Images representing the morphology of Tri-Tab[®] particles under 10x magnification, and B. the physical mixture of gabapentin and Tri-Tab[®] particles under 4x magnifications.

The results of the study to test the effect of excipients on gabapentin's degradation strongly suggested a role of the excipients on solid-state degradation of gabapentin, as seen in Figures 21 and 22. A significant (95% confidence interval, $n = 3$) increase in lactam formation over the entire study duration can be seen in the physical mixtures of gabapentin with each of the excipients relative to lactam formation in their absence. Two different shapes for the lactam formation profile were observed, which varied with the type of excipient used. Amongst the physical mixtures, the gabapentin-Tri-Tab[®] mixture demonstrated the highest lactam formation at 697 h, followed in relative order by the mixtures of gabapentin with A-Tab[®], starch, Mono-Tab, Emcompress[®], Talc, HPC, and HPMC. However, it is important to note the shape of each degradation profile. It can be seen in Figure 21, that binary mixtures of gabapentin with excipients Tri-Tab[®], A-Tab[®], Emcompress[®], talc, HPMC, and HPC have a similar degradation profile. In these profiles, a significant increase in the initial rate of lactam formation (<192 h) is observed relative to the degradation profile for gabapentin. However, no distinct rise in lactam concentration over time, representative of the branching/ termination phase was seen. The other profile for lactam formation is shown in Figure 22, observed for gabapentin and the physical mixtures of gabapentin with Mono-Tab and starch. These lactam formation profiles demonstrated a lower initial rate of lactam formation relative to other excipients in the study. However, a distinct branching phase is seen in their degradation profiles.

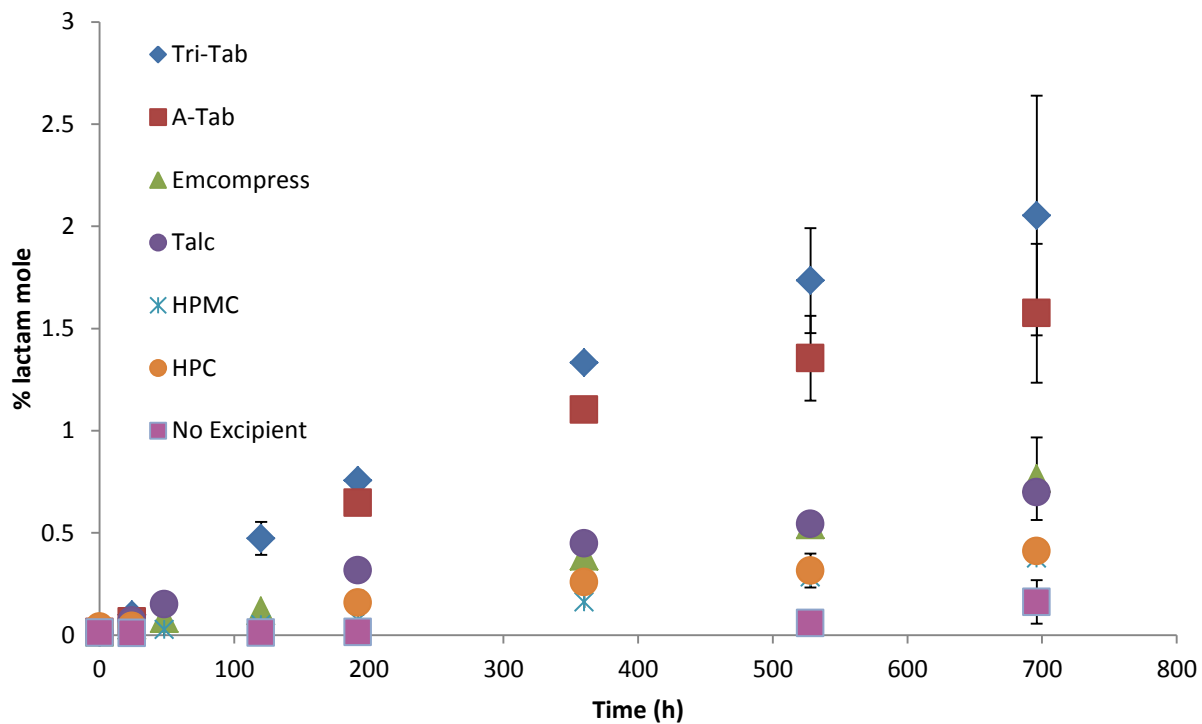


Figure 21: Effect of the excipients on the solid-state degradation of gabapentin I. Mean lactam formation (% mole) across time (h) for gabapentin excipient physical mixtures. Degradation profiles represent significant (95% C.I., n = 3) an accelerated lactam formation in the presence of excipients relative to gabapentin. Curves represent accelerated initial rate of lactam formation (<192 h) but the absence of a distinct branching phase in the degradation kinetics.

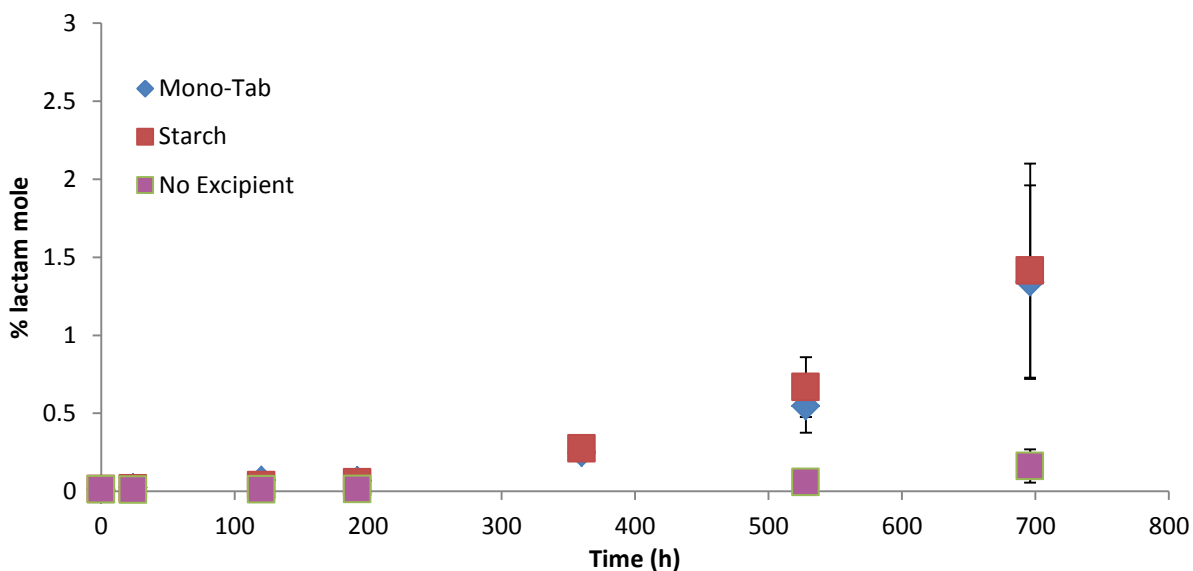


Figure 22: Effect of the excipients on the solid-state degradation of gabapentin II. Mean lactam formation (% mole) across time (h) for the gabapentin excipient physical mixtures. Degradation profiles represent significant (95% C.I., n = 3) accelerated lactam formation in the presence of excipients relative to gabapentin. The excipients did not affect the initial rate of lactam (<192 h) formation as much as the other excipients in Figure 21. The degradation profile clearly showed a distinct branching phase (>200 h) in the degradation kinetics.

To attribute the observed accelerated lactam formation solely to the presence of the excipients, it was important to negate the role of the mixing procedure on gabapentin's degradation. This experiment was performed to see if the mechanical shear experienced by gabapentin was not a major contributor to the accelerated lactam formation. The results as seen in Figure 23, demonstrate no significant (95% confidence interval, n = 3) change in the rate of lactam formation across all time points for the gabapentin samples on application of the mixing procedure.

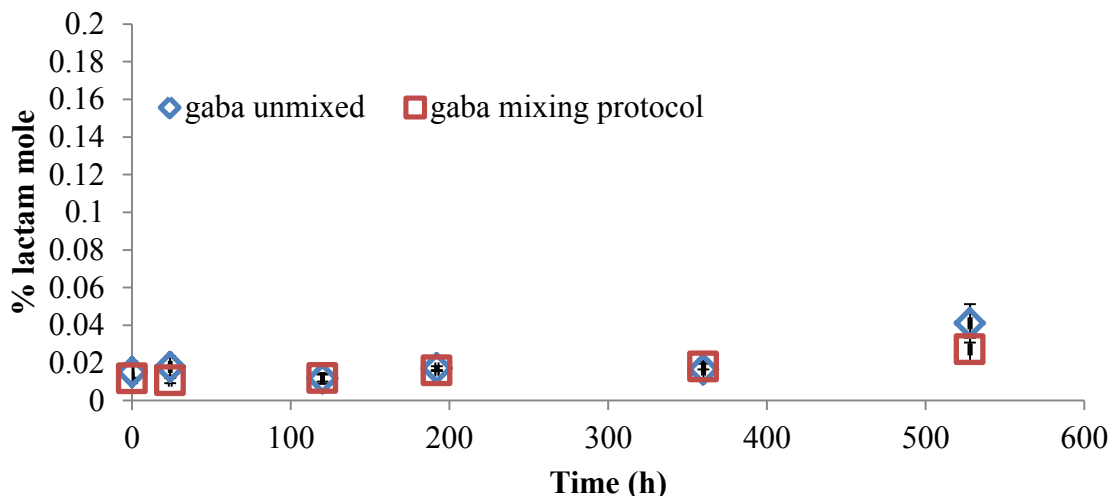


Figure 23: Effect of the mixing procedure on the solid-state degradation of gabapentin. The mean lactam concentration (% mole, n = 3) over time (h) for samples of unprocessed gabapentin in the presence and absence of simple mixing protocol. The error bars represent a 95% confidence interval. No significant difference between lactam formation across all time points is observed on the application of the mixing procedure.

Another factor that needed investigation, before attributing the observed accelerated lactam formation to the presence of the excipients, was the moisture content of the excipient. The results as seen in Figure 24, demonstrate no significant difference (95% confidence interval, n = 3) in lactam formation until 697 h for the physical mixtures of gabapentin and Mono-Tab with variable moisture content (0.01% w/w and 1% w/w). A moisture content of 1% w/w in the case of Mono-Tab was selected to match the moisture content (0.95% w/w) of Tri-Tab[®] since Tri-Tab[®] was the inorganic excipient demonstrating the highest effect amongst the excipients on the rate of lactam formation. The moisture-induced stabilization of gabapentin molecules was not observed in the case of the mixtures of gabapentin with Mono-Tab since the physical mixture with the higher moisture content showed greater lactam formation. However, to confirm absence of an accelerating effect on lactam formation as seen at 697h in Figure 24, further investigation (collection of stability data points between 296-697 h) will have to be performed in case of Mono-Tab.

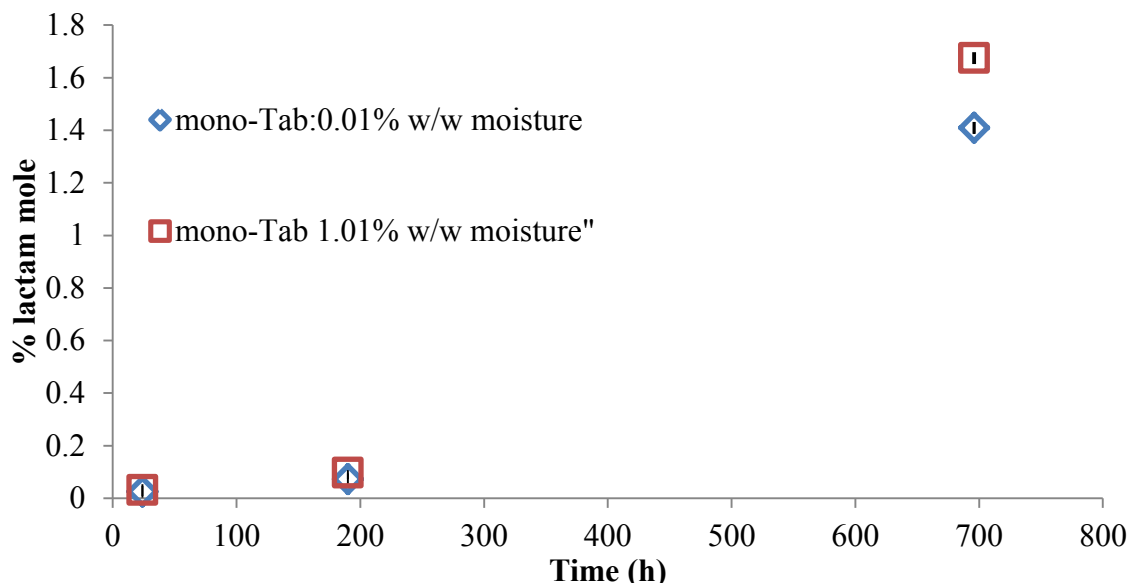


Figure 24: Effect of varying moisture content in Mono-Tab on the solid-state degradation of gabapentin. The mean lactam concentration (% mole, n = 3) over time (h) for samples of the gabapentin-Mono-Tab physical mixtures with variable moisture content. The error bars represent a 95% confidence interval.

In the second study with HPMC, despite variable moisture content (6.66% w/w and 2.21% w/w) in the HPMC samples, no significant (95% confidence interval, n = 3) difference between the degradation profiles of gabapentin and HPMC with variable moisture content was observed (Figure 25). This finding negated the role of excipient moisture in accelerating the degradation kinetics, which was thought to be a possibility in the case of the gabapentin-Mono-Tab physical mixtures as discussed above.

The results from the above studies confirmed the absence of a stabilizing effect of excipient moisture on the degradation kinetics of gabapentin, especially in case of HPMC and Mono-Tab. Based on the above results, the likelihood of excipient moisture content affecting the degradation kinetics of unprocessed gabapentin seems less likely.

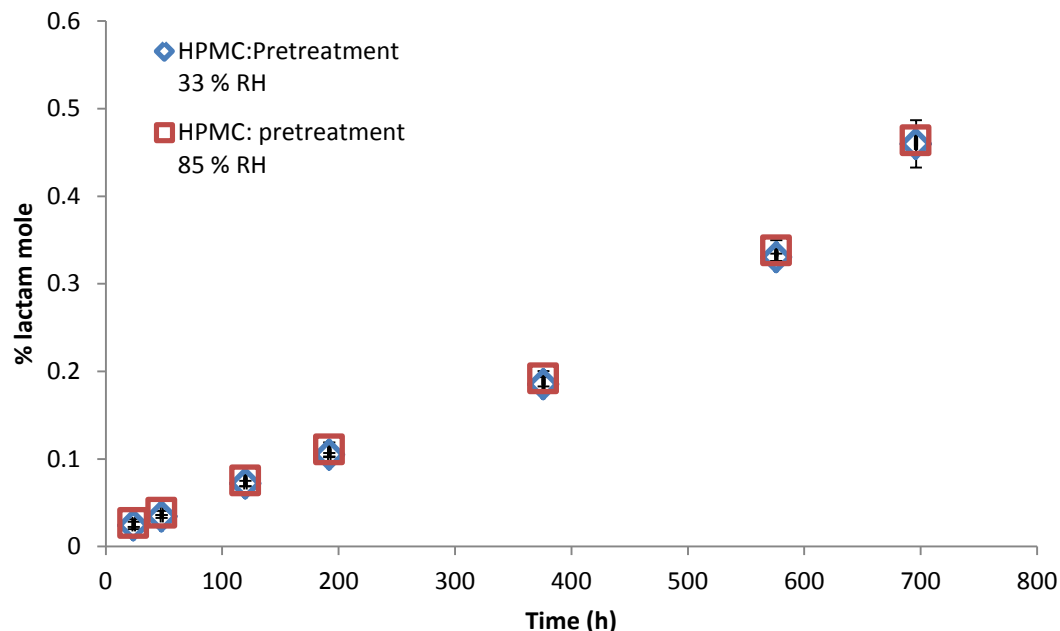


Figure 25: The effect of varying moisture content in HPMC on the solid-state degradation of gabapentin. The mean lactam concentration (% mole, n = 3) over time (h) for samples of the gabapentin-HPMC physical mixtures. HPMC, possessed variable moisture content of 6.66% w/w at 85% RH and 2.21% w/w at 33% RH. The error bars represent a 95% confidence interval.

Application of the Kinetic Model to the Observed Lactam Profiles

To apply the existing kinetic model to the data and estimate rate constants, the first step involved development of an Excel[®] worksheet to solve the series of differential equations using the Runge-Kutta approximation. The Excel[®] worksheet developed was successfully validated using the ode45 function handle on MATLAB[®]. A comparison of the observed data with the predicted degradation profile approximated by the MATLAB[®] routine and the Excel[®] spreadsheet can be seen in Figure 26.

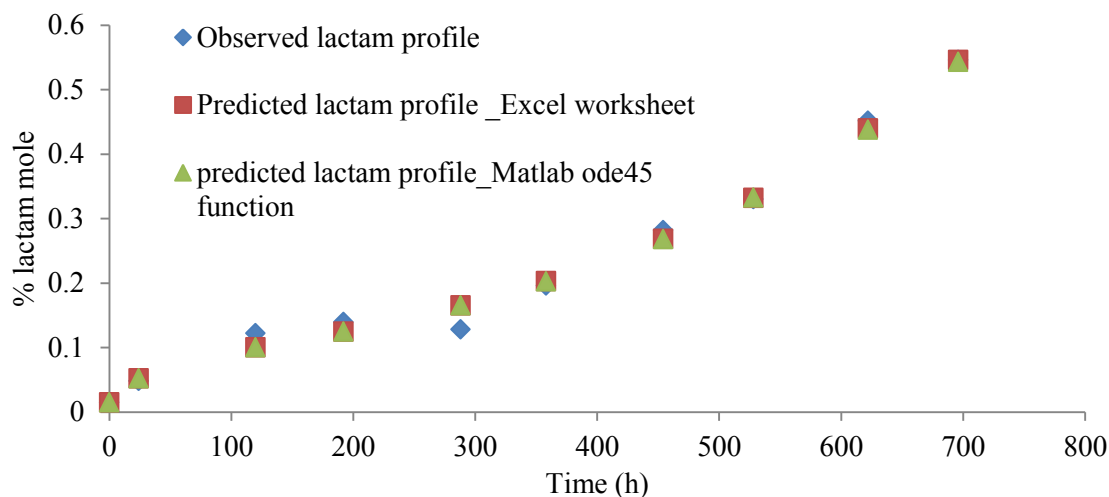


Figure 26: Comparison of approximated lactam content (% mole) using the Runge-Kutta method on Excel[®] and Matlab[®] routine relative to the observed lactam content (% mole) over time for the gabapentin-excipient compact stored under accelerated temperature (50 °C) and humidity conditions (5% RH).

The next step involved use of the Solver function in Excel[®] to optimize rate constants and initial concentration of reactive molecules (gaba_0^*), describing the degradation kinetics of gabapentin.

First optimization of the rate constants was performed on the data for unprocessed gabapentin by fixing a lower value of gaba_0^* . The value of gaba_0^* was selected to be ~ 0.027 which was substantially lower than the value (0.46% mole) of gaba_0^* published previously¹ (by a separate research group) for milled (15 min using ball mill at speed 5) gabapentin samples in the absence of excipients. The lower value (0.027% mole.) of gaba_0^* was selected than that published previously since a greater concentration of reactive molecules in an unprocessed gabapentin sample was less likely. The results as shown in Figure 27 and Table 14 for unprocessed gabapentin (red unfilled squares) demonstrate a good fit between the data predicted by the model and the experimentally observed data. The optimized rate constant values for gabapentin data were also similar to those published previously.¹ However, when the same lower value of gaba_0^* was fixed to estimate the rate constants in the case of gabapentin- Tri-Tab[®] mixture

(Figure 27: navy blue triangles) the model-predicted curve failed to provide a reasonable fit resulting in a high SSE value, as shown in Figure 27 (green dashed line). A poor fit was obtained irrespective of altering all the other rate constants in the model. This observation is due to greater initial lactam formation (>0.7% mole at 200h) in the case of the gabapentin-Tri-Tab[®] physical mixture relative to gabapentin (>0.02% mole at 200 h). As per the assumptions of the kinetic model, the initial lactam formation is described predominantly by rate constant k_2 and the concentration of gaba_0^* . Thus a noticeably higher concentration of lactam in the case of the gabapentin-Tri-Tab[®] physical mixture suggests a higher concentration of gaba_0^* present inherently in the gabapentin sample used for the degradation study.

When Excel[®] solver was allowed to optimize all of the rate constants and the value for gaba_0^* for the gabapentin-Tri-Tab[®] mixture data, the optimized value for gaba_0^* was ~3% mole. The predicted lactam profile provided a good fit with the observed lactam concentration-time profile, as seen in Figure 27 (navy blue dashed line). However, the estimated value of gaba_0^* was far greater than that reported previously.

The next step was to ascertain if the higher value of gaba_0^* was able to predict the lactam concentration for the gabapentin data published in the literature. Based on the published literature values of the rate constants (Equations 4-6), a concentration-time profile for lactam formation was generated (simulated) as seen in Figure 28 and Table 15. The estimated value for the rate constants and higher value of gaba_0^* were used to generate a lactam formation profile as seen in Table 15 and Figure 28. Despite a higher value of gaba_0^* , the predicted profile closely matched the simulated lactam profile with a low (0.00009) SSE value. However, it is important

to note the value of k_2 in Table 15 changed significantly with the change in the value of gaba_0^* . This observation is due to the correlation of the two parameters defining the initial rate of lactam formation, as seen in Equation 3.

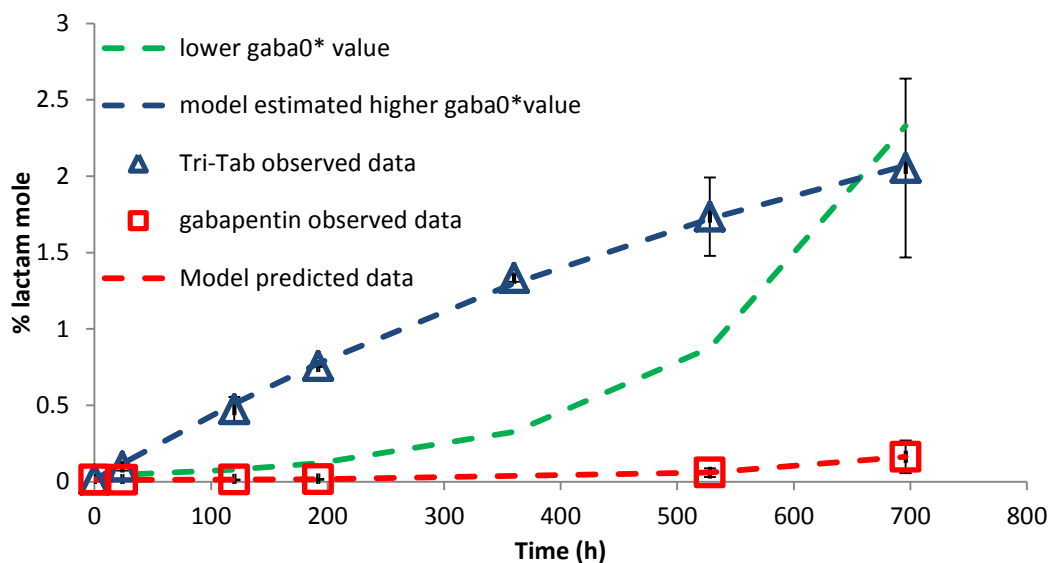


Figure 27: Optimization of the parameters in gabapentin and the gabapentin-Tri-Tab[®] physical mixture. The observed lactam concentration-time profiles for gabapentin (red squares) and the gabapentin-Tri-Tab[®] physical mixture (blue triangles) are compared to the model-predicted lactam profiles represented by dashed lines. The dashed line for the gabapentin-Tri-Tab[®] model predicted data demonstrates the model predictions at higher (blue lines) and lower value (green lines) of gaba_0^* respectively.

Table 14: The model estimated parameters for the gabapentin and gabapentin-Tri-Tab[®] physical mixture. A poor curve fit of model-predicted data is observed for the gabapentin-Tri-Tab[®] physical mixture after fixing for lower values of gaba_0^* .

Parameter	Gabapentin Fixing gaba_0^* at 0.027 and Optimizing Other Parameters	Tri-Tab[®] Fixing gaba_0^* at 0.027 and Optimizing Other Parameters	Tri-Tab[®] Model Estimated Data
k_1 ($\text{mol}^{-1}\text{h}^{-1}$)	6.8×10^{-5}	5.9×10^{-5}	1.4×10^{-6}
k_2 (h^{-1})	2.5×10^{-4}	0.64	1.5×10^{-3}
k_3 ($\text{mol}^{-1}\text{h}^{-1}$)	1.0×10^{-12}	1.0×10^{-8}	1.0×10^{-8}
gaba_0^* (% mole)	0.027	0.027	3.000
SSE	3.80×10^{-6}	3.39	3.60×10^{-3}

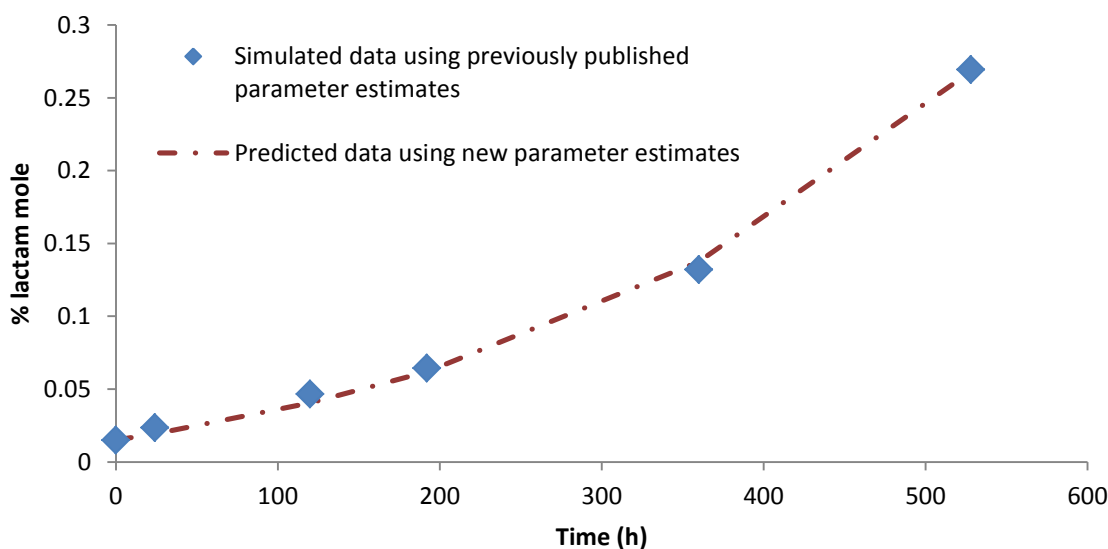


Figure 28: Comparison of simulated and predicted lactam concentration-time profiles for gabapentin, stored under accelerated temperature (50°C) and humidity (5% RH) conditions. The simulated lactam profile is generated using the literature-reported rate constants for gabapentin.¹ The predicted lactam profile is generated using new parameter estimates with estimated gaba_0^* greater than that reported previously.

Table 15: The model-estimated parameter values for unprocessed gabapentin relative to the previously estimated model parameters. No major alteration in the curve fit was observed post-application of new parameter estimates with a greater value of gaba_0^* .

Parameter	Simulated Data with Previously Published Parameter Estimates ¹	Predicted data With New Parameter Estimates
k_1	6.0×10^{-5}	7.5×10^{-5}
k_2	1.5×10^{-2}	5.1×10^{-5}
k_3	7.6×10^{-5}	3.8×10^{-5}
gaba_0^*	0.027	3.30
SSE	NA	9.0×10^{-5}

To confirm that a true solution was obtained after parameterization of the gabapentin-Tri-Tab[®] data, non-linear regression was performed using 25 different sets of input values. The parameter optimization resulted in an estimate of gaba_0^* that was 3% mole.

A clear increase in the sum of square error value and a poor fit of the model-predicted data was observed when the value of gaba_0^* was fixed below 3% mole in the gabapentin-Tri-Tab[®] data. A poor fit was obtained even after the alteration of other parameters, as seen in table 16.

Gaba_0^* was redefined as the combination of surface molecules and disordered molecules in the bulk of the gabapentin crystal. Based on the results obtained for the gabapentin-Tri-Tab[®] data, constraint on the value of gaba_0^* was set up to not be less than 3% mole. This constraint was established when assessing profiles for other gabapentin-excipient mixtures since, in unprocessed binary mixtures of gabapentin concentration of gaba_0^* was not expected to change.

The change in the concentration of gaba_0^* is not expected since it represents the inherently present reactive molecules in the gabapentin sample used in the study.

Table 16: Parameter estimates for the gabapentin-Tri-Tab[®] physical mixture, post-fixing for different values of gaba_0^* . The table demonstrates an increase in the sum of square error (SSE) value for the model-predicted fit after fixing for the value of gaba_0^* below 3% mole.

Parameter	Input Value	Optimized Output Estimate
k_1	1.4×10^{-6}	6.7×10^{-6}
k_2	0.0014	0.0022
k_3	1.0×10^{-8}	1.0×10^{-8}
Fixed gaba_0^*	2.00	2.00
SSE	1.270	0.009
k_1	1.4×10^{-6}	9.0×10^{-6}
k_2	0.0014	0.0032
k_3	1.0×10^{-8}	1.0×10^{-8}
Fixed gaba_0^*	1.50	1.50
SSE	4.480	0.010
k_1	1.4×10^{-6}	1.5×10^{-5}
k_2	0.0014	0.0050
k_3	1.0×10^{-8}	1.0×10^{-8}
Fixed gaba_0^*	1.00	1.00
SSE	1.073	0.045
k_1	1.4×10^{-6}	2.2×10^{-5}
k_2	0.0014	0.0190
k_3	1.0×10^{-8}	1.0×10^{-8}
Fixed gaba_0^*	0.5	0.5
SSE	6.818	0.180

The kinetic model for the solid-state degradation of gabapentin was successfully applied to the data and a good correlation between predicted and measured lactam concentration was observed, with a low sum of square error (SSE <0.001) value across all gabapentin-excipient mixtures, as seen in Table 16 and Figure 29. As can be seen from the Figure 29, a higher value (3% mole) of gaba_0^* was able to provide good model fits to all of the gabapentin-excipient mixture data unlike

a lower value ($<2\%$ mole) of gaba_0^* , which only fit a few gabapentin-excipient mixture profiles. Thus the primary reason for a noticeable difference in the magnitude of the estimated value of gaba_0^* between the previously published study¹, and presented research could be due to the initial development of the existing kinetic model only with processed gabapentin in the absence of excipients. The model assumed no catalytic effect of the excipient on the rate constant k_2 . Rate constant k_2 and gaba_0^* are responsible for the rate of initial lactam formation, hence a change in k_2 value would impact the estimated value of gaba_0^* from that reported previously.

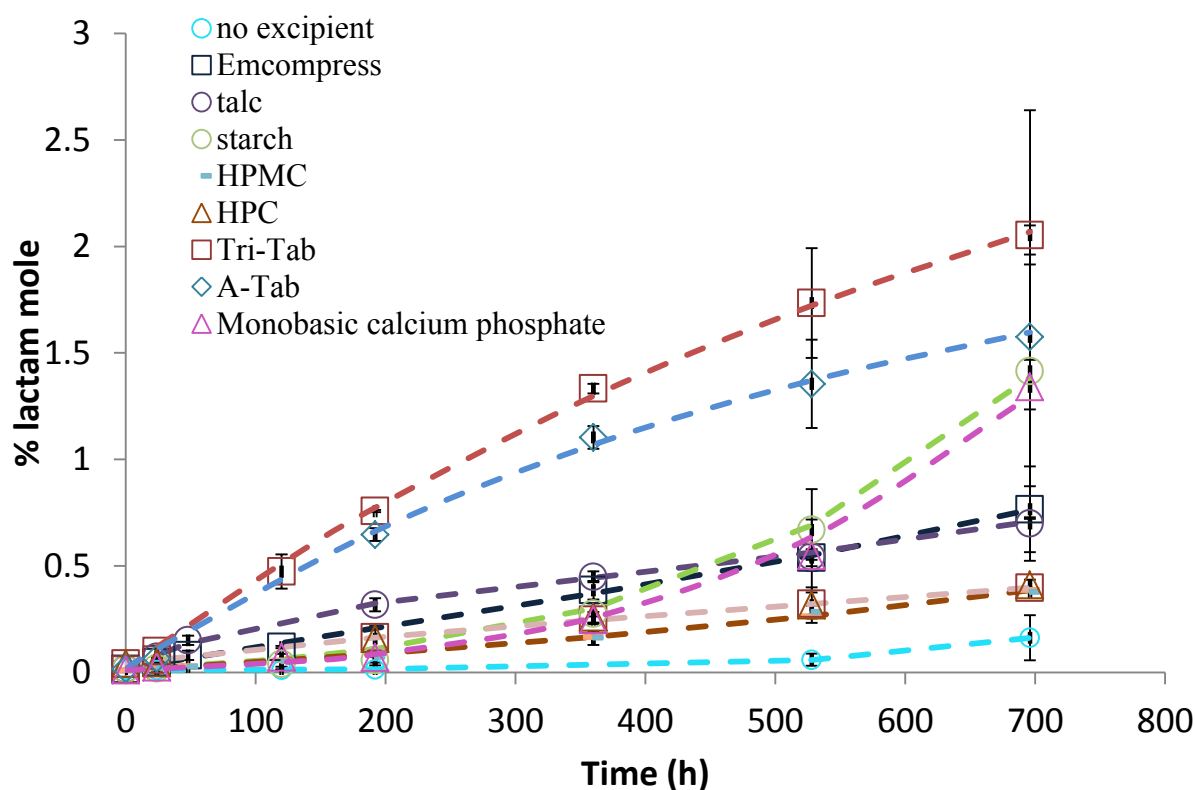


Figure 29: A comparison between observed and model predicted lactam formation in gabapentin and its physical mixture with excipients. Observed lactam concentration is indicated by legends, while the dashed lines indicate model predicted fit. The error bars represent a 95% confidence interval for three replicates across all time points. The above data suggests a good fit between the data predicted by the model and the observed values of lactam concentration.

After assessing the differential equations, (Equations 1-3), two parameters k_2 and gaba_0^* seem to be correlated. The correlation made it difficult to optimize the independent estimate values for the two parameters with great precision. Thus, to increase certainty in estimation of rate constant k_2 the value for gaba_0^* was fixed at 3% mole and estimates for other rate constants were obtained. Rate constants estimated for the data associated with gabapentin-excipient physical mixtures is reported in Table 17. The table also provides values of SSE and coefficient of determination (R^2) between the observed and the model predicted lactam concentration values.

Table 17: Summary of Optimized Rate Constants for the Degradation of Gabapentin with the Excipients

Constant	Tri-Tab [®]	A-Tab [®]	talc	Emcompress [®]	HPC	HPMC	Mono-Tab	starch	no excipient
k ₁	1.4x10 ⁻⁶ ±9.7x10 ^{-8*}	1.0x10 ⁻⁸ ±1.2x10 ^{-7*}	1.4x10 ⁻⁴ ±1.7x10 ^{-7*}	1.2x10 ⁻⁴ ±9.5x10 ^{-7*}	7.3x10 ⁻⁵ ±1.5x10 ^{-6*}	8.6x10 ⁻⁵ ±7.4x10 ^{-6*}	1.2x10 ⁻⁴ ±3.1x10 ^{-5*}	1.2x10 ⁻⁴ ±1.3x10 ^{-5*}	7.7x10 ⁻⁵ ±4.5x10 ^{-4*}
k ₂	1.4x10 ⁻³ ±9.4x10 ^{-7*}	1.3x10 ⁻³ ±9.4x10 ^{-7*}	1.0x10 ⁻³ ±1.1x10 ^{-6*}	3.5x10 ⁻⁴ ±4.3x10 ^{-7*}	2.2x10 ⁻⁴ ±3.1x10 ^{-7*}	1.1x10 ⁻⁴ ±2.8x10 ^{-7*}	6.9x10 ⁻⁵ ±3.9x10 ^{-7*}	6.5x10 ⁻⁵ ±1.3x10 ^{-7*}	7.2x10 ⁻⁶ ±1.0x10 ^{-7*}
k ₃	1.0x10 ⁻⁸ ±1.4x10 ^{-7*}	5.5x10 ⁻⁶ ±1.8x10 ^{-7*}	2.3x10 ⁻⁴ ±3.0x10 ^{-7*}	1.3x10 ⁻⁴ ±1.0x10 ^{-6*}	8.4x10 ⁻⁵ ±1.6x10 ^{-6*}	7.3x10 ⁻⁵ ±7.6x10 ^{-6*}	6.7x10 ⁻⁵ ±3.2x10 ^{-5*}	5.8x10 ⁻⁵ ±1.3x10 ^{-5*}	1.4x10 ⁻⁵ ±4.5x10 ^{-4*}
gaba ₀ [*]	3	3	3	3	3	3	3	3	3
SSE	0.0036	0.0035	0.0005	0.0009	0.0004	0.0007	0.0108	0.0018	0.0005
R ²	0.9990	0.9980	0.9980	0.9980	0.9920	0.9940	0.9920	0.9980	0.9680

* Estimated standard error using partial differentials and matrix inversion method

The presence of excipients in the physical mixtures with gabapentin resulted in an increased value of the rate constant, k_2 (h^{-1}), as seen in Figure 30. The highest value for k_2 (0.00149 h^{-1}) was obtained in the gabapentin-Tri-Tab[®] mixture, while the lowest value for k_2 ($6.39 \times 10^{-5} \text{ h}^{-1}$) was obtained for starch. The magnitude of k_2 in the absence of excipients was significantly lower ($7.20 \times 10^{-6} \text{ h}^{-1}$) than that in presence of excipients, strongly suggesting that excipients had a catalytic effect on lactam formation.

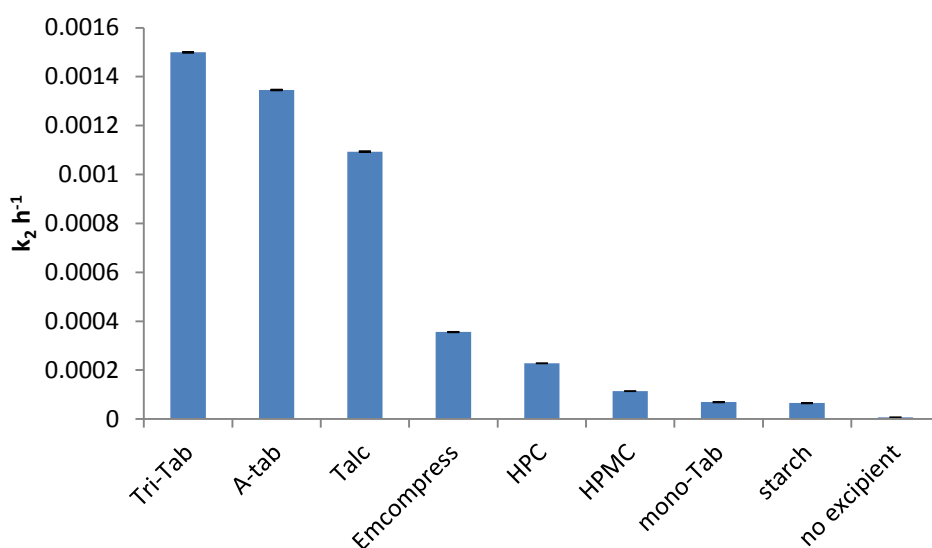


Figure 30: Estimated value for the rate constant k_2 across the gabapentin-excipient physical mixtures. Up to a 200-times increase in the value of the rate constant is observed for the gabapentin-Tri-Tab[®] mixture relative to its value in the absence of excipients.

The rate constant k_1 , associated with autocatalytic branching, was estimated to be $7.75 \times 10^{-5} \text{ mol}^{-1} \text{ h}^{-1}$ in case of unprocessed gabapentin as seen in Figure 31. This estimate was similar to the value of k_1 ($7.1 \times 10^{-5} \text{ mol}^{-1} \text{ h}^{-1}$) reported in the literature.¹ In the presence of excipients, the estimated value of the rate constant k_1 was $8.45 \times 10^{-5} \pm 0.000053 \text{ mol}^{-1} \text{ h}^{-1}$.

The value of the rate constant k_3 which was responsible for reaction termination was $7.45 \times 10^{-5} \pm 0.000073 \text{ mol}^{-1}\text{h}^{-1}$ across gabapentin and the gabapentin-excipient mixtures, as seen in Figure 32.

Although the rate constants k_1 and k_3 did not change significantly in the presence of most excipients, much lower values were estimated for the mixtures of gabapentin with Tri-Tab[®] and A-Tab[®] (Figures 31 and 32). This effect was possibly due to the significantly higher magnitude of the rate constant k_2 , which could be potentially masking the impact of the other two rate constants (k_1 and k_3) in the degradation profiles of gabapentin with Tri-Tab[®] and A-Tab[®]. Lactam profiles for Tri-Tab[®] and A-Tab[®] do not display the characteristic acceleration associated with the autocatalytic branching phase defined by the current model (Figure 22). On the other hand, the autocatalytic phase is seen distinctly in gabapentin and its physical mixtures with starch and Mono-Tab, with lower estimated values of the rate constant k_2 . It is observed that as the initial rate of lactam formation (<192 h) increases, branching phase starts to get less prominent as seen in Figure 21, which possibly makes estimation of the rate constants k_1 and k_3 difficult.

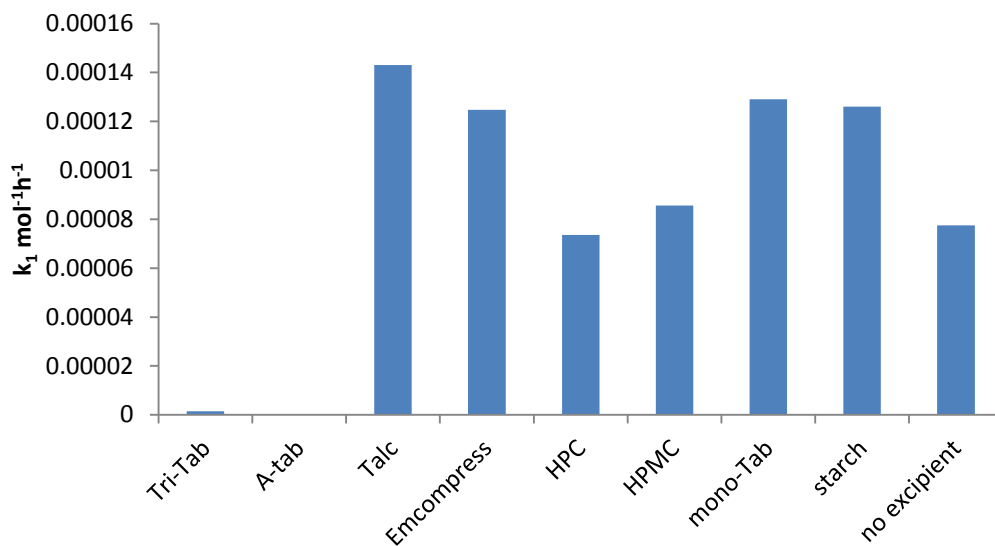


Figure 31: Estimated values for the rate constant k_1 (mol⁻¹h⁻¹) across the gabapentin-excipient physical mixtures. The significantly lower value of k_1 in the case of A-Tab[®] and Tri-Tab[®], is thought to be due to the higher magnitude of k_2 masking the actual branching/termination phase (described by k_1) in the degradation kinetics of gabapentin.

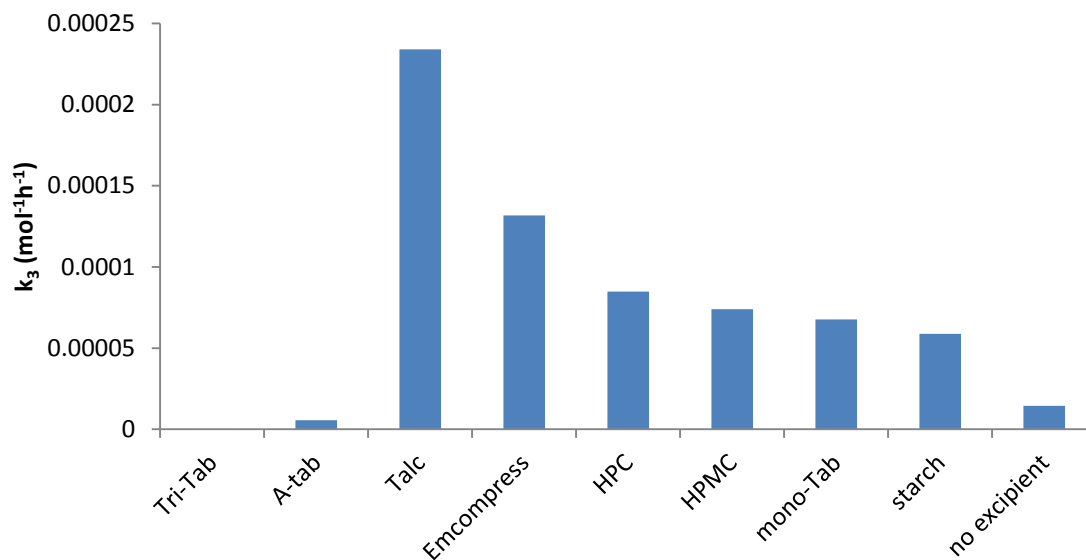


Figure 32: Estimated values for the rate constant k_3 (mol⁻¹h⁻¹) from the lactam concentration time profiles for the gabapentin-Excipient physical mixtures. The significantly lower value of k_3 in the case of A-Tab[®] and Tri-Tab[®], is thought to be due to higher magnitude of k_2 masking the actual branching/termination phase (described by k_3) in the degradation kinetics of gabapentin.

3.4. Conclusion

The major objective of this chapter was to provide evidence for the effect of excipients on the solid-state degradation of gabapentin. The objective was accomplished, when clear impact of the excipients on the solid-state degradation of gabapentin was confirmed in unprocessed powder mixtures. The method for preparation of the powder mixtures and the initial excipient moisture content were not found to affect the lactamization kinetics.

The central hypothesis of the research was that the **physicochemical properties of the excipients will accelerate the solid-state degradation of gabapentin, increasing the rate constant for lactam formation (k_2). The degradation kinetics, predominantly the initial rate of lactam formation, will be further accelerated by compaction of the gabapentin-excipient physical mixtures.**

The results from this chapter proved the hypothesis that conversion of reactive gabapentin to lactam driven by the rate constant k_2 was affected greatly by the presence of excipients. The magnitude of the rate constant k_2 was almost 200-times higher in the case of the gabapentin-Tri-Tab[®] physical mixture relative to its value for gabapentin. A possible reason for this effect could be general base catalysis in solid-state catalyzed by basic materials like Tri-Tab[®]. However, the subsequent chapter (Chapter 4) will focus on understanding the role of excipient properties responsible for the increased value of rate constant (k_2) catalyzed by the excipients. The Rate constants k_3 and k_1 , responsible for autocatalytic branching and the branching termination steps in the kinetic scheme were less affected in the presence of most excipients.

The value of gaba_0^* was estimated to be around 3% mole which included the surface molecules and other disordered molecules in the gabapentin crystal. The estimated value was found to be higher than that reported in the literature for the degradation of gabapentin. Further studies will have to be carried out to confirm and justify the unexpectedly greater value of gaba_0^* .

Chapter 4

Expansion of the Kinetic Model of Gabapentin Degradation to Account for the Physicochemical Properties of Excipients

4.1. Introduction

In chapter 3, the accelerated degradation of unprocessed gabapentin in the presence of excipients was studied. This chapter will focus on understanding the impact of excipient concentration, and excipient particle size on the degradation of gabapentin.

The observation of accelerated degradation of gabapentin in the presence of excipients prompted modification of the existing kinetic model to account for the presence of excipients. To expand the model and incorporate the excipient effect, it was important to confirm the catalytic effect of excipient concentration on degradation kinetics.

One of the critical aims of this chapter will be the expansion of the kinetic model to account for the excipient effect. The aim is to establish a relationship between the physical properties of excipients, such as particle size, particle shape, density, specific surface area and molecular cross sectional area, with the rate constant for lactam formation.

4.2. Materials and Methods

4.2.1. Materials

The materials used in the study are similar to those used in chapter three. However this chapter mainly focuses on the impact of excipient (A-Tab[®]) mass and particle size on the degradation of gabapentin. The physical properties of calcium phosphate dibasic dihydrate (Emcompress[®], E. Mendell. Co. Inc, New York), monobasic calcium phosphate (V-90 grade, Innophos, New Jersey), dibasic calcium phosphate anhydrous (A-Tab[®], Innophos, New Jersey), tribasic calcium phosphate anhydrous (Tri-Tab[®], Innophos, New Jersey), modified corn starch (Uni-pure[™] DW, National Starch LLC, New Jersey), hydroxypropyl cellulose (HPC, Klucel EF[®], Ashland Aqualon Functional Ingredients., Delaware), hydroxypropyl methyl cellulose (HPMC, Methocel[™] E50 Prem LV, The Dow Chemical Co., Michigan) and talcum (Talc, Fisher Scientific, Massachusetts) were measured. All other reagents and solvents used for the analytical quantitation were HPLC grade.

4.2.2. Study Designs

The particle size fractions of gabapentin and the excipients were obtained by sieve classification using a set of standard sieves (Gilson Company, Inc.) and a sieve shaker (Performer III Model SS-3, Gilson Company, Inc.) as described in chapter 3. The particle size fractions of A-Tab[®] (75-125 μm , 125-250 μm , 250-500 μm) were separated to study the effect of surface contact between gabapentin and the excipient on gabapentin's degradation

Gabapentin was maintained under controlled conditions of temperature ($20^{\circ}\text{C} \pm 2^{\circ}\text{C}$) and humidity (33% RH, magnesium chloride) for a week prior to the studies due to its higher stability under these conditions. The excipients were stored under controlled conditions of temperature (50°C) and humidity (5% RH, Drierite[®]) for at least one week prior to the study to ensure a minimal confounding effect of excipient moisture content on gabapentin's degradation.

To confirm the catalytic effect of excipient mass in the binary mixture, gabapentin was physically mixed ($n = 3$) with different concentrations (5%, 20%, 35%, 50% w/w) of A-Tab[®] controlled for their size (125-250 μm). Concentrations of excipient greater than 50% w/w were not considered for the study since gabapentin is a low potency drug, commercially available as tablets in a 600-800 mg dose. Hence, the concentration of excipients greater than 50% in a gabapentin formulation is less likely.

Assuming the catalytic effect of the excipients follows the Law of Mass Action, the rate constant for degradation should be proportional to the number of excipient molecules in contact with gabapentin molecules. Accordingly, it was hypothesized that increasing the particle size of the excipients would decrease the rate constant for lactam formation by decreasing the number of surface molecules available for interaction. To test this hypothesis and understand the effect of the contact area between gabapentin and excipient particles, physical mixtures of gabapentin and different particle size fractions (75-125 μm , 125-250 μm and 250-500 μm) of A-Tab[®] were prepared in a 1:1 proportion by weight.

All of the above physical mixtures were stored in scintillation vials (20 ml) under controlled conditions of temperature (50 °C) and humidity (5% RH) for the entire study duration (697 h). Samples (n = 3) of the mixtures were withdrawn periodically for quantitation of gabapentin and its degradation product lactam. Deionized and filtered (0.45 µm sized filter) water was used to prepare the samples. The samples were filtered using a 0.45 µm nylon syringe filter and analyzed using a validated analytical method as discussed in chapter 2.

The existing kinetic model for solid-state degradation of gabapentin was applied to the generated data.¹ The Runge-Kutta 4th order numerical approximation method was used to solve the series of differential equations (Equations 1-3) defining the kinetic model.¹ The data collected was further parameterized using non-linear regression by applying the least squares approach using Excel[®] Solver (Excel[®] 2010). Constraints on the values of gaba_0^* and the rate constant k_1 and k_3 were set up as discussed in chapter 3. To understand the role of the physical properties of the excipients on gabapentin's degradation, a thorough characterization of the excipient's physical properties, such as particle size (µm), particle shape, true density (g/cm³), molecular cross-sectional area (A_x , m²), and specific surface area ($\overline{S_E}$, m²/g), was performed.

4.2.3. Particle Size and Shape Determination

The varying morphology of gabapentin and the excipients required measurement of the mean particle size (Ferret diameter) using an optical microscope. Measuring the Ferret diameter (cm) was especially valuable for materials with a needle shaped or rectangular prismatic morphology.

Images of gabapentin and excipient particles ($n \gg 200$) were acquired using a light microscope (Model BX-51, Olympus, Pennsylvania). The images were visualized under 10x objective for most excipients and 50x objective in the case of talc. The images were processed using Image J software (U.S. National Institutes of Health, Bethesda, Maryland, version 1.41o), to calculate the mean Feret diameter.

An optical microscope was also used to visualize the particle morphology for all excipients and measure the dimensions (length and breadth) of rectangular particles. Excipient particles ($n \gg 100$) were analyzed using the Image J software, to determine particle circularity according to Equation 25.

$$\text{Circularity} = 4\pi \times \frac{\text{Area of a particle}}{\text{Perimeter of a particle}^2} \quad \text{Equation 25}$$

Circularity values typically range from 1 in the case of a perfect circle to 0 in the case of an infinitely long polygon. The circularity values helped differentiate the morphology of the different materials.

4.2.4. Determination of Molecular Cross-Sectional Area

To compute the cross-sectional area of the excipient molecule, the 2-dimensional (2-D) chemical structure of each excipient was acquired using ChemDraw[®] software (version 13.0, PerkinElmer, Massachusetts). In the case of polymers, the structures of the monomer units were considered for the determination of the molecular cross-sectional area. The 2-dimensional chemical structure was transformed to a 3-dimensional structure using Molecular Operating Environment (MOE 2013.08, Chemical Computing Group, Quebec, Canada) software. Energy minimization was performed using force field MMF94X and a 0.05 gradient. The van der Waals radii of atoms

were taken into account, and the contours of the projections were smoothed using a water probe of 1.4 Å radius. The lengths of the major and minor axis of the projected surface in two orientations were measured to compute the average cross-sectional area of the molecule assuming an ellipsoidal geometry. The computed molecular surface and the axis measured for the cross-sectional area determination are depicted in appendix 2.

4.2.5. Specific Surface Area Measurements

One of the most important physical properties of a material is its specific surface area (\overline{S}_E , m²/g). This property becomes especially important when understanding interactions at the drug-excipient interface. The measurements of specific surface area were made using nitrogen vapor adsorption data (FlowSorb II 2300, Micromeritics Instrument Corporation, Georgia) with subsequent application of Brauner, Emmett and Teller (BET) model. Helium was employed as the carrier gas and liquid nitrogen served as the external coolant. Approximately 1.0-1.5 g of the excipient was filled into a clean, dry sample tube. The samples were outgassed for more than 24 h at higher temperatures (50-200°C) for calcium phosphates (anhydrous grade) and talc. To prevent alteration of any physical properties, materials such as dibasic calcium phosphate dihydrate, modified corn starch, HPC, and HPMC were outgassed at 50°C for more than 24 h and further degassed at 50°C for 5 h. A single sample of each material was analyzed. Measurements were conducted at a series of relative pressures (p/p_0) of 0.05, 0.10, 0.15, 0.20, 0.25, and 0.30, and the moles of nitrogen adsorbed (n) at each of the partial pressures was analyzed with the BET equation (Equation 26), given below in its linear form.

$$\frac{\frac{P}{P_0}}{n\left(1 - \frac{P}{P_0}\right)} = \frac{1}{c \times n_m} + \frac{(c - 1)\frac{P}{P_0}}{c \times n_m} \quad \text{Equation 26}$$

Linear regression analysis was used to estimate the moles of nitrogen adsorbed at monolayer coverage (n_m) and the affinity constant (c). The specific surface area was taken as a quotient of the sample's total surface area and mass. The cross-sectional area of a nitrogen molecule was assumed to be 16.2 \AA^2 in all of the calculations.

4.2.6. True Density Measurement

The true density of the materials was used to estimate the number of excipient and drug particles in the mixture considering for their volume and mass. The measurements were also used to estimate the solid fraction of gabapentin-excipient compacts, which will also be discussed in chapter 5. This measurement uses helium pressure and Boyle's law (the product of pressure and volume is constant for a closed system at a fixed temperature) to calculate the volume occupied by powder particles. The true density of each material weighing between 5-10 g was measured in triplicates using helium pycnometry (Model: SPY-6DC, Quantachrome Instruments, Boynton Beach, Florida). The samples were degassed for 30 min. To determine the effective powder density, the volume was normalized by the final powder mass.

4.2.7. Theoretical Estimation of the Fraction Surface Area of the Excipient Particle in Contact with Gabapentin Particle

In binary mixtures of gabapentin with excipients, it is expected that a single particle of gabapentin will be in contact with multiple particles of excipients and gabapentin. To calculate the fraction of excipient surface area in contact with gabapentin, the first step involved

estimating the number-fraction of excipient particles and gabapentin particles around a single gabapentin particle in the mixture.^{89,90} The Komatsu model⁸⁹ was used for this purpose. This model was developed for binary mixtures. It assumes as per Equation 27, the number ratio of the individual component particles in the mixture (N_A and N_B) to be equal to the ratio of each component particle (n_A and n_B) contacting a single particle in the binary mixture (Equation 27).^{89,90}

$$\frac{n_A}{n_B} = \frac{N_A}{N_B} \quad \text{Equation 27}$$

Assuming, a binary mixture of two components A and B, n_A and n_B are the number of particles of component A and B in contact with a single particle of component B.

The total number of individual component particles (N_B and N_A) in the binary mixture is estimated using the molar mass (Mw), true density (ρ) and volume (V) of the individual components (Equation 28).^{89,90}

$$\frac{N_A}{N_B} = \frac{V_B \times \rho_B \times Mw_A}{V_A \times \rho_A \times Mw_B} \quad \text{Equation 28}$$

The Komatsu model was used to estimate the total number of individual component particles (N_B and N_A) and the number-fraction of component A (excipient) particles and component B (gabapentin) particles around a single particle B (gabapentin) in the binary mixture (Equation 29-30).^{89,90} The volumes of the excipient and gabapentin particles were determined based on the morphology, and the dimensions of the particles measured using optical microscopy.

$$\frac{n_A}{(n_A+n_B)} = \frac{\frac{N_A}{N_B}}{1+\frac{N_A}{N_B}} \quad \text{Equation 29}$$

$$\frac{n_B}{(n_A+n_B)} = \frac{1}{1+\frac{N_A}{N_B}} \quad \text{Equation 30}$$

The next step involved the use of Equation 31 to estimate the total number of particles (N_T) (excipient + gabapentin) contacting a single particle of gabapentin. This was calculated using the surface area of the gabapentin particle and the contact surface area (CSA) between the excipient and gabapentin particles.

$$N_T = \frac{\text{Surface area gabapentin particle}}{\left(\frac{n_A}{n} \times \text{CSA excipient}\right) + \left(\frac{n_B}{n} \times \text{CSA gabapentin}\right)} \quad \text{Equation 31}$$

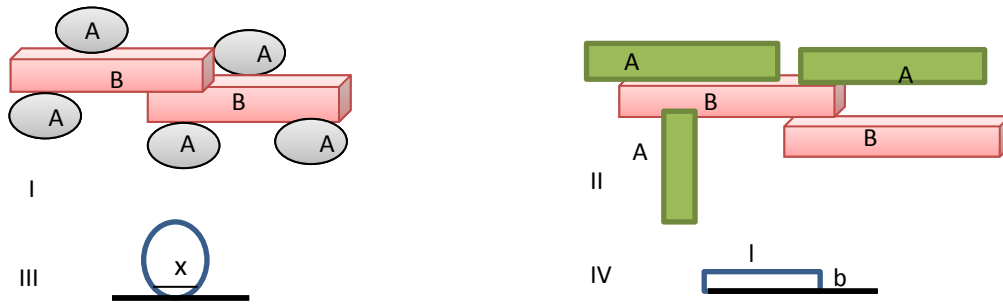


Figure 33: Graphical representation of the physical mixture of gabapentin (rectangular prismatic) particles (B) with excipient particles (A) of different shapes, I. Spherical or nearly spherical excipient particles. II. Rectangular prismatic excipient particles. III. Contact area between particles of gabapentin and spherical excipients IV. Contact area between particles of gabapentin and rectangular excipients

The surface area of the gabapentin particle was estimated by measuring its dimensions (length and breadth) using optical microscopy. The height of the gabapentin particle was assumed to be equal to its breadth considering the limitation of 3-D imaging on an optical microscope. The cross-sectional area (CSA) of the excipient and gabapentin particles were calculated based on the particle morphologies. In the case of rectangular particles, two different orientations were

possible; in these cases the mathematical average of the contact surface area for the two orientations were used to estimate the total number of particles, as per Equation 31. In the case of spherical excipient particles in contact with gabapentin, the point of contact would typically be a point on the spherical surface contacting gabapentin (Figure 33, I). Since it is difficult to measure the area of a point contact, the area of interaction (Van-der-Waals) between a sphere and a plane (πx^2) was calculated as the particle contact area. The distance x (Figure 33 III) was measured using optical microscopy in conjunction with the image J software. The range for PCA between the gabapentin and excipient particle with a rectangular prismatic morphology (Figure 33 II) was calculated using the formula for area of contact between two rectangular bodies (length \times breadth). The dimensions of excipient particles (rectangular prismatic) were also measured using optical microscopy (Fig. 33 IV).⁶³ After estimating N_T as per Equation 31, the number of excipient (N_E) and gabapentin particle around a single gabapentin particle was calculated using Equation 32.

$$N_E = \frac{n_A}{n} \times N_T \quad \text{Equation 32}$$

Finally, the fraction surface area (f) of the excipients in contact with gabapentin was calculated using Equation 33. This equation helped in calculating the fraction surface area of the excipient in contact with gabapentin, accounting for the effects of size, shape, and density of both the gabapentin and excipient particles.

$$f = \frac{N_E \times PCA (m^2)}{\text{Surface area of excipient } (m^2)} \quad \text{Equation 33}$$

4.3. Results and Discussion

The results in chapter 3, have demonstrated the impact of excipients on the solid-state degradation of gabapentin. The results in Figure 34, strongly suggests an increase in lactam formation with an increase in the concentration of the excipient (A-Tab[®]) in the binary mixture with gabapentin. This observation supported the hypothesis that excipient molecules play a role in the kinetics of gabapentin's degradation in a concentration-dependent manner. Consequently, the existing kinetic model needed modifications to account for the presence of excipients.

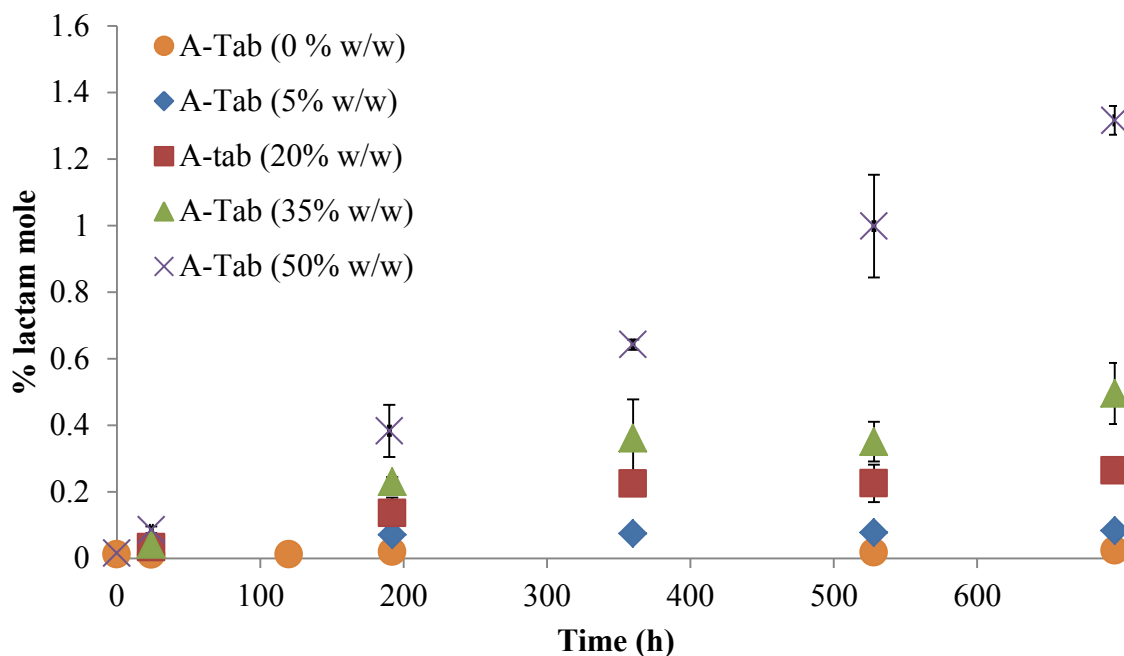


Figure 34: Effect of excipient concentration on the degradation of gabapentin. The graph represents mean lactam concentration (% mole) over time (h) with increasing concentration of the A-Tab[®] in the binary mixture. The error bars represents confidence interval (95%) for three replicates.

The results presented in Figure 35 also suggested lactam formation to be inversely proportional to the particle size of A-Tab[®]. It was observed that physical mixtures of gabapentin with a

smaller particle size fraction (75-125 μm) of A-Tab[®] showed a greater concentration of lactam (1.63% mole at 696 h) relative to the lactam content (1.31% mole and 1.10% mole respectively at 696 h) in physical mixtures with larger size fractions (125-250 μm and 250-500 μm) of A-Tab[®]. This observation indicated a key role of the surface molecules of excipient in accelerating lactam formation. However, a major difference in the specific surface areas of the different size fractions of A-Tab[®] was not observed (Figure 35 inset). This observation indicated that a large fraction of A-Tab's molecules were contained in the pores on the particle surface. The molecules within the pores are less likely to be in direct contact with the gabapentin particles. This observation highlighted the importance of external surface area in driving the degradation kinetics, relative to the overall specific surface area of the material.

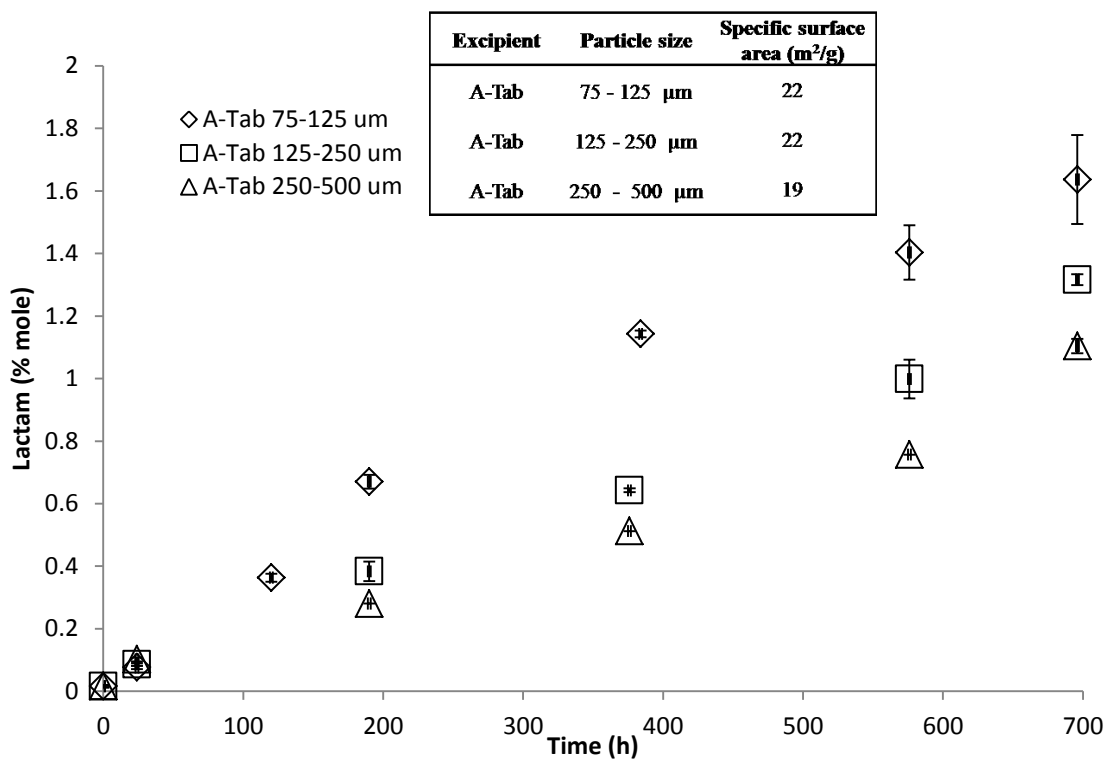


Figure 35: Effect of excipient particle size on the degradation of gabapentin. (\diamond) A-Tab[®] 75-125 μm , (\square) A-Tab[®] 125-250 μm , (Δ) A-Tab[®] 250-500 μm . The above data suggests the role of the external surface area of excipient on the degradation of gabapentin.

4.3.1. Modification of the Kinetic Model for Degradation of Gabapentin to Incorporate the Excipient Effect

The existing kinetic model for the degradation of gabapentin does not account for the catalytic effect of the excipient on gabapentin's degradation. To incorporate the excipient effect, the model was modified by the addition of a new, catalyzed pathway between reactive gabapentin and gabapentin lactam. The rate constant describing the kinetics of the pathway was denoted as k_4 (Figure 36). The expansion of the kinetic model resulted in modification of the differential equations (Equations 34-38) associated with the model.

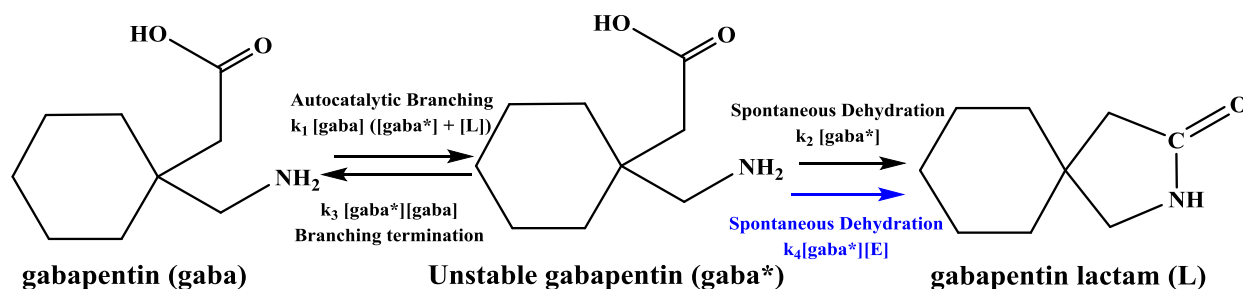


Figure 36: Expanded kinetic model for the solid-state degradation of gabapentin in the presence of excipients. Rate constant k_4 was added to the model to represent the rate constant catalyzed by the excipient molecules (E).

$$\frac{d[gaba]}{dt} = -k_1 [gaba] [gaba^* + L] + k_3 [gaba] [gaba^*] \quad \text{Equation 34}$$

$$\frac{d[gaba^*]}{dt} = k_1 [gaba] [gaba^* + L] - k_3 [gaba] [gaba^*] - k_2 [gaba^*] - k_4 [gaba^*][E] \quad \text{Equation 35}$$

$$\frac{d[L]}{dt} = k_2 [gaba^*] + k_4 [gaba^*][E] \quad \text{Equation 36}$$

$$\frac{d[L]}{dt} = gaba^* (k_2 + k_4 E) \quad \text{Equation 37}$$

$$(k_2 + k_4 E) = k_2^* \quad \text{Equation 38}$$

k_2^* is the newly derived apparent rate constant for the conversion of reactive gabapentin to lactam. This rate constant is the sum of both the excipient catalyzed and the uncatalyzed rate constants. E represents the concentration (% mole) of surface molecules on the excipient particle. The concentration of surface molecules on the excipient particle is further described by combination of physical properties of the excipients as seen in Equation 39.

$$E = \left[\frac{\frac{\overline{S}_E}{A_x \times N_A}}{\frac{m_E}{Mw_E} + \frac{m_G}{Mw_G}} \times 100 \right] m_E \quad \text{Equation 39}$$

As seen in Equation 39, \overline{S}_E (m²/g) is the specific surface area of the excipient, A_x (m²/ molecule) is the molecular cross-sectional area of the excipients, N_A (molecules/mole) is Avogadro's number, m_E (g) is the mass of the excipient, m_G (g) is the mass of gabapentin in the physical mixture, and Mw (g/mol.) is the molecular weight of the excipient (Mw_E) or gabapentin (Mw_G).

The representation of E using the physical properties of the excipients facilitated the development of a relationship that accounted for the effect of major physical properties of the excipients on the apparent rate constant for lactam formation, as seen in Equation 40.

$$k_2^* = k_2 + k_4 \times \left[\frac{\frac{\overline{S}_E}{A_x \times N_A}}{\frac{m_E}{Mw_E} + \frac{m_G}{Mw_G}} \times 100 \right] m_E \quad \text{Equation 40}$$

Where k_2 (h⁻¹) is the rate constant for lactam formation in the absence of excipient molecules, k_4 (h⁻¹ mol⁻¹) is the excipient catalyzed rate constant for the conversion of gaba* to lactam in the presence of excipients.

The developed relationship had multiple limitations. First, it assumed the total surface molecules of the excipient to be catalyzing the reaction. This assumption is unlikely especially when considering simple physical mixtures. Second, the relationship failed to take into account important physical properties such as the particle size and shape of both the excipient and the gabapentin particle. Third, the above relationship could lead to overestimation of the concentration of excipient molecules for catalysis, in the case of porous excipient materials like A-Tab[®], where greater concentration of the molecules would be contained in the pores.

To overcome the above limitations, a factor that could assist in estimating the actual surface area of the excipient in contact with gabapentin based on the particle size, shape and density of both gabapentin and excipient particles was included in the model.

The relationship was modified to include a factor (f), as seen in Equation 41.

$$k_2^* = k_2 + k_4 \times f \times \left[\frac{\frac{\overline{S}_E}{A_x \times N_A}}{\frac{m_E}{MW_E} + \frac{m_G}{MW_G}} \times 100 \right] m_E \quad \text{Equation 41}$$

Factor (f) represents the fraction surface area of the excipients in contact with gabapentin. This theoretical estimation was based on the principles of the Komatsu model to determine the contact area between components in a binary mixture.⁸⁹

Cumulative lists of all the measured physical properties of the excipients are summarized in Table 18. The moisture content of the excipients was recorded to be less than 1% w/w for most excipients, except starch (2.69 ±0.28% w/w) and HPC (1.97±0.38% w/w) due to their ability to absorb greater amounts of moisture. However, the minimal effect of excipient moisture on the degradation kinetics of gabapentin in the unprocessed state was observed in chapter 3. The

excipients under study showed wide variations in their surface properties. As seen in Table 18, the highest specific surface areas, 54.00 m²/g and 22.40 m²/g, were recorded for the porous excipients Tri-Tab[®] and A-Tab[®]. Lower porosity materials, such as Mono-Tab and starch, demonstrated lower specific surface area values of 0.70 m²/g and 0.22 m²/g, respectively. The molecular cross-sectional area varied between 2.30x10⁻¹⁹ m² and 8.60x10⁻¹⁹ m² between excipients. The highest molecular cross-sectional area was recorded for HPC, while, the lowest molecular cross-sectional area was recorded for A-Tab[®] (Appendix 2).

Table 18: Cumulative List for the Various Physical Properties of Excipients

Excipient	M_{wE} (g/mole)	True Density (g/cm ³)	\overline{S}_E (m ² /g)	A_x (m ² /molecule)	Moisture Content (% w/w)	Particle Dimension (cm)	Morphology & Circularity (C)
Tri-Tab [®]	502.3	3.11 (± 0.004)	54.54	7.2x10 ⁻¹⁹	0.95 (± 0.12)	0.0122 [#]	C = 0.77 
A-Tab [®]	136.0	2.92 (± 0.009)	22.41	2.3x10 ⁻¹⁹	0.25 (± 0.03)	0.0118 [#]	C = 0.68 
talco	379.3	2.55 (± 0.003)	9.03	5.8x10 ⁻¹⁹	0.04 (± 0.00)	0.000325 [#]	C = 0.63 
Emcompress [®]	172.1	2.61 (± 0.002)	4.53	2.8x10 ⁻¹⁹	0.22 (± 0.01)	0.0153 [#]	C = 0.63 
HPMC	279.0	1.25 (± 0.005)	0.97	6.1x10 ⁻¹⁹	0.44 (± 0.08)	(0.013, 0.0011, 0.0011)*	C = 0.06 
Mono-Tab	234.0	2.60 (± 0.004)	0.70	4.2x10 ⁻¹⁹	0.01 (± 0.00)	(0.016, 0.0035, 0.0035)*	C = 0.07 
HPC	321.0	1.23 (± 0.009)	0.93	8.6x10 ⁻¹⁹	1.97 (± 0.38)	(0.0125, 0.0039, 0.0039)*	C = 0.04 
starch	164.0	1.44 (± 0.003)	0.22	6.7x10 ⁻¹⁹	2.69 (± 0.28)	0.0125 [#]	C = 0.82 

[#] = Mean Feret Diameter for spherical or nearly spherical particle

* = measured length, breadth of a rectangular prismatic excipient particle. Thickness was assumed to be equal to the breadth.

The excipients were either spherical (or nearly spherical) or possessed a rectangular prismatic geometry. Particles with circularity values above 0.6 were considered to be nearly spherical while those below 0.6 were classified as rectangular prismatic. Amongst the spherical excipients, the mean Feret diameter recorded was highest in the case of Emcompress[®] (0.0153 cm) and lowest in the case of talc (0.000325 cm). On the other hand in the case of excipients with rectangular prismatic geometry two orientations of the molecule contacting gabapentin could be imagined. Amongst the excipients, Mono-Tab demonstrated greater particle dimensions ($l = 0.016$ cm and $b = 0.0035$ cm) relative to the particle dimensions for HPMC ($l = 0.0130$ cm and $b = 0.0011$ cm) and HPC ($l = 0.0125$ cm and $b = 0.0039$ cm).

The total molecular concentration on the surface of the excipient particle, capable of accelerating gabapentin's degradation was calculated and is reported in Table 18. As expected, the specific surface area of the excipient particle played a critical role where excipients with greater specific surface area values, such as Tri-Tab[®] and A-Tab[®] had greater concentrations of total surface moles available for interaction. Similarly, excipients with lower specific surface area values, such as starch and Mono-Tab displayed a lower concentration of molecules at the surface. Amongst the excipients, HPC despite of relatively higher surface area value than Mono-Tab, showed a similar concentration of molecules at the surface; this was due to the higher molecular cross-sectional area of HPC relative to that of Mono-Tab. It was observed that the molecular cross-sectional area and specific surface area of the excipients together played an important role in estimating the total surface molar concentration. After addition of the factor (f) to estimate the fraction surface area of the excipient particle in contact with gabapentin, a more accurate

representation of the concentration of excipient molecules expected to be in contact with gabapentin was reported as seen in Table 19.

Table 19: Estimation of surface molar concentration on the excipient particle available for catalyzing lactam formation

Excipients	N_E	Total % Mole on Surface of Excipient Particle	f	Estimated Actual % Mole on Excipient Particle in Contact with Gabapentin
Tri-Tab [®]	0.05	1.339	0.00007	0.00010
A-Tab [®]	0.06	0.453	0.00026	0.00012
Emcompress [®]	0.03	0.091	0.00117	0.00010
talc	859.64	0.155	0.00736	0.00114
starch	0.10	0.002	0.05377	0.00015
HPC	0.59	0.012	0.02188	0.00081
HPMC	4.90	0.019	0.33649	0.00241
Mono-Tab	0.30	0.013	0.15980	0.00084

The value for (f) (0.02-0.33) was estimated to be higher in the case of particles with a rectangular shape relative to the estimated value of (f) (0.00007-0.053) in the case of spherical particles. This was due to the greater PCA between two rectangular particles relative to a sphere and a rectangular-shaped particle. However, in the case of starch and gabapentin physical mixture, the value of (f) (0.053) was higher relative to other spherical excipients due to the greater contact surface area (CSA) between gabapentin and starch particles relative to most other spherical excipients. Hence the total estimated surface area of starch in contact with gabapentin was higher relative to the total available surface area of starch in the mixture.

Talc, despite its spherical shape, had a greater magnitude for (f) relative to other spherical particles of excipients due to the smaller particle size of talc relative to other excipients, which

resulted in a higher estimated number of talc particles in contact with gabapentin. In the case of HPMC, greater numbers of HPMC particles (4.9 particles) were estimated to be covering a surface of gabapentin relative to other excipients in the study, which was a result of its higher estimated (f) value. The actual surface molecules of the excipients in contact with gabapentin were calculated to be greater in the case of talc and HPMC due to the higher estimated value of (f) relative to other excipients in the study.

In summary, the theoretically estimated fraction of surface moles in contact with gabapentin was found to be dependent mainly on the shape, size, density and molecular weight of the excipient. This estimation facilitated calculation of the rate constant k_4 using Equation 41 for lactam formation in the presence of excipients (Figure 37).

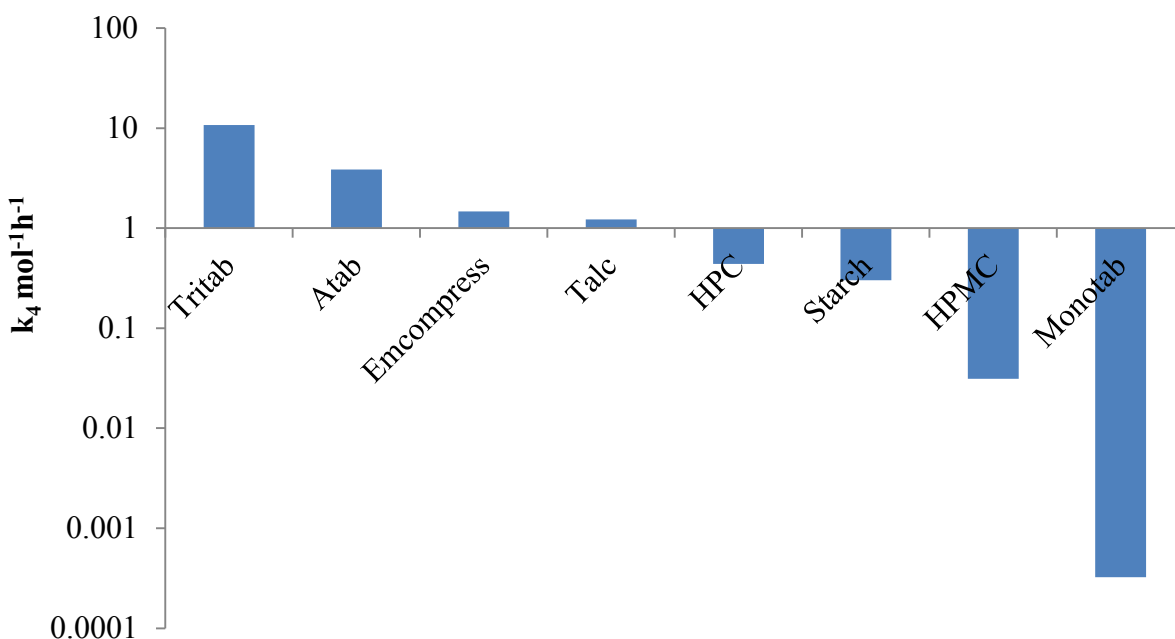


Figure 37: Estimated catalytic rate constant k_4 ($\text{h}^{-1} \text{mol}^{-1}$) for lactam formation in the presence of excipients. The plot is in logarithmic scale for the y-axis to show the magnitude of difference in the effect of excipient type on gabapentin's degradation. Maximal effect is shown by inorganic basic excipients relative to inorganic acidic excipients and polymers.

The estimation of rate constant k_4 helps in determining a role of the excipient's chemical properties in catalyzing lactam formation. However, the present data was unable to pinpoint a direct connection between the rate constant k_4 and a chemical property of the excipient. However, the results indicated a greater impact of inorganic salts of basic nature (Tri-Tab[®] (pKa 12.12), A-Tab[®] (pKa 7.4), talc (pKa 9.19), and Emcompress[®] (pKa 7.4)) relative to inorganic excipients of acidic nature (Mono-Tab (pKa 2.12)). Polymers (HPMC, HPC, and starch) had a lower impact on the degradation of gabapentin relative to the inorganic excipients. A possibility of a general base catalysis similar to that observed in the solution state degradation kinetics of gabapentin cannot be ignored. In the case of polymers and organic excipients, it could be hypothesized that the presence of impurities of a basic nature could be driving the catalysis of the reaction. However, further investigation will have to be planned in order to test this hypothesis. Nevertheless, to make a strong conclusion, and relate a particular chemical property of the excipients to affect lactam formation, the existing library of excipients will have to be expanded.

Currently, the ability to estimate k_4 from the developed relationship helps to facilitate excipient selection and the separation of a certain chemical class of excipients capable of catalyzing gabapentin's degradation.

On further validation, the model has the potential to be used as a tool in screening excipients and facilitating their selection for solid formulations of gabapentin. The model will enable risk assessment and identify formulations exceeding the regulated lactam content upon alterations in the physical properties of excipients due to batch-to-batch variation or change in the source for excipient procurement.

4.4. Conclusion

The results confirmed a catalytic effect of the excipient concentration on gabapentin's degradation profile. To account for the effect of excipient properties, the existing kinetic model for gabapentin's degradation was modified, and rate constant k_4 for lactam formation in the presence of excipients was incorporated. On modification of the kinetic model, the rate constant k_2^* (combination of rate constants k_2 and k_4) was defined as the "apparent rate constant" that accounted for lactam formation in the presence and absence of excipients.

Referring back to the research hypothesis, which stated that **physicochemical properties (such as specific surface area, molecular weight, particle size, particle shape and, acidic or basic strength) of the excipients will accelerate the solid-state degradation of gabapentin, increasing the rate constant (k_2) for lactam formation.** The results from this chapter proved the hypothesis and concluded major physical properties of the excipient such as their particle size, morphology, specific surface area, molar weight, and molecular cross-sectional area to be impacting the rate constant (k_2) for lactam formation. However no specific chemical properties of the excipients were found to be impacting the lactamization kinetics.

An inverse relationship between the particle size of the excipient and the rate of lactam formation was concluded. This finding prompted a strong need to theoretically estimate the actual surface moles of the excipient in contact with gabapentin after considering for the effect of particle size, shape, and density. Model expansion resulted in the development of a relationship between the apparent rate constant (k_2^*) and surface molar concentration of the excipient in contact with gabapentin based on the physical properties of the excipients. The proposed

relationship has the potential to be used as a tool to assess the effect of different physical and chemical properties of the excipient on the solid-state degradation of gabapentin.

Chapter 5

Effect of Compaction and Powder Properties of Excipients on the Solid-State Degradation of Gabapentin

5.1. Introduction

In chapter 4 we studied the effects of the physical properties of excipients on gabapentin's degradation. We also developed a theoretical model to predict how lactam content changes over time as excipient properties change. The results in chapter 4 are based on the physical mixing of gabapentin and excipients. Commercially, gabapentin is mainly available as tablets. Hence, it is also important to study the effects of compaction.

We hypothesized that in addition to the catalytic effect of excipients, compaction stress will accelerate lactam formation. It was expected that in the case of a highly crystalline drug like gabapentin, compaction stress would cause crystal damage and increase the concentration of reactive gabapentin molecules available for lactam formation. It was also expected that compaction in the presence of excipients would accelerate lactam formation by increasing the area of contact or the number of points of contact between gabapentin and the excipient molecules.

In this chapter we will study the effect of compaction stress, compact porosity, compaction energy, yield pressure and moisture content of the excipient as potential factors affecting the solid-state degradation of gabapentin.

5.2. Materials and Methods

5.2.1. Materials

Compacts for the study were prepared using physical mixtures of gabapentin and excipients in a 1:1 proportion. The excipients used for the study were dibasic calcium phosphate dihydrate (Emcompress[®], E. Mendell. Co. Inc, New York), modified corn starch (Uni-pure[™] DW, National Starch LLC, New Jersey), hydroxypropyl cellulose (HPC, Klucel EF[®], Ashland Aqualon Functional Ingredients, Delaware), hydroxypropyl methyl cellulose (HPMC, Methocel[™] E50 Prem LV, The Dow Chemical Co., Michigan) and talcum (Talc, Fisher Scientific, Massachusetts). All other reagents and solvents used for the analytical quantitation were HPLC grade.

5.2.2. Material Pretreatment

All solid materials including gabapentin and the excipients were stored under controlled conditions of temperature and humidity (21°C and 33% RH) for 1 week prior to compaction. The materials were not controlled for their particle size and were used as received from the supplier.

5.2.3. Determination of Moisture Content

The moisture content (% w/w) of the excipients was determined using thermogravimetric analysis (TGA Q-500, TA Instruments, Delaware). The average and standard deviation of two replicate measurements has been reported.

5.2.4. True Density Determination

The true density was determined using helium pycnometry (Model: SPY-6DC, Quantachrome Instruments, Boynton Beach, Florida) as described in chapter 4 and was performed in triplicates for each excipient.

5.2.5. Study Protocol

Gabapentin and excipients were mixed individually for every compact, in a 1:1 weight ratio (200 mg each) in a geometric proportion. Batch mixing of gabapentin with the excipients was avoided to eliminate sampling related inhomogeneity issues. In the case of gabapentin without excipients, 400 mg of gabapentin was weighed for compaction. Compacts of the physical mixtures (n = 3/time-point) were prepared using Instron Universal Testing System (Model 5869, Instron Corporation, Norwood, Massachusetts) at a compaction speed of 240 mm/min to a maximum pressure of 36.6 kN, measured using a 50 kN load cell in a 13 mm steel cylindrical die. Decompression using the same crosshead speed began immediately after the maximum load was reached. Punch separation distance was corrected for deformation of the tooling. This was done by adding the displacement measured during compression of the punches in an empty die to the punch separation distance measured during formation of each compact. The compact thickness and the diameter were measured immediately after ejection from the die using a set of digital calipers. Extra compacts for every set of gabapentin-excipient mixtures were prepared in triplicate and stored for 4-5 consecutive days under ambient temperature (21°C) and humidity conditions (31-33% RH) to allow for viscoelastic relaxation. This step was important to measure the “out of die” thickness of the tablets after the relaxation process in order to calculate the

compact porosity. This measurement of the “out of die” thickness was especially critical in the case of gabapentin compacts with viscoelastic materials like starch.

Compact porosity was calculated using the mass of the compact and the true density of individual components using Equation 42. In the case of physical mixtures, the true density of the mixture was calculated as the weighted sum of the true densities of the individual components based on their mass ratio.

$$\varepsilon = 1 - \frac{4m}{\pi (D)^2 t \rho} \quad \text{Equation 42}$$

In the above equation, ε denotes porosity, m is mass of the compact, D is the diameter of the compact, t is the compact thickness after viscoelastic relaxation, and ρ is the true density of the physical mixture.

As discussed in chapter 1, the Heckel model for consolidation was used to calculate the yield pressure (P_y) of different physical mixtures, as per Equation 21.

The mechanical energy values were determined using the Blue Hill Software Package (Instron, Norwood, Massachusetts). The work of compression (W_c) and work of decompression (W_d) were determined by integration of the force vs. displacement plots. Work of compression values represent the amount of work absorbed by the sample during compression that is not released during decompression.

$$W_{c/d} = W_c + W_d \quad \text{Equation 43}$$

In equation 43, $W_{c/d}$ represents the irreversible work (J/g) utilized in making the compact.

The compacts ($n = 3$) for the gabapentin-excipient physical mixtures for every time point were stored under accelerated conditions of temperature and humidity (50°C and 5% RH) and analyzed for the concentrations of gabapentin and lactam using a validated HPLC analytical method across 624 h.

The expanded kinetic model for the solid-state degradation of gabapentin as derived in chapter 4 was applied to the generated data.¹ The Runge-Kutta 4th order numerical approximation method was used to solve the series of differential equations defining the kinetic model.¹The data collected was parameterized by non-linear regression using the Solver function (Excel[®] 2010). The initial values for the parameters were the optimized parameter estimates obtained after parameterizing the stability data in chapter 3.

The parameters expected to change on compaction and with the presence of excipients included, gaba_0^* , due to increased concentration of the reactive gabapentin molecules on exposure to mechanical stress, and the rate constant k_4 (part of k_2^*), due to the greater contact area between gabapentin and excipients. The possible effect of excipient moisture in stabilizing the degradation of gabapentin could result in alteration in the value of k_3 . Hence, gaba_0^* , k_2^* , and k_3 were optimized, followed by the optimization of k_1 . The values for k_3 and k_1 were constrained to be greater than 10^{-8} to obtain non-zero estimates for the parameters.

The nature of the differential equation for lactam formation, as shown in Equation 36, demonstrates mathematical links between k_2^* and gaba_0^* . We have not attempted to separate their effects in compacted samples. We have therefore compared the initial rate for lactam formation

represented by $k_2^* \text{gaba}_0^*$ to determine the effect of compaction and the presence of excipients on the degradation of gabapentin.

5.3. Results and Discussion

Lactam formation results for compacted mixtures can be seen in Figure 38. The results demonstrate accelerated lactam formation in compacted physical mixtures of gabapentin with excipients relative to gabapentin compacted by itself. Application of the expanded kinetic model to the data resulted in good fit (indicated by dashed line in Figure 38) between the model-predicted data and the observed data points with low sum of square error (SSE <0.005) values across the different gabapentin-excipient mixtures.

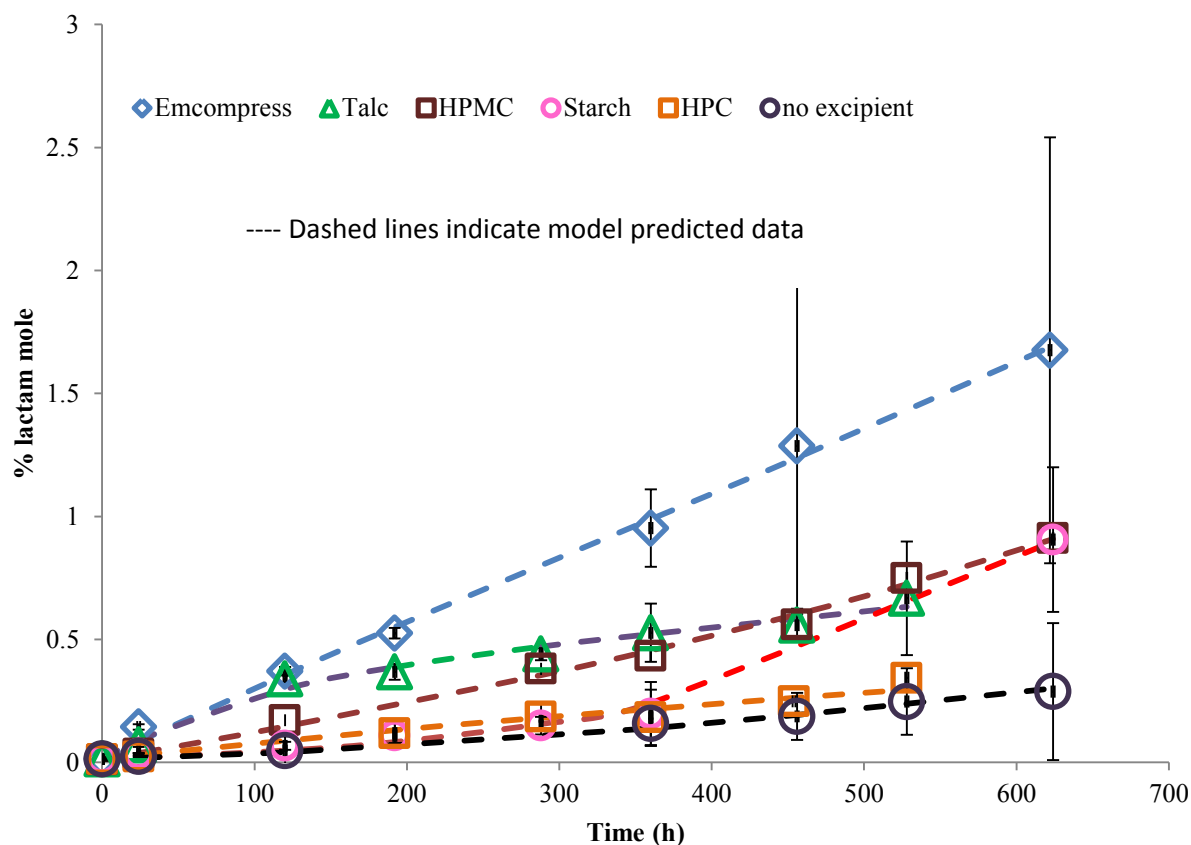


Figure 38: Effect of compaction and the presence of excipients on the solid-state degradation of gabapentin. Dashed lines indicate model-predicted data. The measured lactam concentration is an average of three replicates in gabapentin compacts and gabapentin-excipient compacts, and the error bars represent a 95% confidence interval.

The effect of compaction was especially prominent when comparing the slope of the initial lactam formation for compacted gabapentin with uncompact gabapentin in Figure 39.

The value of $k_2^* \text{gaba}_0^*$, which represents the initial rate of lactam formation, was found to be approximately 90% higher in the case of compacted gabapentin in the absence of any excipients relative to uncompact gabapentin.

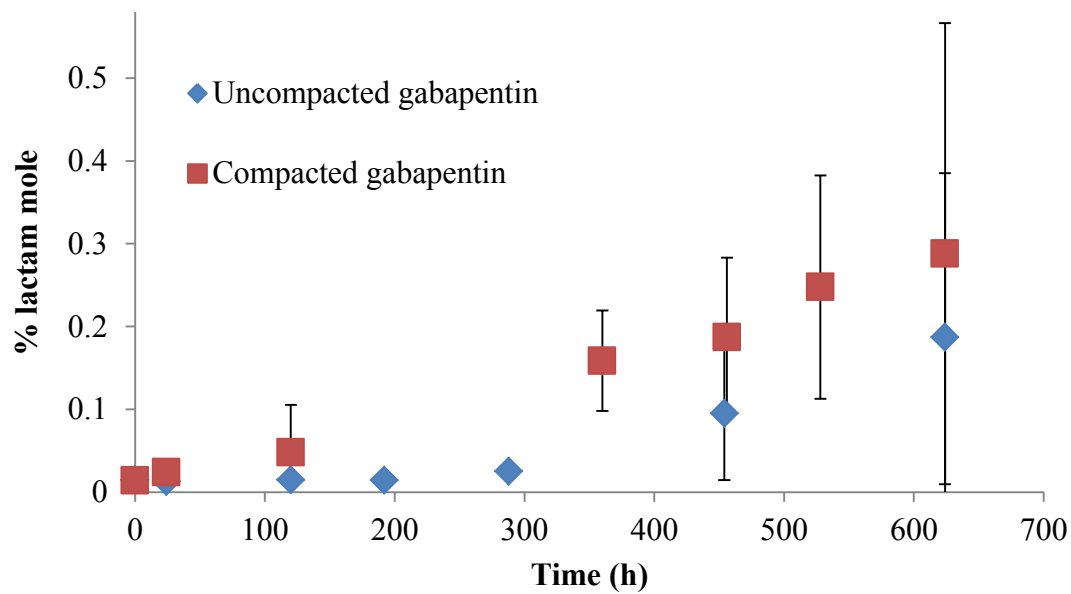


Figure 39: Effect of compaction on gabapentin’s degradation. The data points represent the concentration of lactam % mole over time (h) in gabapentin compacts (n = 3) and gabapentin uncompacted (n = 3). The error bars represent a 95% confidence interval.

In the case of compacts of physical mixtures of gabapentin and excipients, the accelerated effect of lactam formation is a combined effect of compaction conditions and the catalytic effect of excipients. Hence, to understand the effect of compaction, the percent increase in the initial rate of lactam formation between the gabapentin physical mixtures and their compacts was compared as seen in Figure 40.

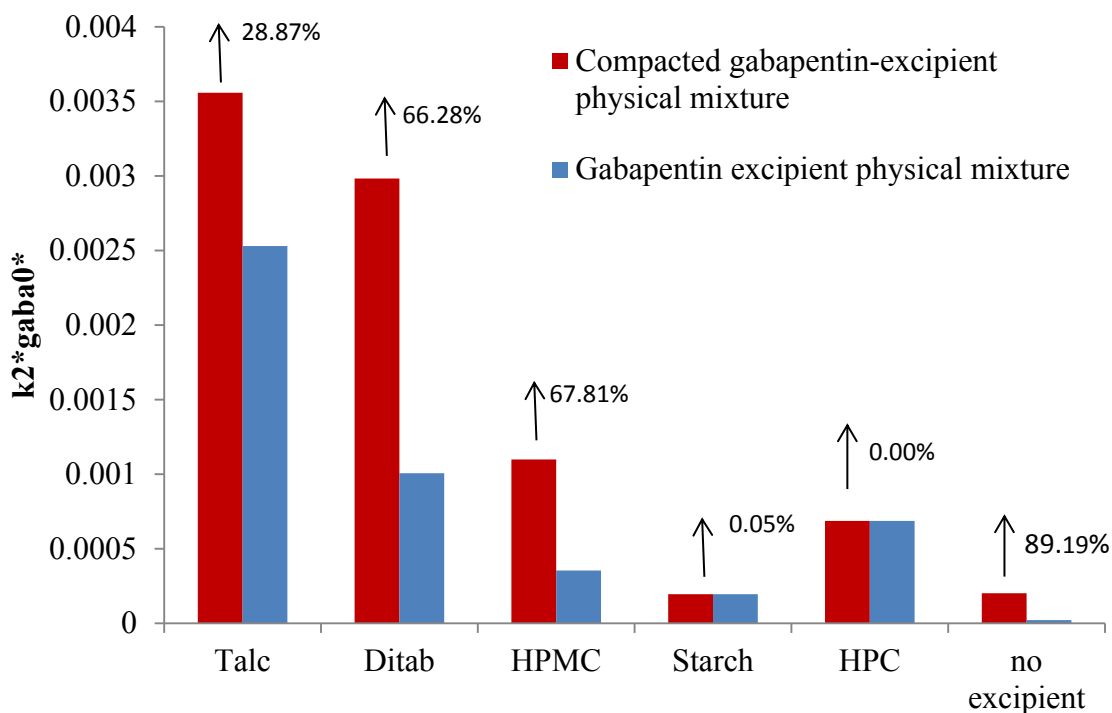


Figure 40: Comparison of the initial lactamization rate ($k_2^* \text{gaba}_0^*$) between the gabapentin-excipient physical mixtures and compacts. The arrows indicate the percent increase in the values of the initial lactamization rate in the case of the compacts of the physical mixtures relative to the value of the initial lactamization rate for physical mixtures.

The initial rate of lactam formation ($k_2^* \text{gaba}_0^*$) increased substantially (68%) in the case of compacts of gabapentin with Emcompress[®] and HPMC relative to the value of $k_2^* \text{gaba}_0^*$ in their physical mixtures. This effect can also be observed as an increase in the initial slope in the lactam formation profiles for mixtures and compacts of gabapentin with excipients in Figure 41 and Figure 42. Compaction is likely to increase the contact area between gabapentin and the excipient particle, accelerating lactam formation by affecting the value of k_2^* . It is important to remember that the rate constant k_2^* incorporates rate constant k_4 , which is catalyzed by the concentration of molecules on the surface of the excipient particle in contact with gabapentin. On the other hand, compaction pressure is also likely to increase the concentration of reactive

disordered molecules (gaba_0^*) of gabapentin, thus accelerating the initial rate of lactam formation.

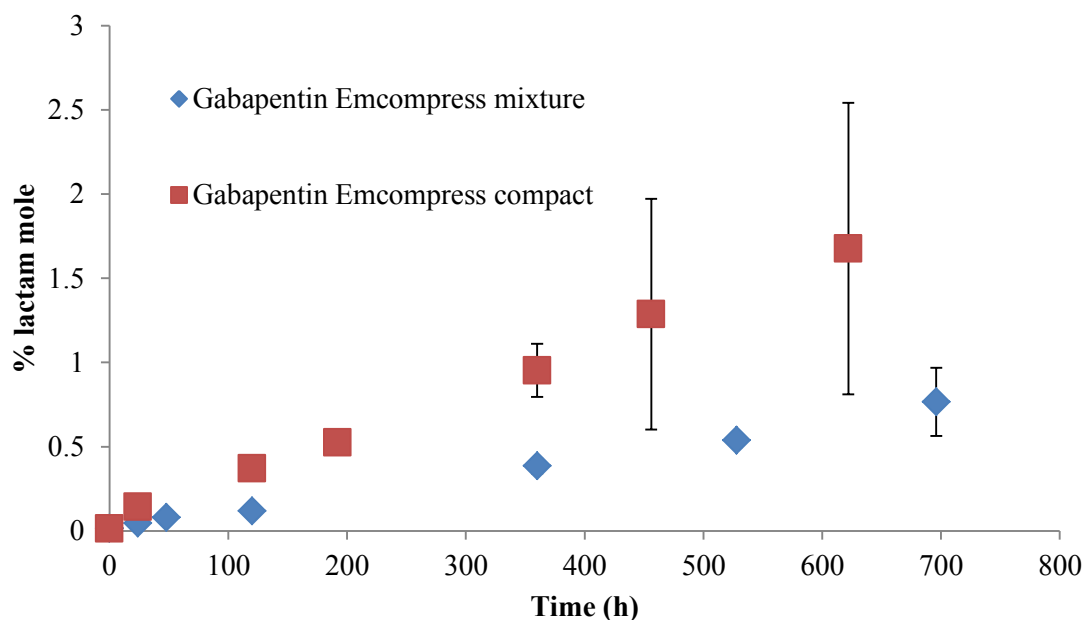


Figure 41: Effect of compaction on gabapentin's degradation in the presence of Emcompress[®]. The legends represent lactam concentration (%mole) over time in the case of physical mixtures and compacts of gabapentin and Emcompress[®]. The error bars represent a 95% confidence interval (n = 3).

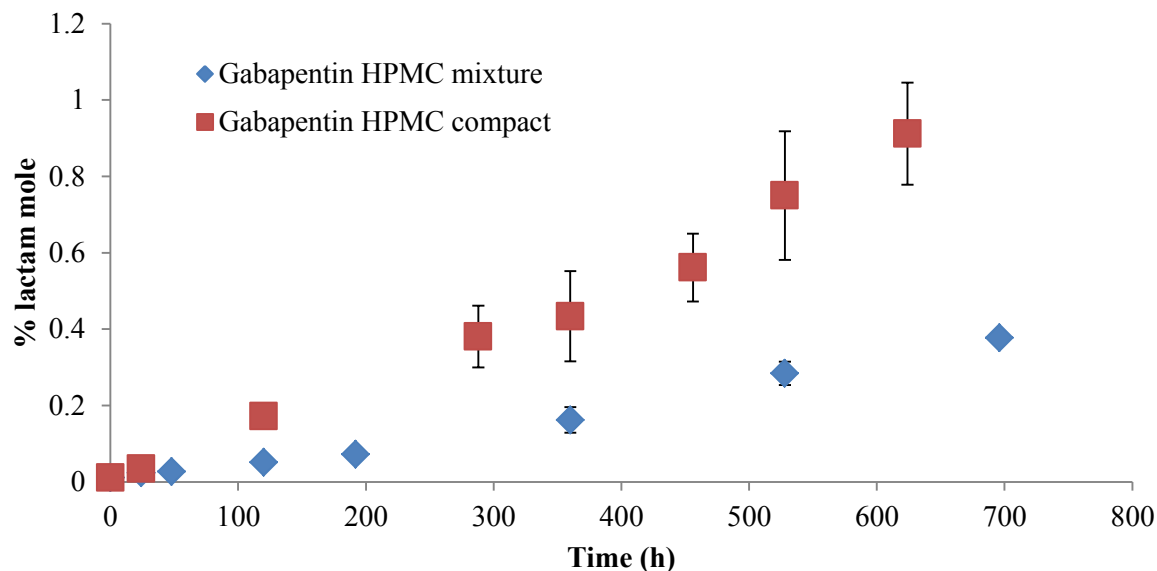


Figure 42: Effect of compaction on gabapentin’s degradation in the presence of HPMC. The legends represent lactam concentration (%mole) over time in the case of the physical mixtures and compacts of gabapentin and HPMC. The error bars represent a 95% confidence interval (n = 3).

It was hypothesized that yield pressure would influence the degradation kinetics of gabapentin. This was expected, due to the possible impact of this material property on the extent of gabapentin’s fragmentation, increasing the area of contact between gabapentin and excipient particles. To understand the effect of yield pressure, a plot of yield pressure for the physical mixtures and initial rate of lactam formation is shown in Figure 43.

It was observed that gabapentin-excipient physical mixtures with higher yield pressure (>200 MPa), which deform predominantly via brittle fracture, were responsible for a greater increase in the rate of initial lactam formation relative to other excipients in the study. Along with the materials deforming by brittle fragmentation, the physical mixture of gabapentin and HPMC undergoing plastic deformation and with a low yield pressure value (<75 MPa) was also

seen to be impacting the initial rate of lactam formation. Hence, the yield pressure of the excipients can be considered one of the critical factors that need to be further explored.

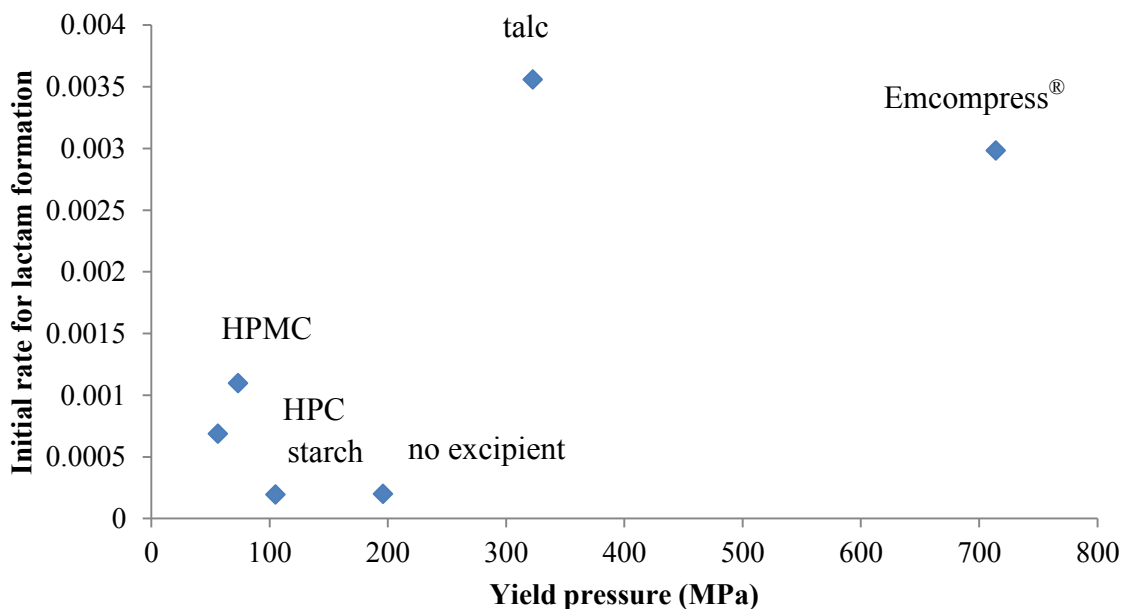


Figure 43: A plot suggesting the relationship between the initial lactam formation rate and the yield pressure of gabapentin-excipient physical mixtures.

Compaction of gabapentin with talc demonstrated no substantial increase in the initial rate of lactam formation relative to their physical mixtures as seen in Figure 44. When comparing the value of $k_2^* \text{gaba}_0^*$ for the compacts and the physical mixture of gabapentin with talc, a 28% increase was observed. The increase in the value of $k_2^* \text{gaba}_0^*$ was relatively lower than that observed in the case of the gabapentin-Emcompress® mixture and compacts with a similar deformation mechanism. This observation was thought to be due to the finer size (~3 μm) of talc particles and their tendency to coat the surface of gabapentin in the physical mixture (Figure 44 (inset)). The coating of talc on the surface of gabapentin is thought to result in a greater level of initial contact between the two materials. The contact area between gabapentin and talc was

thought to not increase substantially on compaction. However, it is important to point out that the initial data points in the degradation profiles for the gabapentin and talc mixtures and the compacts have less number of data points to make a conclusive statement. Collecting more data points across the initial degradation profile will be important to better support our conclusion.

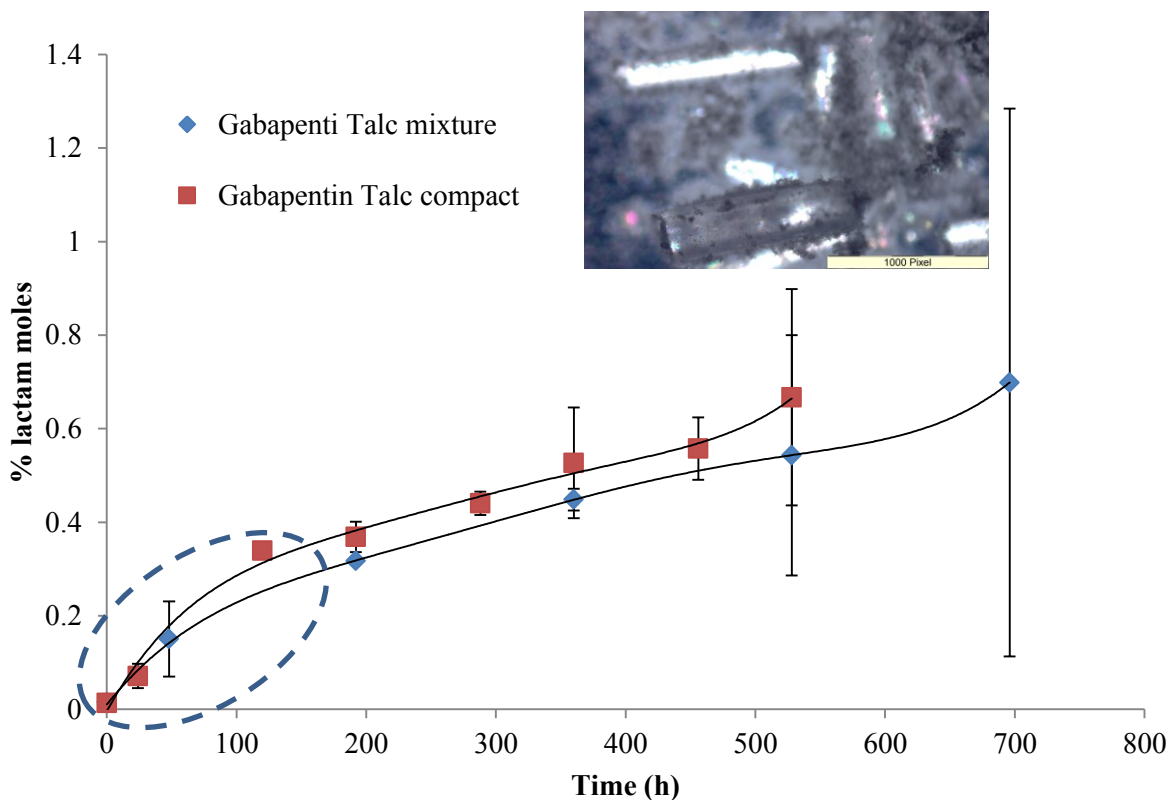


Figure 44: Effect of compaction on gabapentin's degradation in the presence of talc. The legends represent lactam concentration (% mole) over time in physical mixtures and compacts of gabapentin and talc. The trend lines across the data points rationalize the slight increase in the initial slope for lactam formation. The error bars represent a 95% confidence interval (n = 3). The inset picture shows a morphological representation of gabapentin particles coated by talc particles in their physical mixture.

The excipient that did not show a substantial increase in lactam formation upon compaction with gabapentin was starch as seen in Figure 45. It is important to highlight that amongst the excipients in the study, starch had the highest moisture content of 9.09% w/w. The literature

findings strongly suggest that moisture stabilizes processed gabapentin by healing the disordered molecules. Hence, we cannot rule out the effect of the moisture contained in starch to be stabilizing the degradation of gabapentin on compaction.

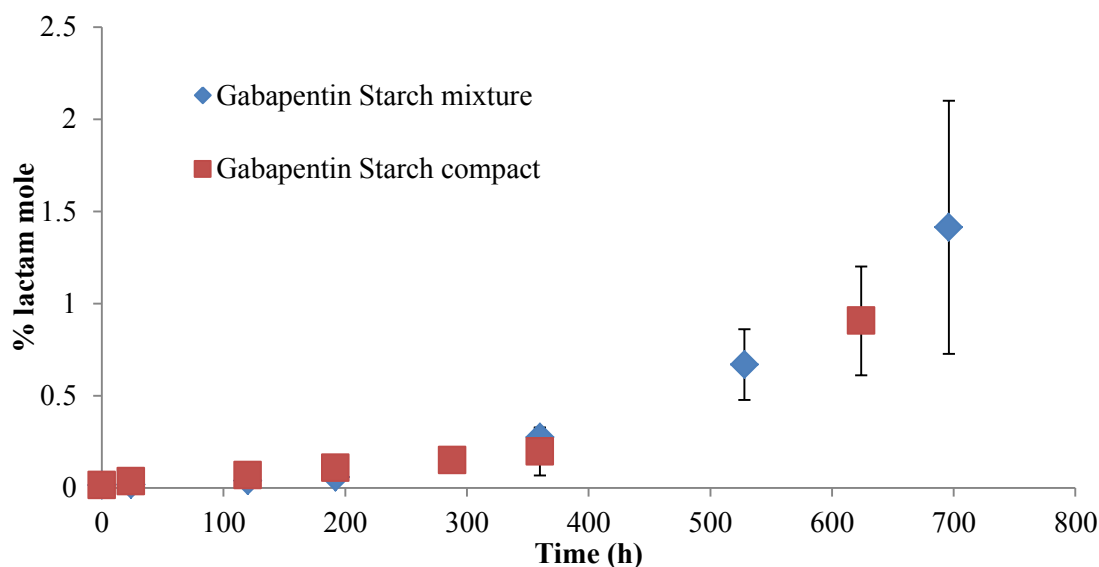


Figure 45: Effect of compaction on gabapentin’s degradation in the presence of starch. The legends represent lactam concentration (% mole) over time in the case of physical mixtures and compacts of gabapentin and starch. The error bars represent a 95% confidence interval (n = 3).

To understand if the moisture contained within the excipients could be one of the factors affecting gabapentin’s degradation, $k_2^* \text{ gaba}_0^*$ and the moisture content (% w/w) of the excipients were plotted as in Figure 46. The results showed a potential connection between the rate of initial lactam formation and the moisture content of the excipients.

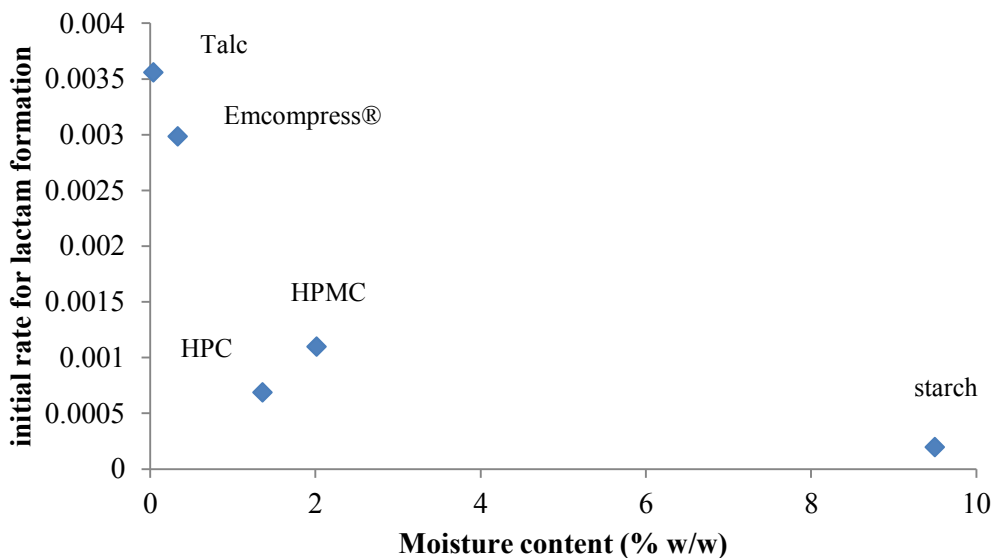


Figure 46: A relationship plot of the initial rate for lactam formation and moisture content of the excipients. A possible stabilization effect of excipient moisture on lactam formation is suggested.

Another excipient that did not show a significant increase in lactam formation on compacting with gabapentin was HPC, as seen in Figure 47. The increase in the rate of initial lactam formation of the gabapentin-HPC compact was lower relative to the increase in the rate of initial lactam formation for the gabapentin-HPMC compact. This was in spite of the moisture content and deformation properties of HPC and HPMC being similar. Interestingly, as seen in Figure 48, the gabapentin compact with HPC demonstrated the lowest porosity value (0.06) of all gabapentin-excipient compacts. HPC was also one of the excipients with higher moisture content. Lower porosity of the compact could suggest greater contact area between gabapentin and HPC. On the other hand, the higher moisture content of HPC in the compact with high solid fraction could potentially stabilize gabapentin by creating a microenvironment with high relative humidity within the compact. Hence, understanding the effect of HPC on gabapentin's

degradation on compaction will require further studies that isolate the effects of compact porosity, excipient moisture, and excipient yield pressure.

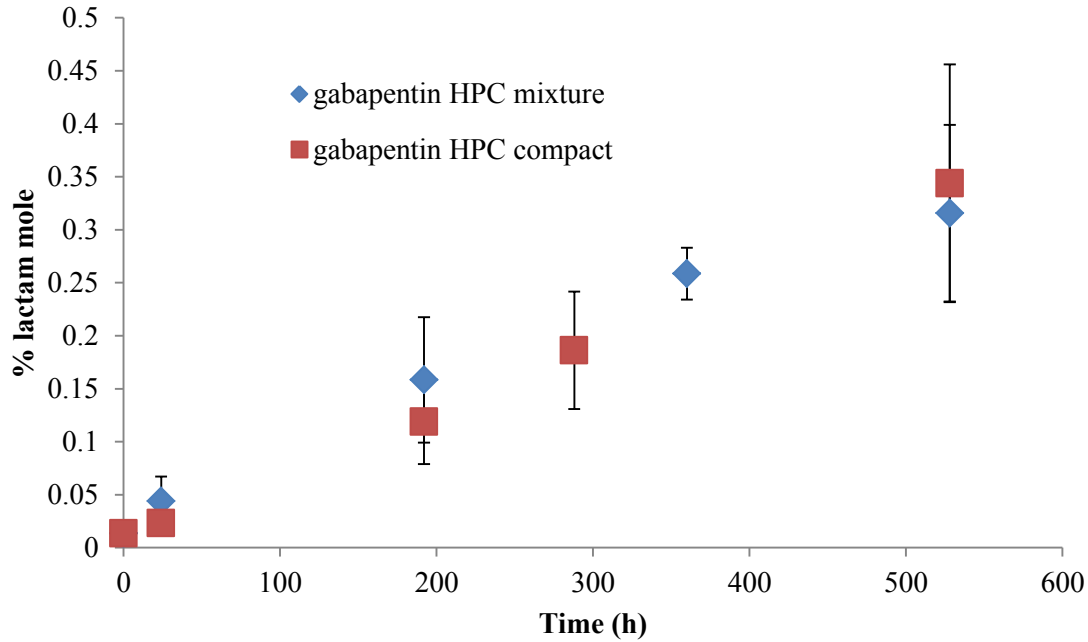


Figure 47: Effect of compaction on gabapentin's degradation in the presence of HPC. The legends represent lactam concentration (% mole) over time in the case of physical mixtures and compacts of gabapentin and HPC. The error bars represent a 95% confidence interval (n = 3).

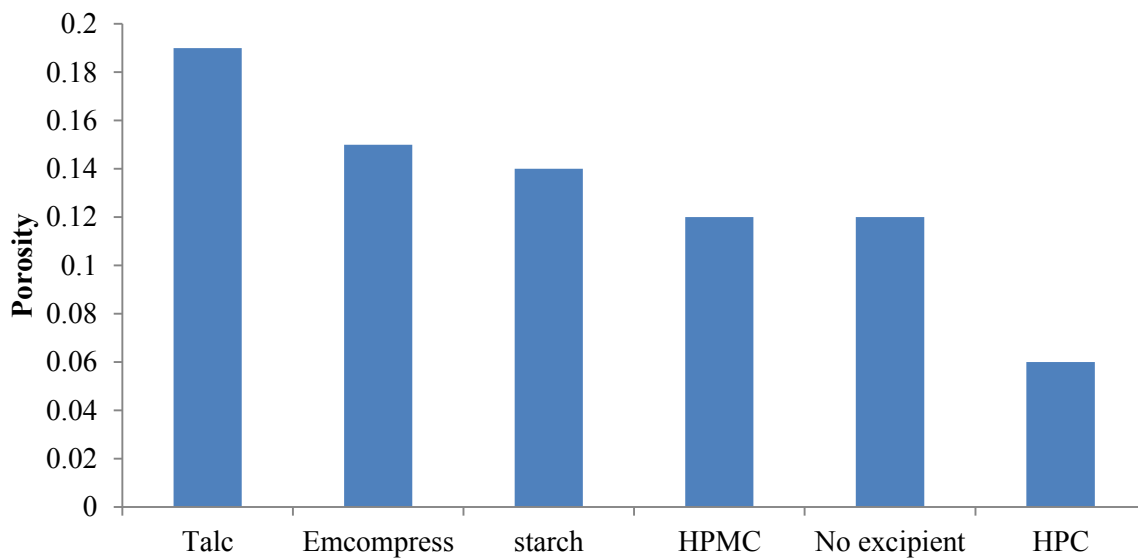


Figure 48: Comparative plot for porosity of the compacts of gabapentin with excipients.

The energy utilized in compact preparation was hypothesized to affect the rate of initial lactam formation. Results indicated no substantial effect from this factor, as observed in Figure 49. However, it is difficult to make any conclusive statement since a number of other confounding factors could be responsible for the observed results.

It is important to note that the data collected from this study is preliminary and only identifies potential factors that could be playing a role in gabapentin's degradation on compaction. Future studies can be designed to better quantify the relationship between lactam formation rate and these factors.

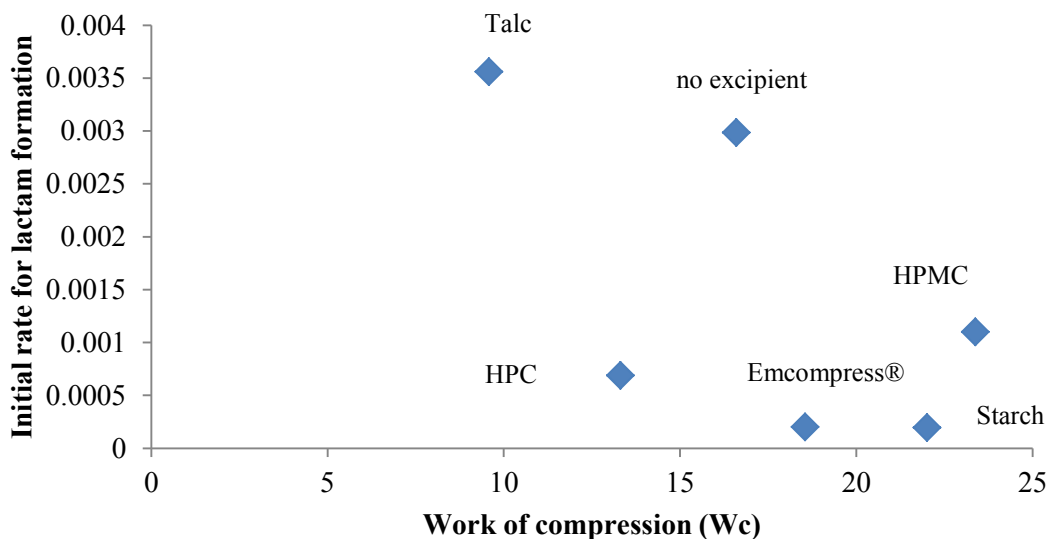


Figure 49: A relationship plot for the initial rate of lactam formation and the work of compression for compacts of gabapentin with excipients. Data indicates poor correlation between the two factors.

The results did not show any substantial effect from the processing conditions and the presence of excipients on the rate constants k_1 and k_3 . No substantial difference in the magnitude of k_3 was observed between the physical mixtures and the compacts of gabapentin with excipients, as seen in Figure 50.

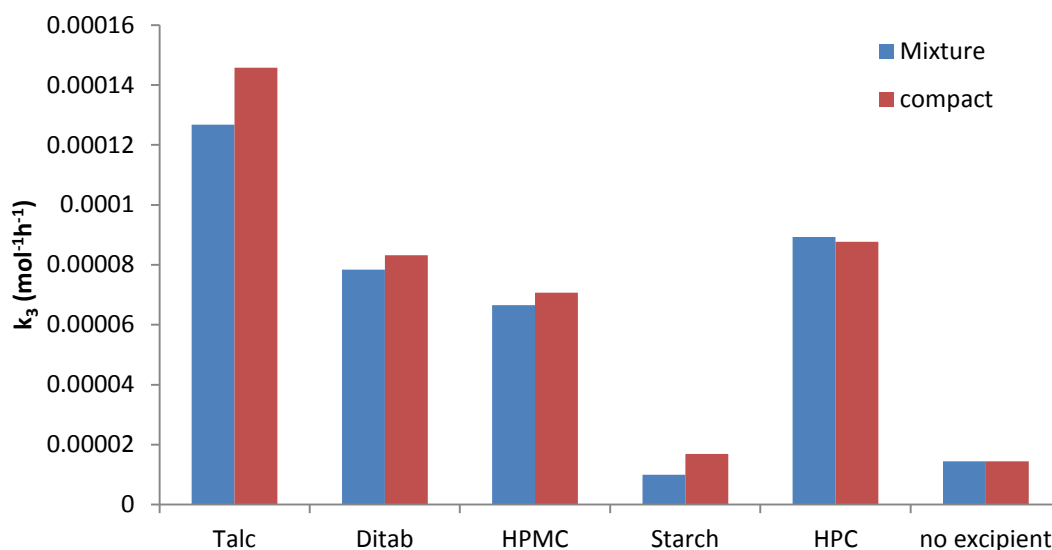


Figure 50: Effect of excipients on the rate constant k_3 in gabapentin’s degradation kinetics

5.4. Conclusion

Compaction pressure accelerated the initial rate of lactam formation in pure gabapentin compacts relative to unprocessed gabapentin. This effect was potentially due to an increase in the concentration of reactive molecules available for lactamization. Accelerated lactam formation in compacts of gabapentin with excipients was expected to be a result of the increased concentration of reactive gabapentin (gaba_0^*) and the increased catalytic effect of excipients due to more intimate contact between gabapentin and the excipients. Rate constants k_1 and k_3 were not impacted substantially by the application of compaction pressure or by the powder properties of excipients.

The above preliminary study suggested a possible effect of yield pressure, moisture content, and particle size of the excipient, and compact porosity on the initial rate for lactam formation in gabapentin-excipient compacts. Further studies are needed to understand the impact of the identified factors on gabapentin's degradation and to quantify the relationship between the factors and the initial rate of lactam formation.

Chapter 6

Conclusion

The objective of the presented research was to understand the role of excipients and compaction conditions on the solid-state degradation of gabapentin. It was hypothesized, that **physicochemical properties (such as specific surface area, molecular weight, particle size, particle shape and, acidic or basic strength) of the excipients will accelerate the solid-state degradation of gabapentin, increasing the rate constant (k_2) for lactam formation. The degradation kinetics, predominantly the initial rate for lactam formation will be further accelerated by compaction of the gabapentin-excipient physical mixtures.**

To test this hypothesis, five specific aims were designed. The **first specific aim** was to develop and validate (ICH Q2A guidelines) a robust analytical method for accurate quantitation of gabapentin and lactam. The results for studies associated with this aim are discussed in chapter 2. The **second specific aim** of the project as discussed in chapter 3 was to provide evidence for the effect of excipients on the solid-state degradation of gabapentin in the absence of any processing conditions. The **third specific aim** of the project as discussed in chapter 4, was to understand the effect of excipient concentration and its particle size on the degradation of gabapentin in solid-state. This aim also included expansion of the existing kinetic model to account for the effect of excipient properties. The **fourth specific aim**, also discussed in chapter 4, was to develop a mechanistic relationship between the physical properties of the excipient (such as shape, size, density, molecular cross sectional area, molecular weight, and surface area) with the rate constant for lactam formation. The relationship has the potential to estimate the effect of excipients based on their physical and chemical properties. The **final specific aim** of the project

as discussed in chapter 5 was to understand the role of compaction conditions and powder properties of excipients on the solid-state degradation of gabapentin.

The results in Chapter 2 highlighted the successful validation of an isocratic HPLC-UV analytical method, as per the ICH Q2A guidelines. The results confirmed the purity of the procured gabapentin sample to be comparable to that of the acquired USP reference standard. Inter-day and intra-day measurements, demonstrated the analytical method to be accurate, precise and robust. The method demonstrated specificity with respect to the elution of gabapentin and lactam in the presence of excipients. The results, confirmed absence of interference either from the filter membrane or from the excipients for extraction of lactam and gabapentin in solution. Lactam was found to be stable both in the mobile phase and in the sample solvent, for the entire duration of the study. On the other hand, the degradation rate of gabapentin in solution was observed to be too low to interfere with the results of solid-state degradation studies.

Results from chapter three provided strong evidence that excipients accelerate the degradation of unprocessed gabapentin to lactam in solid-state. Application of the existing kinetic model highlighted that the excipients significantly ($p > 0.05$) affect the initial rate of lactam formation. This initial rate is described by rate constants k_2 and the concentration of reactive gabapentin molecules (gaba_0^*). The results partly proved the hypothesis that “properties of the excipients will accelerate the rate constant (k_2) for spontaneous lactam formation”. Fixing a lower value of gaba_0^* and a value of k_2 , as established previously in the literature, successfully predicted the gabapentin degradation profile with a high R^2 value (> 0.97). However, the same lower value of gaba_0^* was unable to fit the data for the gabapentin-excipient binary mixture, which had the

highest lactam formation rate. The higher estimated value for gaba_0^* in most cases of gabapentin-excipient binary mixtures was the result of high lactam formation, measured in the initial time period of the stability study. As per the model assumption, the initial lactam formation is predominantly due to the spontaneous conversion of gaba_0^* . Thus, to observe the high initial lactam content as seen in the results from chapter 3, a greater concentration of gaba_0^* will have to be present as indicated by the model predicted estimate. The lowest value of gaba_0^* that provided a good fit ($R^2 < 0.99$) was 3% mole. Fixing the value of gaba_0^* lower than 3% mole resulted in a poor model fit to the data. Interestingly, higher value of gaba_0^* provided a good fit for the gabapentin data with an R^2 value of (> 0.97) and sum of square error value of 0.0005. The fit was comparable (similar values for R^2 and SSE) to that obtained for the gabapentin data with lower value of gaba_0^* .

The lower estimated value of gaba_0^* in previously established studies is entirely based on the data generated after milling gabapentin in the absence of excipients. Thus, greater initial lactam formation is attributed to the higher concentration of gaba_0^* on milling. However, after accounting for the catalytic effect of the excipients on the rate constant k_2 , the value of gaba_0^* was estimated to be 3% mole for unprocessed gabapentin present in all the binary mixtures. The concentration of reactive gabapentin molecules was defined as the sum of all surface molecules and other disordered molecules in the crystal. The concentration of reactive molecules was unexpectedly higher and hence will require further investigation.

The rate constant k_2 showed a significant ($p < 0.05$) increase in the presence of excipients relative to its value for gabapentin. Amongst the excipients tested, inorganic excipients (Tri-Tab[®],

A-Tab[®], Talc and Emcompress[®]) were seen to impact the degradation kinetics of gabapentin far more than polymers (HPMC, HPC and starch). Rate constants k_1 and k_3 were relatively less affected in the presence of most excipients. However, in physical mixtures of gabapentin with Tri-Tab[®] and A-Tab[®] the value of k_1 and k_3 was estimated to be significantly lower than that of gabapentin by itself. This effect is likely due to the higher magnitude ($\times 100$) of k_2 relative to k_1 and k_3 , resulting in masking the branching and termination phase in the solid-state degradation profile. The branching phase described by rate constants k_1 and k_3 , is observed clearly in the case of the degradation profiles for gabapentin, starch and Mono-Tab, which have lower values of k_2 .

Concentration dependent catalytic effect of the excipients was observed in the results from chapter 4 where, as the mass of the excipient in the binary mixture with gabapentin increased, there was an increase in the lactam content. This concentration dependent catalytic effect of the excipients was incorporated into the existing kinetic scheme. The kinetic model was expanded by addition of rate constant k_4 , surface molar concentration of excipients (E) and apparent rate constant k_2^* . Apparent rate constant k_2^* , was the sum of catalytic rate constant k_4 and uncatalyzed rate constant k_2 .

The final set of differential equations to predict lactam formation for the degradation of gabapentin in the **presence of excipients** would be as follows:

$$\frac{d[\text{gaba}]}{dt} = -k_1[\text{gaba}][\text{gaba}^* + L] + k_3[\text{gaba}][\text{gaba}^*] \quad \text{Equation 44}$$

$$\frac{d[\text{gaba}^*]}{dt} = k_1[\text{gaba}][\text{gaba}^* + L] - k_3[\text{gaba}][\text{gaba}^*] - k_2[\text{gaba}^*] - k_4[\text{gaba}^*][E] \quad \text{Equation 45}$$

$$\frac{d[L]}{dt} = \text{gaba}^* k_2 \quad \text{Equation 46}$$

$$(k_2 + k_4E) = k_2^* \quad \text{Equation 47}$$

In the above equations:

k_1 ($\text{mol}^{-1}\text{h}^{-1}$) is the autocatalytic rate constant

k_2 (h^{-1}) is the uncatalyzed rate constant for spontaneous lactam formation

k_3 ($\text{mol}^{-1}\text{h}^{-1}$) is the termination rate constant catalyzed by environmental moisture

k_4 ($\text{mol}^{-1}\text{h}^{-1}$) is the excipients catalyzed rate constant for spontaneous lactam formation

k_2^* (h^{-1}) is the apparent rate constant for spontaneous lactam formation, which is the sum of both the catalyzed and the uncatalyzed rate constant

gaba (% mole) is the concentration of stable gabapentin molecules

gaba* (% mole) is the concentration of reactive gabapentin

L (% mole) is the lactam concentration

t (h) is time.

Total molar concentration (E) on the surface of the excipient particle was represented using the specific surface area, the molecular cross sectional area and the molecular weight of the excipient. Results in chapter 4, also demonstrated an effect of excipient particle size on the rate

of lactam formation. Increasing particle size of the excipient molecules demonstrated decrease in rate of lactam formation. This finding highlighted the importance of estimating actual surface contact between gabapentin and the excipient based on their particle morphology and size. The fraction of molar concentration on the excipient surface which is in contact with gabapentin, was estimated (based on particle size, true density, the morphology of the excipient and gabapentin), by using the Komatsu model.⁸⁹ Results from chapter 4 proved the hypothesis that both the physical and the chemical properties of the excipients affect the lactamization kinetics.

The major physical properties of the excipients were measured and incorporated into the developed model which helped estimate the rate constant k_4 as it is affected by chemical properties of the excipients. Estimation of the excipient catalyzed rate constant, indicated greater impact of inorganic salts of basic nature (Tri-Tab[®] (pKa 12.12), A-Tab[®] (pKa 7.4), Talc (pKa 9.19) and Emcompress[®] (pKa 7.4)) relative to inorganic excipients of acidic nature (Mono-Tab (pKa 2.12)). Polymers (HPMC, HPC and starch) had a lower impact on the degradation of gabapentin relative to the inorganic excipients. However, considering the limited number of excipients used, it was difficult to strongly conclude that any particular chemical property was impacting degradation kinetics of gabapentin. Further expansion of the excipient library will be required to establish relationships between chemical properties of the excipients and the rate constants describing the degradation kinetics.

Comparing the initial rate ($k_2^* \text{ gaba}_0^*$) of lactam formation between gabapentin-excipient physical mixtures and their compacts in Chapter 5, showed that compaction pressure and powder properties affected gabapentin's degradation. Results from the study proved the hypothesis that

“The degradation kinetics, predominantly the initial rate of lactam formation will be further accelerated by compaction of gabapentin-excipient physical mixtures”. Results indicated accelerated initial rate of lactam formation in case of compacted gabapentin. This is hypothesized to be due to damage caused to its crystals, which would lead to increased concentration of reactive molecules. Results also indicated the potential role of compact porosity, yield pressure of physical mixtures, and moisture content of excipient and excipient particle size in accelerating lactam formation.

In summary, excipients impacted solid-state degradation of gabapentin. This impact was incorporated into the previously established kinetic model. The developed relationship between the apparent rate constant for lactam formation and the physical properties of excipients can be further explored, as a risk assessment tool. This tool would help predict lactam formation in gabapentin formulations over time, with variations in the physical properties of excipients and compaction conditions.

Bibliography

1. Zong, Z.; Qiu, J.; Tinmanee, R.; Kirsch, L. E. Kinetic Model for Solid State Degradation of Gabapentin. *J. Pharm. Sci.* **2012**, *101* (6), pp 2123-2133.
2. Byrn, S. R.; Xu, W.; Newman, A. W. Chemical Reactivity in Solid-State Pharmaceuticals: Formulation Implications. *Adv. Drug Delivery Rev.* **2001**, *48* (1), pp 115-136.
3. Salameh, A. K.; Taylor, L. S. Physical Stability of Crystal Hydrates and their Anhydrides in the Presence of Excipients. *J. Pharm. Sci.* **2006**, *95* (2), pp 446-461.
4. Ahlneck, C.; Zografi, G. The Molecular Basis of Moisture Effects on the Physical and Chemical Stability of Drugs in the Solid State. *Int. J. Pharm.* **1990**, *62* (2-3), pp 87-95.
5. Zong, Z.; Desai, S. D.; Kaushal, A. M.; Barich, D. H.; Huang, H. S.; Munson, E. J.; Suryanarayanan, R.; Kirsch, L. E. The Stabilizing Effect of Moisture on the Solid-State Degradation of Gabapentin. *AAPS PharmSciTech* **2011**, *12* (3), pp 1-8.
6. Chawla, G.; Bansal, A. K. Challenges in Polymorphism of Pharmaceuticals. *Current Research and Information on Pharmaceutical Society (CRIPS)* **2004**, *5* (1), pp 9-12.
7. Lin, S. Y.; Hsu, C. H.; Ke, W. T. Solid-State Transformation of Different Gabapentin Polymorphs Upon Milling and Co-milling. *Int. J. Pharm.* **2010**, *396* (1-2), pp 83-90.
8. Datta, S.; Grant, D. J. Crystal Structures of Drugs: Advances in Determination, Prediction and Engineering. *Nat. Rev. Drug Discovery* **2004**, *3* (1), pp 42-57.
9. Morris, K. R.; Griesser, U. J.; Eckhardt, C. J.; Stowell, J. G. Theoretical Approaches to Physical Transformations of Active Pharmaceutical Ingredients During Manufacturing Processes. *Adv. Drug Delivery Rev.* **2001**, *48* (1), pp 91-114.
10. Chaumeil, J. Micronization: A Method of Improving the Bioavailability of Poorly Soluble Drugs. *Methods Finds. Exp. Clin. Pharmacol.* **1998**, *20* (3), pp 211-216.
11. Rasenack, N.; Miller, B. W. Micron-size Drug Particles: Common and Novel Micronization Techniques. *Pharm. Dev. Technol.* **2004**, *9* (1), pp 1-13.
12. Brittain, H. G. Effects of Mechanical Processing on Phase Composition. *J. Pharm. Sci.* **2002**, *91* (7), pp 1573-1580.
13. Brittain, H.; Fiese, E. Effects of Pharmaceutical Processing on Drug Polymorphs and Solvates. *Polymorphism in Pharmaceutical Solids*; Swarbrick J. (Ed.); Marcel Dekker: New York, **1999**, *95*, pp 331-361.

14. Vippagunta, S. R.; Brittain, H. G.; Grant, D. J. W. Crystalline Solids. *Adv. Drug Delivery Rev.* **2001**, *48* (1), pp 3-26.
15. Zambon, E.; Giovanetti, R.; Cotarca, L.; Pasquato, L. Mechanistic Investigation on 2-aza-spiro [4, 5] decan-3-one Formation from 1-(aminomethyl) Cyclohexylacetic Acid (gabapentin). *Tetrahedron* **2008**, *64* (28), pp 6739-6743.
16. Jensen, A. A.; Mosbacher, J.; Elg, S.; Lingenhoehl, K.; Lohmann, T.; Johansen, T. N.; Abrahamsen, B.; Mattsson, J. P.; Lehmann, A.; Bettler, B. The Anticonvulsant Gabapentin (Neurontin) Does Not Act Through-Aminobutyric acid-B receptors. *Mol. Pharmacol.* **2002**, *61* (6), pp 1377.
17. Taylor, C. P. Emerging Perspectives on the Mechanism of Action of Gabapentin. *Neurology* **1994**, *44* (6 Suppl 5), S10-6, discussion S31-2.
18. Baillie, J. K.; Power, I. The Mechanism of Action of Gabapentin in Neuropathic Pain. *Curr. Opin. Invest. Drugs* **2006**, *7* (1), pp 33-39.
19. Potschka, H.; Feuerstein, T. J.; Löscher, W. Gabapentin-lactam, a Close Analogue of the Anticonvulsant Gabapentin, Exerts Convulsant Activity in Amygdala Kindled Rats. *Naunyn-Schmiedeberg's Arch. Pharmacol.* **2000**, *361* (2), 200-205.
20. Clinical pharmacology and Biopharmaceutical Review for Neurontin. Center of Drug Evaluation and Research (CDER), U.S. Government Printing Office: Washington DC **2011**.
21. FDA. Generic Firm Commences Gabapentin Recall Due to Excessive Impurities. *FDA news Drug Daily Bulletin* **2007**, *4* (226).
22. Chawla, M.; Raghuvanshi, R.; Rampal, A. Sustained Release Oral Tablets of Gabapentin and Process for Their Preparation. WO Patent 2,005,020,978 March 10, **2005**.
23. Augart, H.; Gebhardt, U.; Herrmann, W. Lactam-Free Amino Acids. US Patent 6,054,482A April 25, **2000**.
24. Singer, C.; Pilarski, G.; Pesachovich, M.; Schwarz, E. Stable Gabapentin Containing More Than 20 ppm of Chlorine Ion. EP Patent 1,430,893 A1 June 23, **2004**.
25. Manikandan, R.; Gogia, A.; Roy, S. B.; Malik, R. Gabapentin Tablets and Method for Their Preparation. WO 200,403,2905 A1 April 22, **2004**.
26. Sherman, B. C. Solid Compositions Comprising Gabapentin Having Improved Stability. US Patent 2,004,014,356 A1 February 19, **2004**.
27. Lloret Perez, S. Solid Pharmaceutical Composition of Gabapentin. WO Patent 2,007,128,495 A3: May 2, **2008**.

28. Camilleri, P.; Ellul, R.; Kirby, A. J.; Mujahid, T. G. The Spontaneous Formation of Amides. The Mechanism of Lactam Formation from 3-(2-aminophenyl) Propionic Acid. *J. Chem. Soc., (Perkin Transactions 2)* **1979**, (12), pp 1617-1620.
29. Guidance for Industry Waiver of In Vivo Bioavailability and Bioequivalence Studies for Immediate-Release Solid Oral Dosage Forms Based on a Biopharmaceutics Classification System. U.S. Department of Health and Human Services, F.D.A, Center for Drug Evaluation and Research (CDER). U.S. Government Printing Office: Washington DC **2000**.
30. Kearney, A.; Mehta, S.; Radebaugh, G. The Effect of Cyclodextrins on the Rate of Intramolecular Lactamization of Gabapentin in Aqueous Solution. *Int. J. Pharm.* **1992**, 78 (1-3), pp 25-34.
31. Reece, H. A.; Levendis, D. C. Polymorphs of Gabapentin. *Acta Crystallogr. Section C: Cryst. Struct. Commun.* **2008**, 64 (3), pp 105-108.
32. Hsu, C. H.; Ke, W. T.; Lin, S. Y. Progressive Steps of Polymorphic Transformation of Gabapentin Polymorphs Studied by Hot-Stage FTIR Microspectroscopy. *J. Pharm. Pharm. Sci.* **2010**, 13 (1), pp 67-77.
33. Braga, D.; Grepioni, F.; Maini, L.; Rubini, K.; Polito, M.; Brescello, R.; Cotarca, L.; Duarte, M. T.; André, V.; Piedade, M. F. M. Polymorphic Gabapentin: Thermal Behaviour, Reactivity and Interconversion of Forms in Solution and Solid-State. *New J. Chem.* **2008**, 32 (10), pp 1788-1795.
34. Zour, E.; Lodhi, S. A.; Nesbitt, R. U.; Silbering, S. B.; Chaturvedi, P. R. Stability Studies of Gabapentin in Aqueous Solutions. *Pharm. Res.* **1992**, 9 (5), pp 595-600.
35. Hsu, C. H.; Lin, S. Y. Rapid Examination of the Kinetic Process of Intramolecular Lactamization of Gabapentin Using DSC-FTIR. *Thermochim. Acta* **2009**, 486 (1-2), pp 5-10.
36. Ciavarella, A. B.; Gupta, A.; Sayeed, V. A.; Khan, M. A.; Faustino, P. J. Development and Application of a Validated HPLC Method for the Determination of Gabapentin and its Major Degradation Impurity in Drug Products. *J.Pharm.Biomed.Anal.* **2007**, 43 (5), pp 1647-1653.
37. Cutrignelli, A.; Denora, N.; Lopodota, A.; Trapani, A.; Laquintana, V.; Latrofa, A.; Trapani, G.; Liso, G. Comparative Effects of Some Hydrophilic Excipients on the Rate of Gabapentin and Baclofen Lactamization in Lyophilized Formulations. *Int.J.Pharm.* **2007**, 332 (1-2), pp 98-106.
38. Rowe, R. C.; Sheskey, P. J.; Owen, S. n. C.; Association, A. P., *Handbook of Pharmaceutical Excipients*; Pharmaceutical Press: London, **2006**; Vol. 6.
39. Schmidt, P.; Herzog, R. Calcium Phosphates in Pharmaceutical Tableting. *Pharm. World Sci.* **1993**, 15 (3), pp 116-122.

40. Khawam, A.; Flanagan, D. R. Basics and Applications of Solid-State Kinetics: A Pharmaceutical Perspective. *J. Pharm. Sci.* **2006**, *95* (3), pp 472-498.
41. Khawam, A.; Flanagan, D. R. Solid-State Kinetic Models: Basics and Mathematical Fundamentals. *J. Phys. Chem. B* **2006**, *110* (35), pp 17315-17328.
42. Byrn, S. R.; Byrn, S. *Solid State Chemistry of Drugs*; Academic Press: New York, **1982**.
43. Jacobs, P. Formation and Growth of Nuclei and the Growth of Interfaces in the Chemical Decomposition of Solids: New Insights. *J. Phys. Chem. B* **1997**, *101* (48), pp 10086-10093.
44. Skrdla, P. J. Use of Coupled Rate Equations to Describe Nucleation-and-Branching Rate-Limited Solid-State Processes. *J. Phys. Chem. A* **2004**, *108* (32), pp 6709-6712.
45. Carstensen, J. T. *Advanced Pharmaceutical Solids*; CRC Press: Florida, **2000**.
46. Prout, E.; Tompkins, F. C. The Thermal Decomposition of Potassium Permanganate. *Trans. Faraday Soc.* **1944**, *40*, pp 488-498.
47. Brown, M. E.; Glass, B. D. Pharmaceutical Applications of the Prout-Tompkins Rate Equation. *Int. J. Pharm.* **1999**, *190* (2), pp 129-137.
48. Brown, M. E. The Prout-Tompkins Rate Equation in Solid-State Kinetics. *Thermochim. Acta* **1997**, *300* (1), pp 93-106.
49. Hairer, E.; Lubich, C.; Roche, M. The Numerical Solution of Differential-Algebraic Systems by Runge-Kutta Methods; Springer-Verlag: Berlin Heidelberg, **1989**; Vol. 1409.
50. Romanelli, M. J. Runge-Kutta Methods for the Solution of Ordinary Differential Equations. *Mathematical Methods for Digital Computers* **1960**, *1*, pp 110-120.
51. Brown, A. M. A Step-by-Step Guide to Non-linear Regression Analysis of Experimental Data Using a Microsoft Excel Spreadsheet. *Computer Methods and Programs in Biomedicine*; Wiley: New Jersey, **2001**, Vol. *65* (3), pp 191-200.
52. Kushnir, M.; Crossett, J.; Brown, P.; Urry, F. Analysis of Gabapentin in Serum and Plasma by Solid-Phase Extraction and Gas Chromatography-Mass Spectrometry for Therapeutic Drug Monitoring. *J. Anal. Toxicol.* **1999**, *23* (1), pp 1-6.
53. Marquardt, D. W. An Algorithm for Least-Squares Estimation of Nonlinear Parameters. *Journal of the Society for Industrial & Applied Mathematics (SIAM)* **1963**, *11* (2), pp 431-441.
54. Burington, R. S.; May, D. C. Handbook of Probability and Statistics with Tables; Handbook Publishers Inc.: Ohio, **1953**.

55. Augsburger, L. L.; Hoag, S. W. *Pharmaceutical Dosage Forms: Tablets*; Informa healthcare: London, **2008**; Vol. 3.
56. Duberg, M.; Nystrom, C. Studies on Direct Compression of Tablets XVII. Porosity-Pressure Curves for the Characterization of Volume Reduction Mechanisms in Powder Compression. *Powder Technol.* **1986**, *46* (1), pp 67-75.
57. Hardman, J.; Lilley, B. Deformation of Particles During Briquetting. *Nature* **1970**, *228*, pp 353-355.
58. Sixsmith, D. The Compression Characteristics of Microcrystalline Cellulose Powders. *J. Pharm. Pharmacol.* **1982**, *34* (5), pp 345-346.
59. Adams, M.; Mullier, M.; Seville, J. Agglomerate Strength Measurement Using a Uniaxial Confined Compression Test. *Powder Technol.* **1994**, *78* (1), pp 5-13.
60. Akande, O.; Rubinstein, M.; Rowe, P.; Ford, J. Effect of Compression Speeds on the Compaction Properties of a 1: 1 Paracetamol and Microcrystalline Cellulose Mixture Prepared by Single Compression and by Combinations of Pre-compression and Main-compression. *Int. J. Pharm.* **1997**, *157* (2), pp 127-136.
61. Altaf, S. A.; Hoag, S. W. Deformation of the Stokes B2 Rotary Tablet Press: Quantitation and Influence on Tablet Compaction. *J. Pharm. Sci.* **1995**, *84* (3), pp 337-343.
62. Amidon, G. E.; Houghton, M. E. The Effect of Moisture on the Mechanical and Powder Flow Properties of Microcrystalline Cellulose. *Pharm. Res.* **1995**, *12* (6), pp 923-929.
63. Israelachvili, J. N. *Intermolecular and Surface Forces*; revised third edition; Academic press: Massachusetts, **2011**.
64. Derjaguin, B.; Abrikosova, I.; Lifshitz, E. Direct Measurement of Molecular Attraction Between Solids Separated by a Narrow Gap. *Q. Rev. Chem. Soc.* **1956**, *10* (3), pp 295-329.
65. Lachman, L.; Lieberman, H.A.; Kanig, J.L. *The Theory of Industrial Pharmacy*; Lea and Febiger: Philadelphia, 1999.
66. Israelachvili, J.; Tabor, D. The Shear Properties of Molecular Films. *Wear* **1973**, *24* (3), pp 386-390.
67. Akande, O. F.; Ford, J. L.; Rowe, P. H.; Rubinstein, M. H. The Effects of Lag-time and Dwell-time on the Compaction Properties of 1: 1 Paracetamol/microcrystalline Cellulose Tablets Prepared by Pre-compression and Main Compression. *J. Pharm. Pharmacol.* **1998**, *50* (1), pp 19-28.
68. Derjaguin, B. V., The force between molecules. *Sci. Am.* **1960**, *203*, pp 47-53.

69. Suzuki, T.; Nakagami, H. Effect of Crystallinity of Microcrystalline Cellulose on the Compactability and Dissolution of Tablets. *Eur. J. Pharm. Biopharm.* **1999**, *47* (3), pp 225-230.
70. Suihko, E.; Lehto, V.-P.; Ketolainen, J.; Laine, E.; Paronen, P. Dynamic Solid-State and Tableting Properties of Four Theophylline Forms. *Int. J. Pharm.* **2001**, *217* (1), pp 225-236.
71. Johansson, B.; Wikberg, M.; Ek, R.; Alderborn, G. Compression Behaviour and Compactability of Microcrystalline Cellulose Pellets in Relationship to Their Pore Structure and Mechanical Properties. *Int. J. Pharm.* **1995**, *117* (1), pp 57-73.
72. Garekani, H. A.; Ford, J. L.; Rubinstein, M. H.; Rajabi-Siahboomi, A. R. Effect of Compression Force, Compression Speed, and Particle Size on the Compression Properties of Paracetamol. *Drug Dev. Ind. Pharm.* **2001**, *27* (9), pp 935-942.
73. Chang, R.-K.; Leonzio, M.; Hussain, M. A.; Hussain, M. Effect of Colloidal Silicon Dioxide on Flowing and Tableting Properties of an Experimental, Crosslinked Polyalkylammonium Polymer. *Pharm. Dev. Technol.* **1999**, *4* (2), pp 285-289.
74. Ohta, K. M.; Fuji, M.; Takei, T.; Chikazawa, M. Effect of Geometric Structure and Surface Wettability of Glidant on Tablet Hardness. *Int. J. Pharm.* **2003**, *262* (1), pp 75-82.
75. Nokhodchi, A. Effect of Moisture on Compaction and Compression. *Pharm. Tech* **2005**, *6*, pp 46-66.
76. Sebhatu, T.; Ahlneck, C.; Alderborn, G. R. The Effect of Moisture Content on the Compression and Bond-Formation Properties of Amorphous Lactose Particles. *Int. J. Pharm.* **1997**, *146* (1), pp 101-114.
77. Bravo-Osuna, I.; Ferrero, C.; Jimenez-Castellanos, M. Influence of Moisture Content on the Mechanical Properties of Methyl Methacrylate and Starch Co-polymers. *Eur. J. Pharm. Biopharm.* **2007**, *66* (1), pp 63-72.
78. Heckel, R. Density-Pressure Relationships in Powder Compaction. *Trans Metall Soc. AIME* **1961**, *221* (4), pp 671-675.
79. Denny, P. Compaction Equations: a Comparison of the Heckel and Kawakita Equations. *Powder Technol.* **2002**, *127* (2), pp 162-172.
80. Van Veen, B.; Bolhuis, G.; Wu, Y.; Zuurman, K.; Frijlink, H. Compaction Mechanism and Tablet Strength of Unlubricated and Lubricated (silicified) Microcrystalline Cellulose. *Eur. J. Pharm. Biopharm.* **2005**, *59* (1), pp 133-138.
81. Wikberg, M.; Alderborn, G. R. Compression Characteristics of Granulated Materials: VI. Pore Size Distributions Assessed by Mercury Penetration of Compacts of Two Lactose Granulations with Different Fragmentation Propensities. *Int. J. Pharm.* **1992**, *84* (2), pp 191-195.

82. Chang, S. Y.; Wang, F.-Y. Determination of Gabapentin in Human Plasma By Capillary Electrophoresis with Laser-induced Fluorescence Detection and Acetonitrile Stacking Technique. *Journal of Chromatogr., B Anal. Technol. Biomed. Life Sci.* **2004**, 799 (2), pp 265-270.
83. Vermeij, T.; Edelbroek, P. Simultaneous High-Performance Liquid Chromatographic Analysis of Pregabalin, Gabapentin and Vigabatrin in Human Serum by Pre-column Derivatization with Phtaldialdehyde and Fluorescence Detection. *Journal of Chromatogr. B. Anal. Technol. Biomed. Life Sci.* **2004**, 810 (2), pp 297-303.
84. Hengy, H.; Kalle, E.-U. Determination of Gabapentin in Plasma and Urine by High-Performance Liquid Chromatography and Pre-column Labelling for Ultraviolet Detection. *Journal of Chromatogr. B Anal. Technol. Biomed. Life Sci.* **1985**, 341, pp 473-478.
85. Ifa, D. R.; Falci, M.; Moraes, M. E.; Bezerra, F. A.; Moraes, M. O.; Nucci, G. d. Gabapentin Quantification in Human Plasma by High-Performance Liquid Chromatography Coupled to Electrospray Tandem Mass Spectrometry: Application to Bioequivalence Study. *J. Mass Spectrom.* **2001**, 36 (2), pp 188-194.
86. Ramakrishna, N.; Vishwottam, K.; Koteswara, M.; Manoj, S.; Santosh, M.; Chidambara, J.; Sumatha, B.; Varma, D. Rapid Quantification of Gabapentin in Human Plasma by Liquid Chromatography/Tandem Mass Spectrometry. *J. Pharm. Biomed. Anal.* **2006**, 40 (2), pp 360-368.
87. Validation of Analytical Procedures: Technical Requirements For The Registration of Pharmaceuticals For Human Use. Int. Conf. on Harmonization (ICH)-Q2A Geneva: **1995**.
88. de Levie, R. Estimating Parameter Precision in Nonlinear Least Squares with Excel's Solver. *J. Chem. Educ.* **1999**, 76 (11), pp 1594-1598.
89. Komatsu, W. Study of Solid-State Reaction. Part 2. Kinetics of Solid-State Reaction. *J. Chem. Soc. Japan* **1953**, 74, pp 601-603.
90. Hao, Y. J.; Tanaka, T. Role of the Contact Points Between Particles on the Reactivity of Solids. *Can. J. Chem. Eng.* **1988**, 66 (5), pp 761-766.

Appendix 1

Supporting data Chapter 1

1. Analytical method validation: Specificity (matrix effect)

- The results confirmed the absence of excipient interaction in the elution of gabapentin and lactam.
- Excipient solutions were analyzed using the HPLC technique, to identify for any peaks specific to the excipients, interfering with the elution of either gabapentin and/or lactam
- The concentration of the excipient solution (4mg/ml) was selected based on the expected concentration in the solutions of their physical mixtures and compacts with gabapentin.

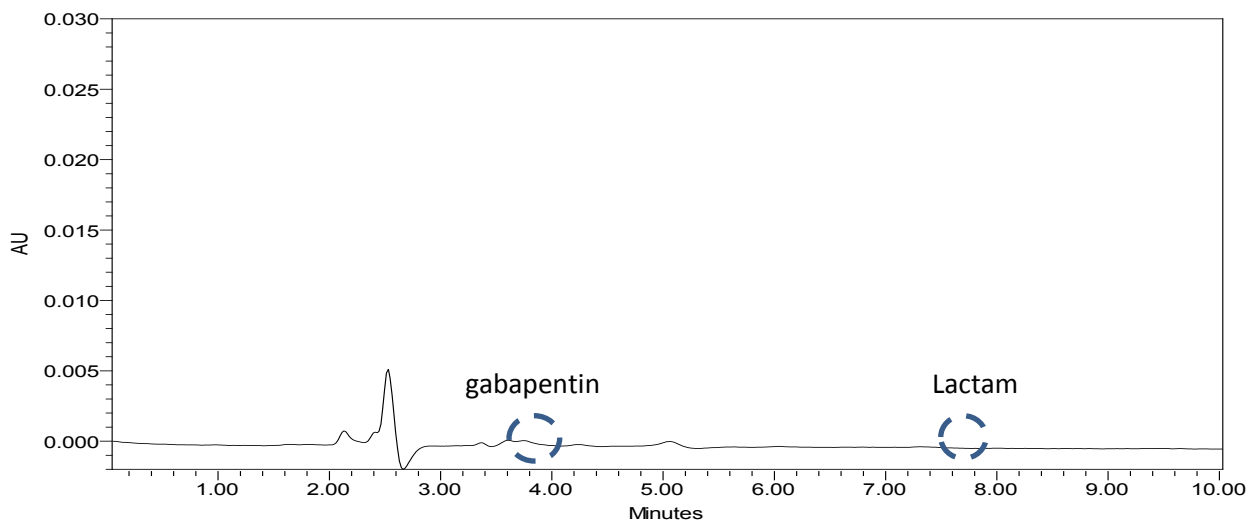


Figure 51: The chromatogram for HPC at a concentration of 4 mg/ml

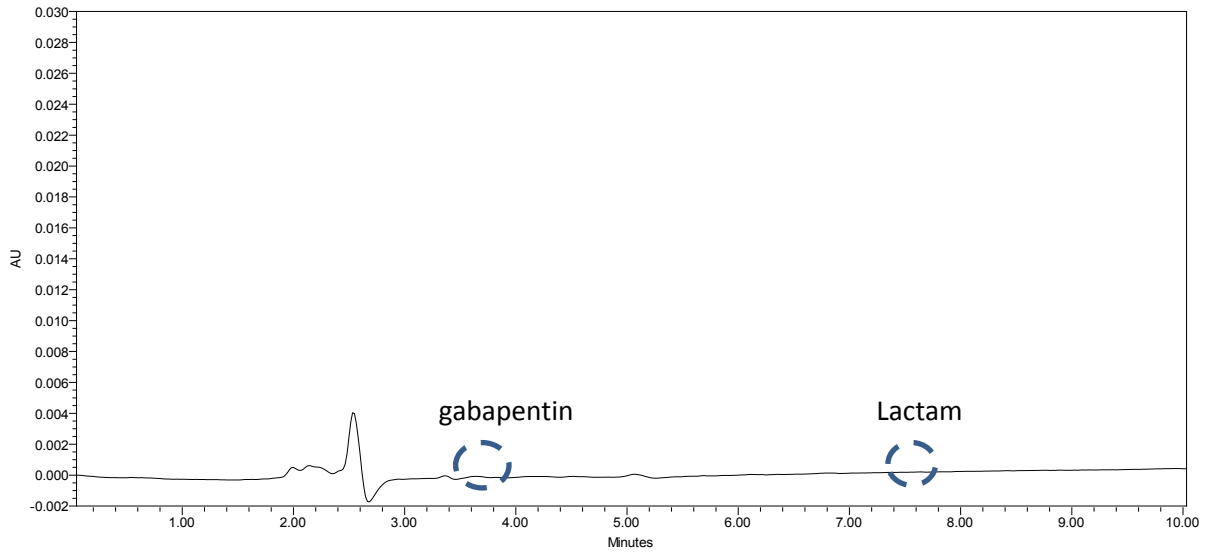


Figure 52: The chromatogram for HPMC at a concentration of 4 mg/ml

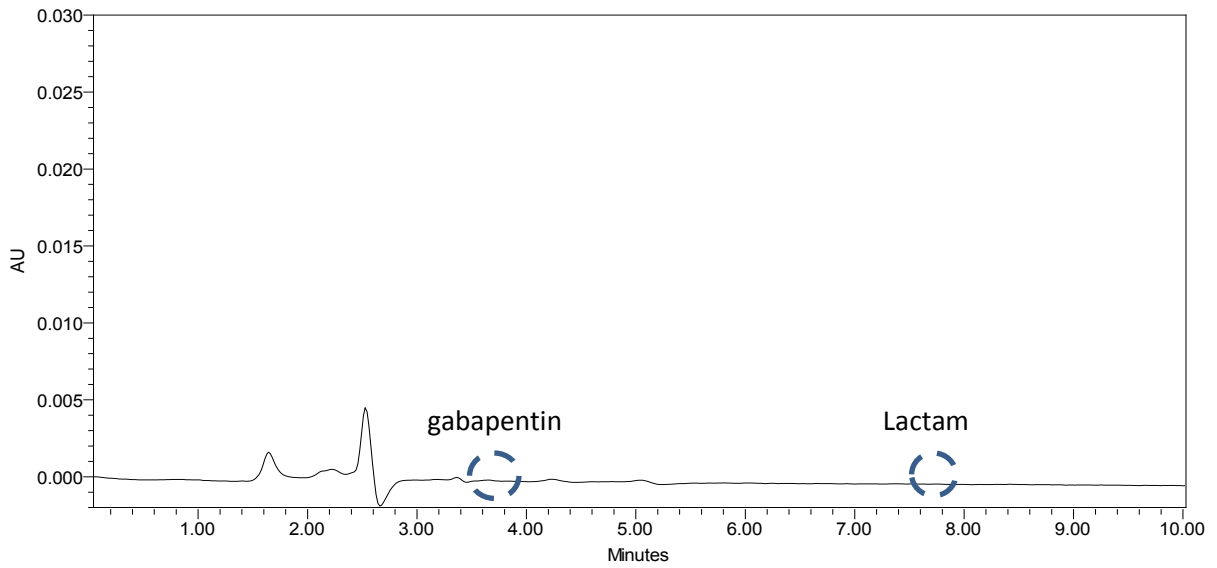


Figure 53: The chromatogram for starch at a concentration of 4 mg/ml

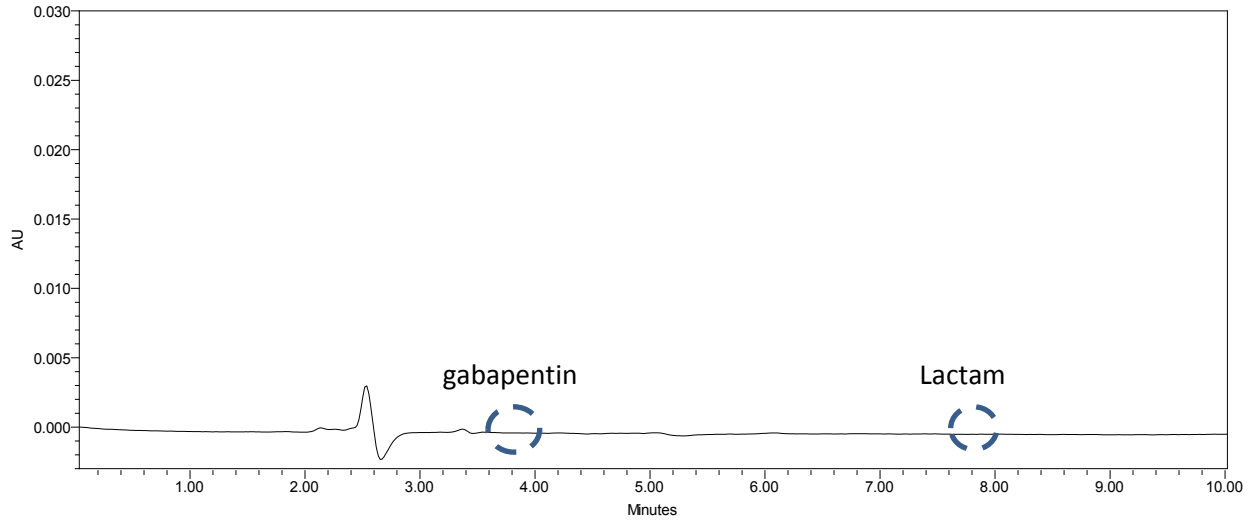


Figure 54: The chromatogram for talc at a concentration of 4 mg/ml

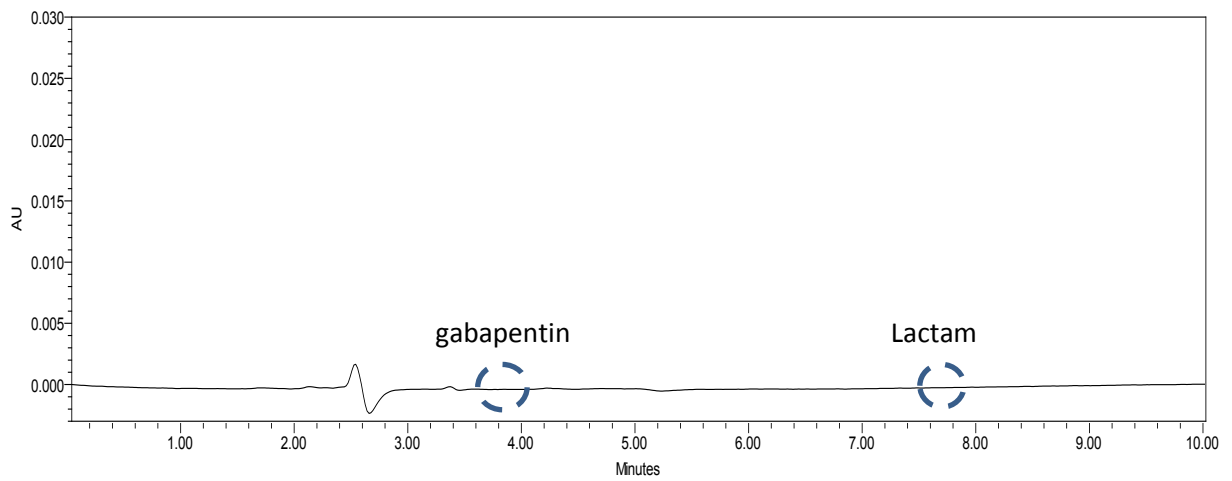


Figure 55: The chromatogram for Emcompress[®] at a concentration of 4 mg/ml

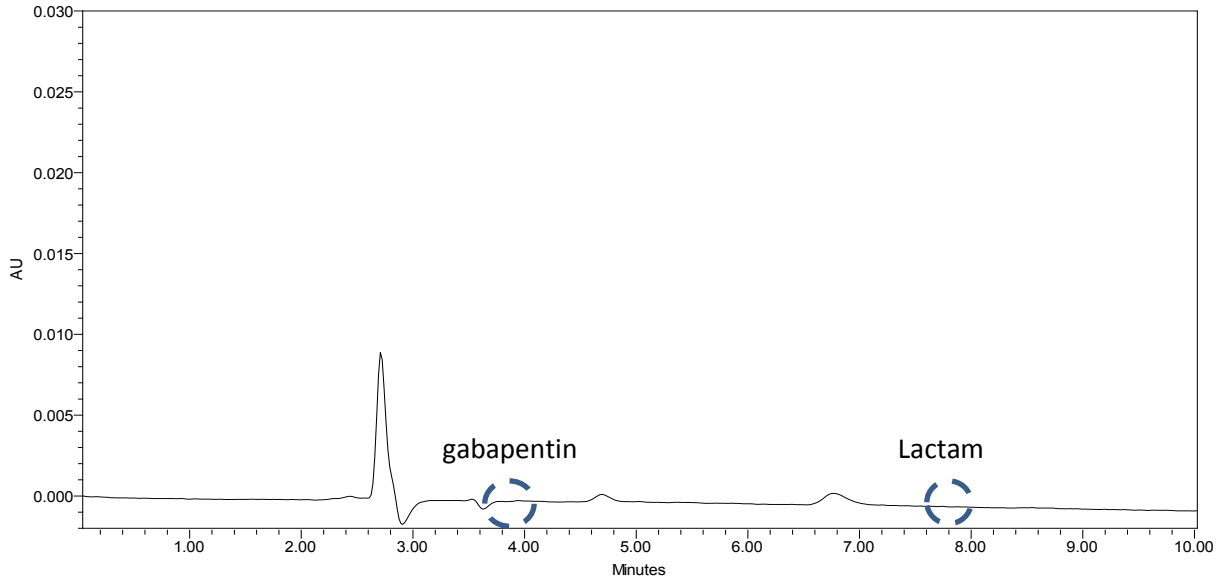


Figure 56: The chromatogram for Tri-Tab[®] at a concentration of 4 mg/ml

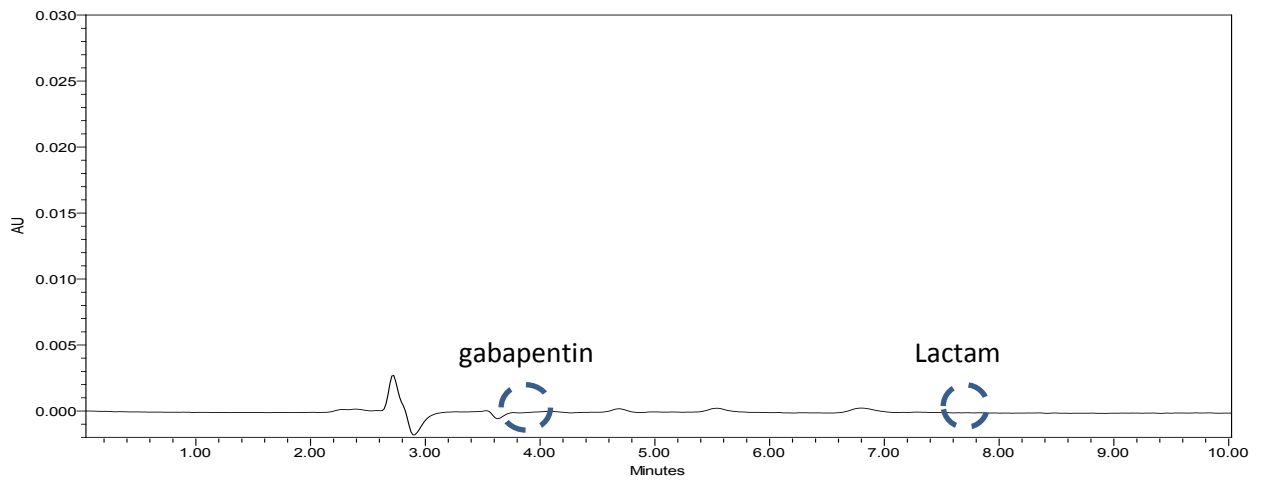


Figure 57: The chromatogram for A-Tab[®] at a concentration of 4 mg/ml

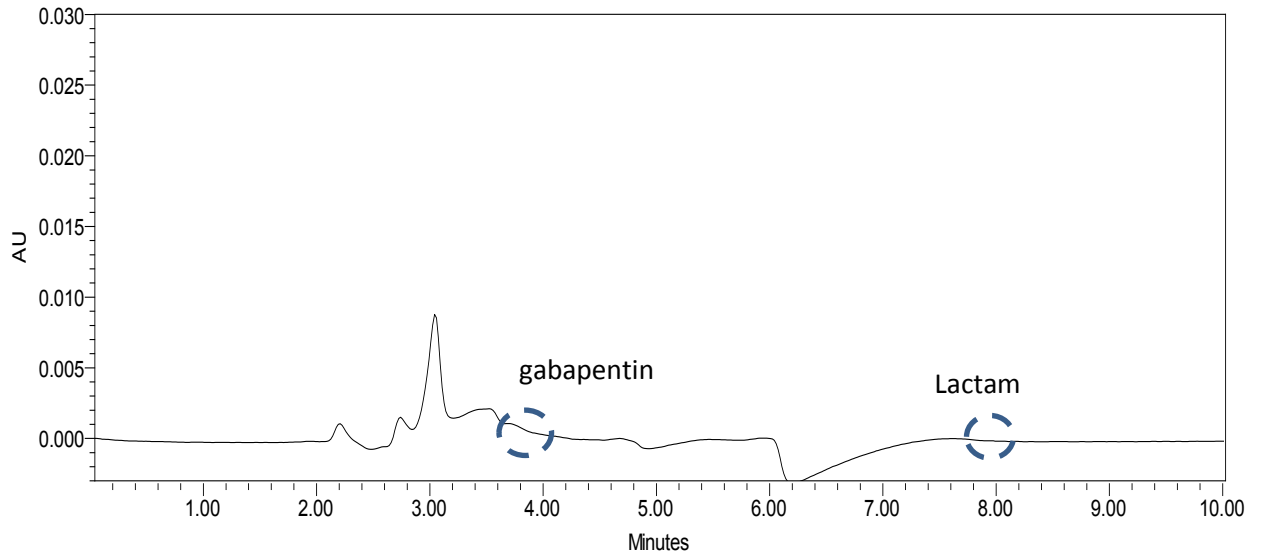


Figure 58: The chromatogram for Mono-Tab at a concentration of 4 mg/ml

Appendix 2

Supporting documentation for chapter 4

Specific surface area measurements

- Multipoint measurements were performed using nitrogen vapor adsorption data with subsequent application of the BET model
- Material weight: 1.00-1.5 g
- Samples were outgassed at high temperatures (50-200°C depending on the material) for more than 24 h.
- Single sample of each excipient was analyzed
- The moles of nitrogen adsorbed at each partial pressure was analyzed using the BET equation (Equation 23)
- Specific surface area was calculated as the quotient of the samples total surface area and mass

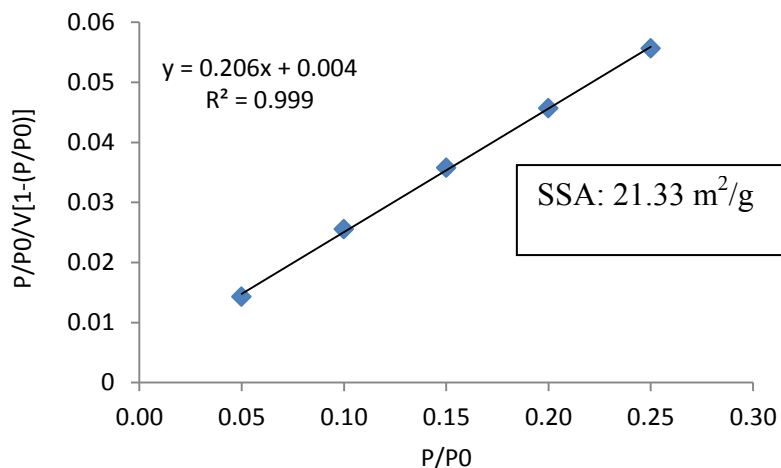


Figure 59: A multi-point BET measurement for Kaolinite reference standard.

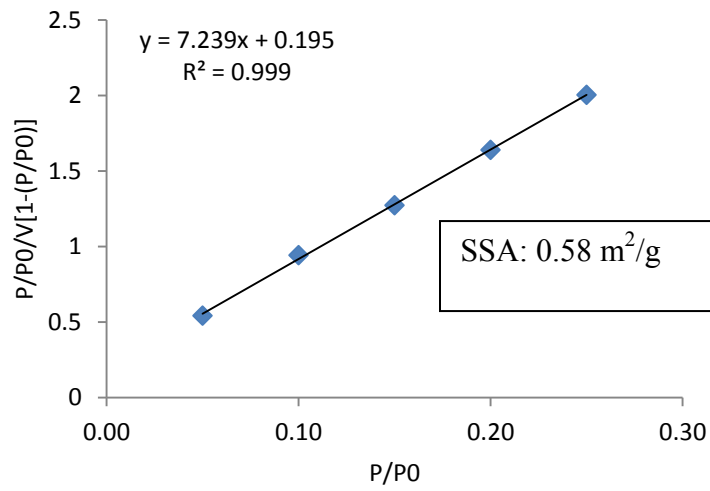


Figure 60: A multi-point BET measurement for Alumina reference standard.

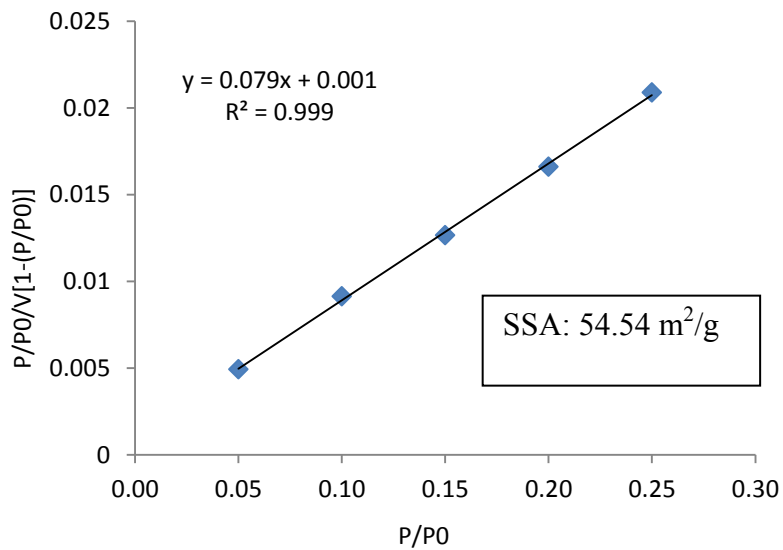


Figure 61: A multi-point BET measurement for Tri-Tab[®]

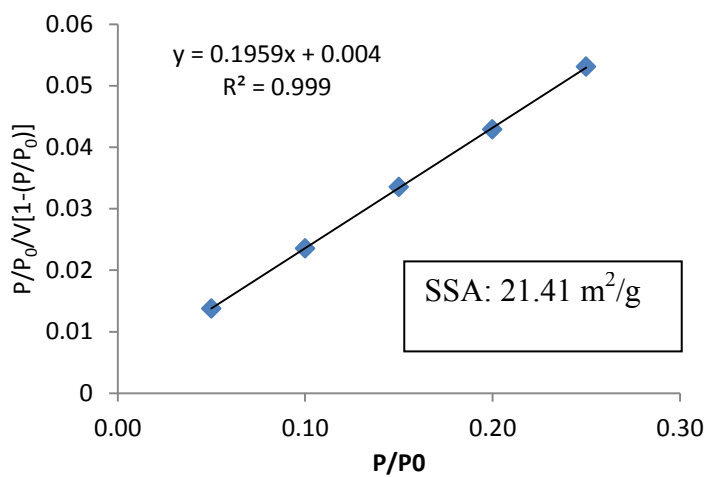


Figure 62: A multi-point BET measurement for A-Tab[®] 75-125µm

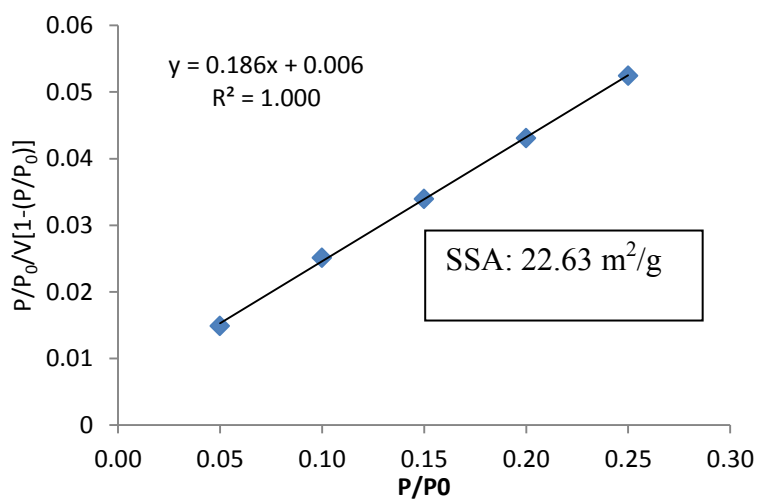


Figure 63: A multi-point BET measurement for A-Tab[®] 125-250µm

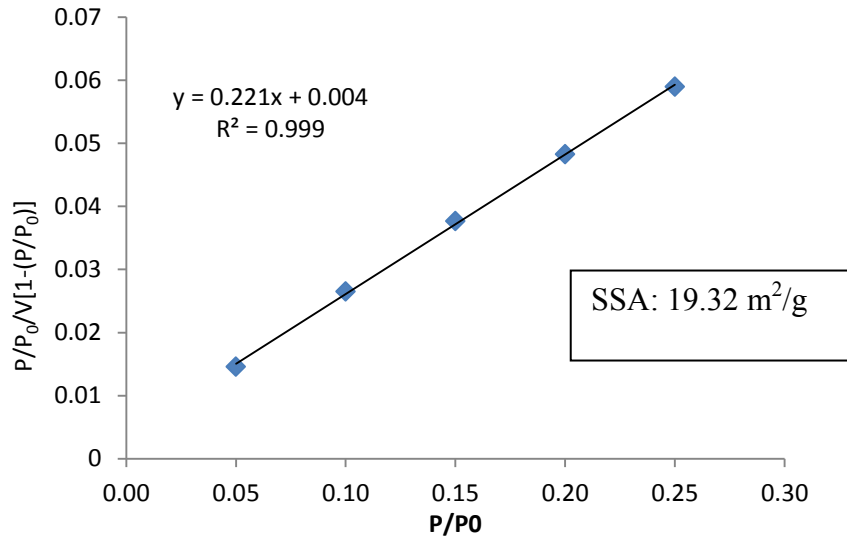


Figure 64: A multi-point BET measurement for A-Tab[®] 250-500 μm

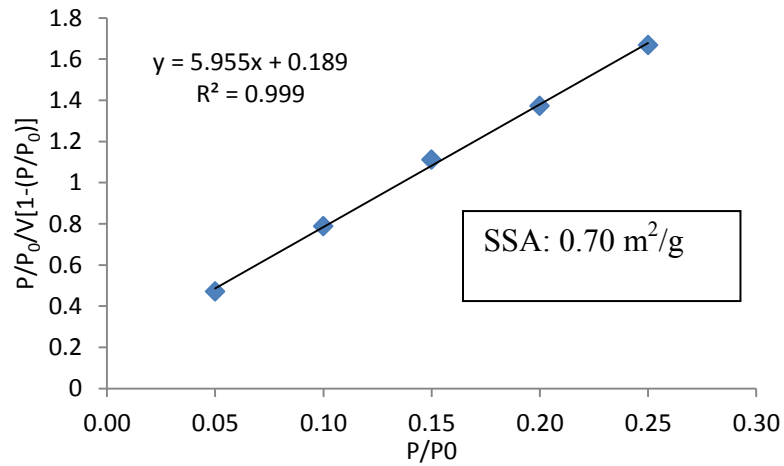


Figure 65: A multi-point BET measurement for Mono-Tab[®]

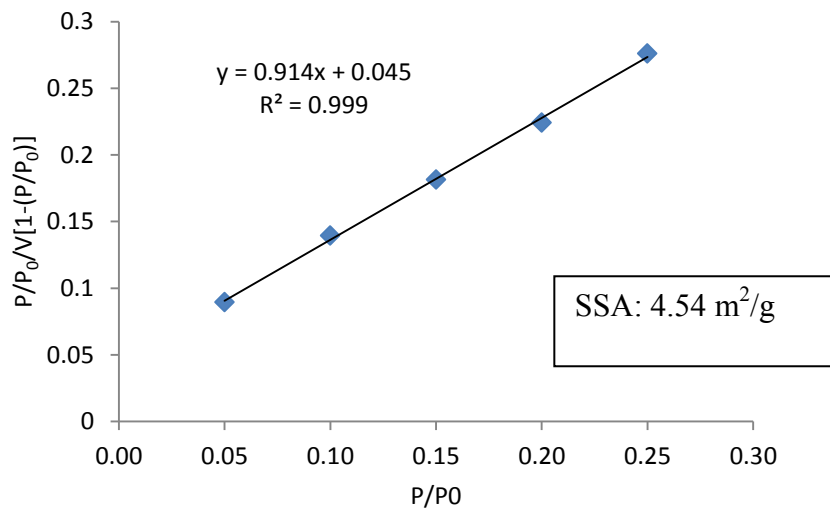


Figure 66: A multi-point BET measurement for Emcompress®

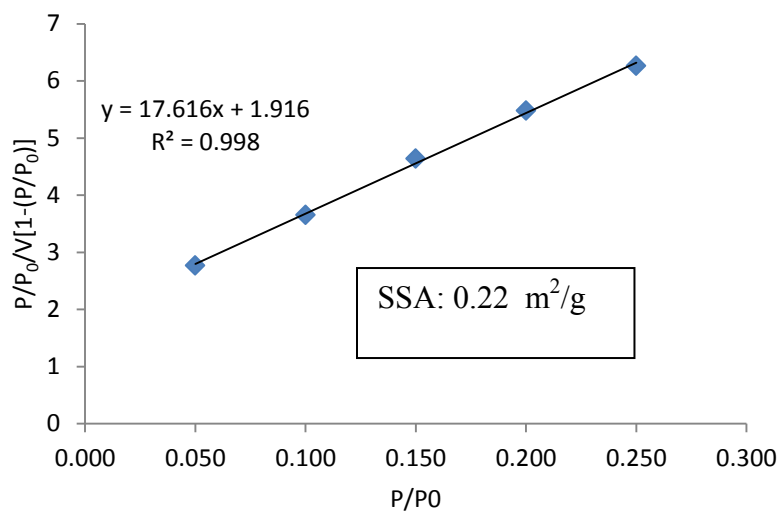


Figure 67: A multi-point BET measurement for starch

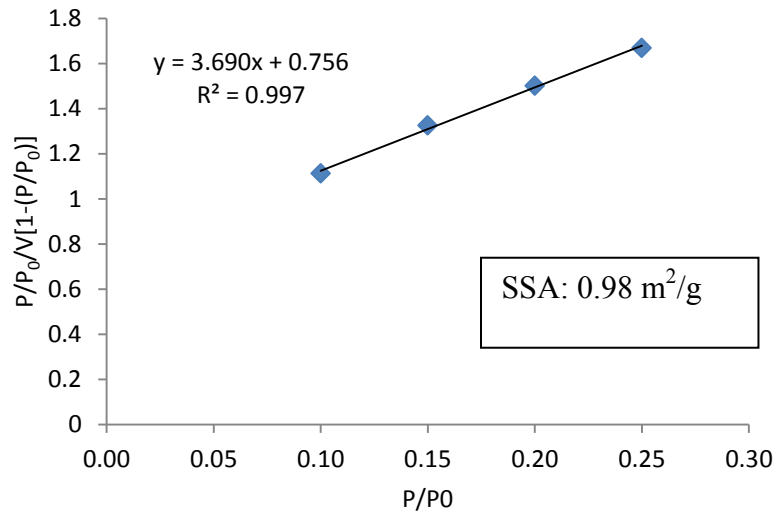


Figure 68: A multi-point BET measurement for HPMC

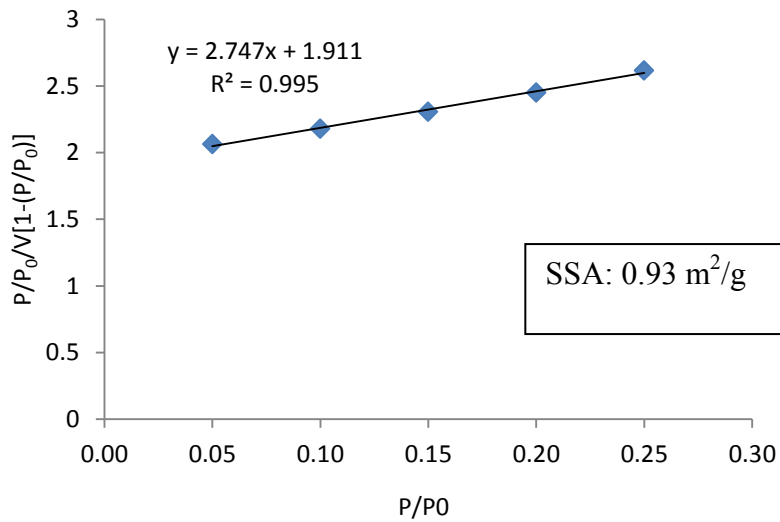


Figure 69: A multi-point BET measurement for HPC

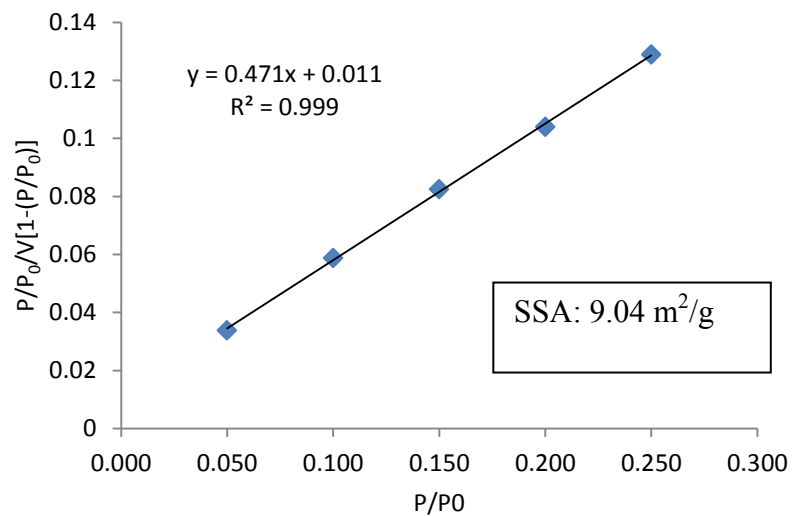


Figure 70: A multi -point BET measurement for talc

Molecular Cross-Sectional area measurements

Computation of molecular cross-sectional area for excipients,

Step 1: Structures of the excipients were constructed using Chem-Draw[®]

Step 2: Transformation of 2-D structures to 3-D structures was performed on MOE[®]

Step 3: Energy minimization was performed using MMF94X force field in MOE[®]

Step 4: Bond distances for different molecular orientations of the excipients were measured. Two major orientations of the molecules on the surface of the excipient particle were assumed.

Step 5: Surface for the excipient structure in 3-D was generated. The colors on the surface were indicative of H-bonding sites (Pink), hydrophobic sites (Blue), and mild polar sites (green).

Step 6: The final distances (length and breadth) across the molecular surface for the two orientations were measured and the van-del-Waals radii for atoms was added to the measured bond lengths

Step 7: The molecular cross sectional area ($A = \pi(\text{length major axis} \times \text{length minor axis})$) was calculated assuming an ellipsoidal geometry at the cross section.

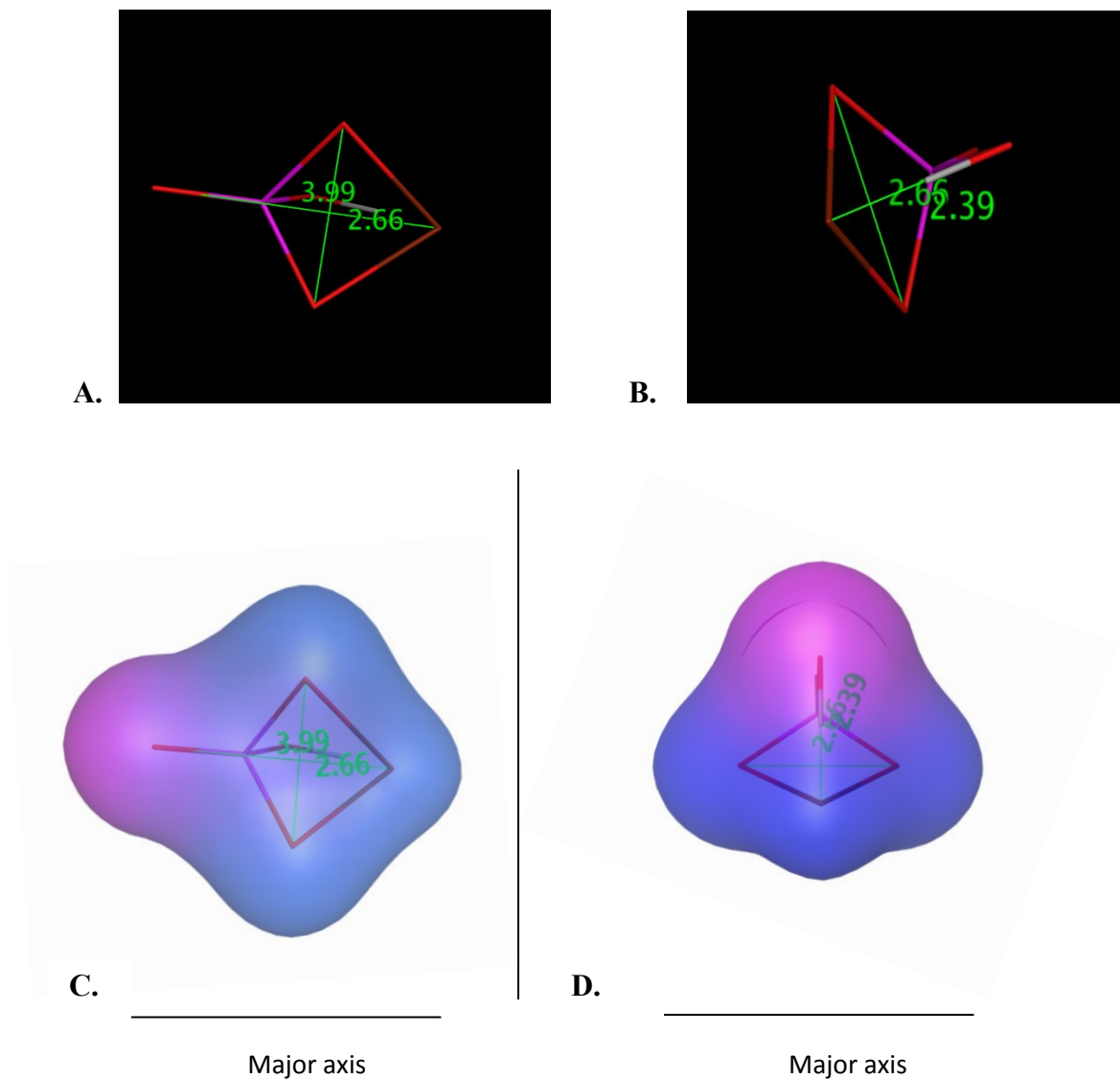


Figure 71: Computation of molecular cross-sectional area for A-tab[®]

A. Measured dimensions (bond length measuring length and breadth) for Orientation 1 of the molecule. **B.** Measured dimensions for orientation 2 of the molecule. **C.** Surface constructed for the molecule in orientation 1. **D.** Surface constructed for the molecule in orientation 2. The surface accounts for the van-der Waals radii of atoms.

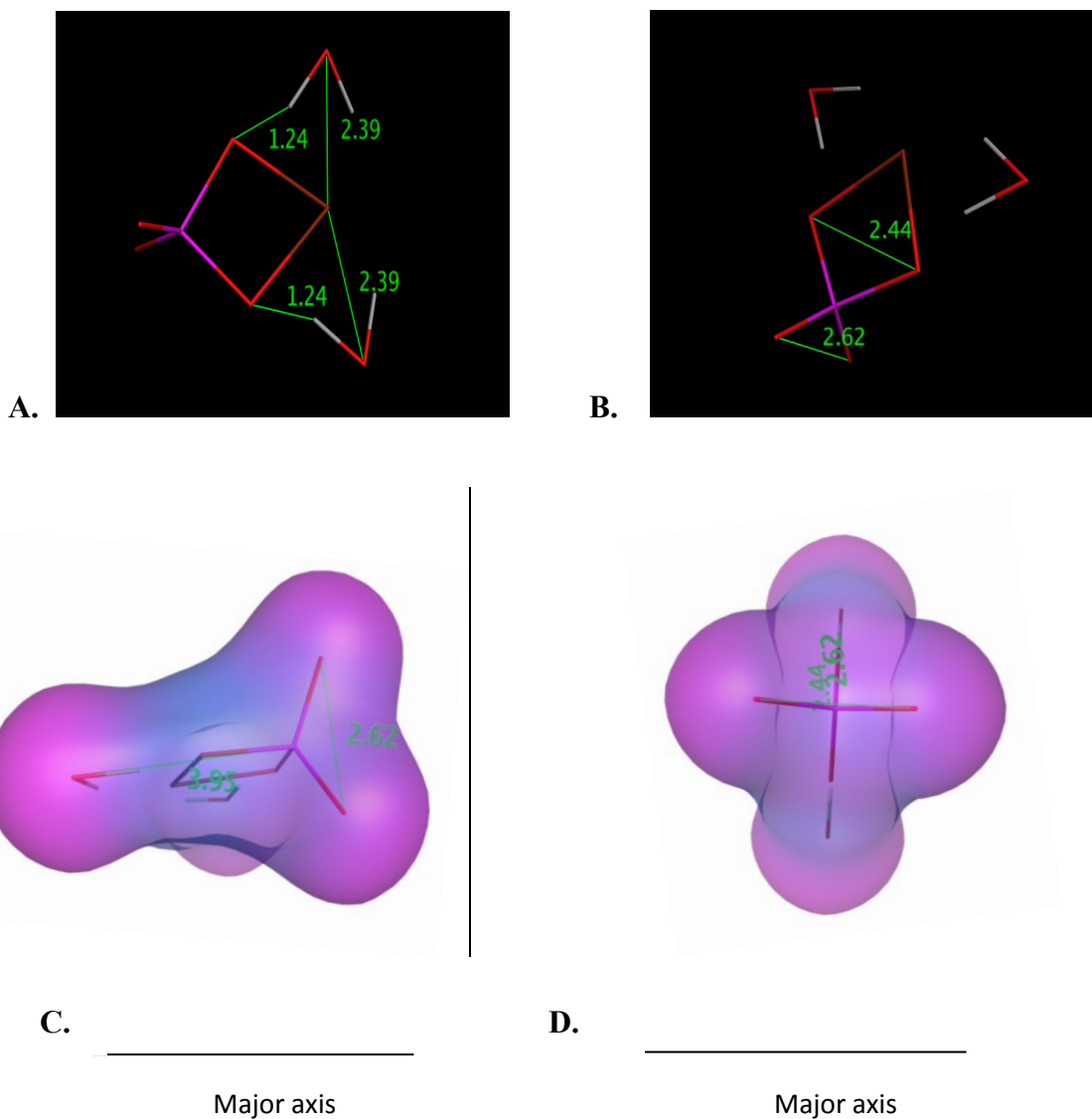


Figure 72: Computation of molecular cross-sectional area for Emcompress[®]

A. Measured dimensions (bond length measuring length and breadth) for Orientation 1 of the molecule. **B.** Measured dimensions for orientation 2 of the molecule. **C.** Surface constructed for the molecule in orientation 1. **D.** Surface constructed for the molecule in orientation 2. The surface accounts for the van-der Waals radii of atoms.

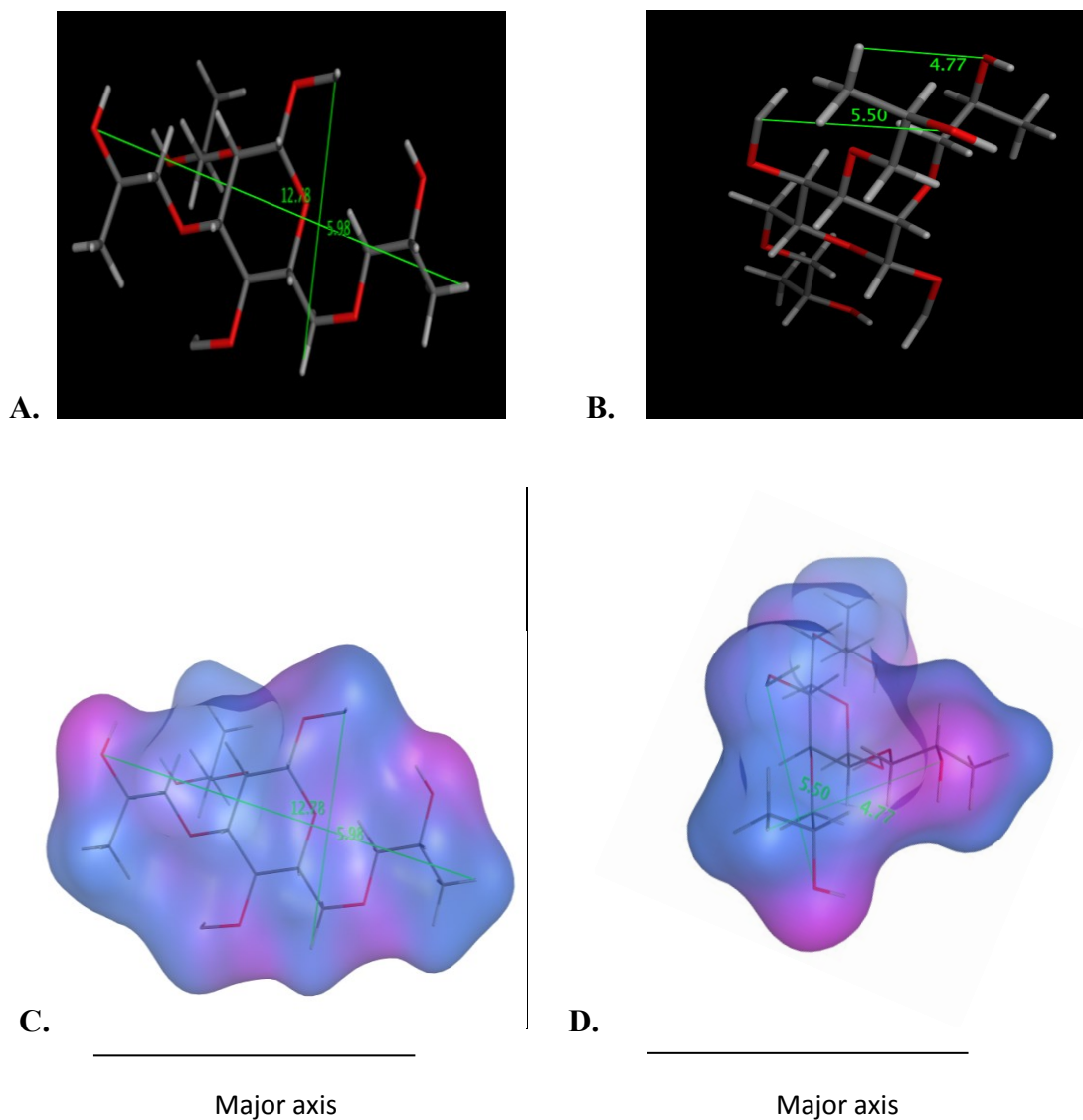


Figure 73: Computation of molecular cross-sectional area for HPC

A. Measured dimensions (bond length measuring length and breadth) for Orientation 1 of the molecule. **B.** Measured dimensions for orientation 2 of the molecule. **C.** Surface constructed for the molecule in orientation 1. **D.** Surface constructed for the molecule in orientation 2. The surface accounts for the van-der Waals radii of atoms.

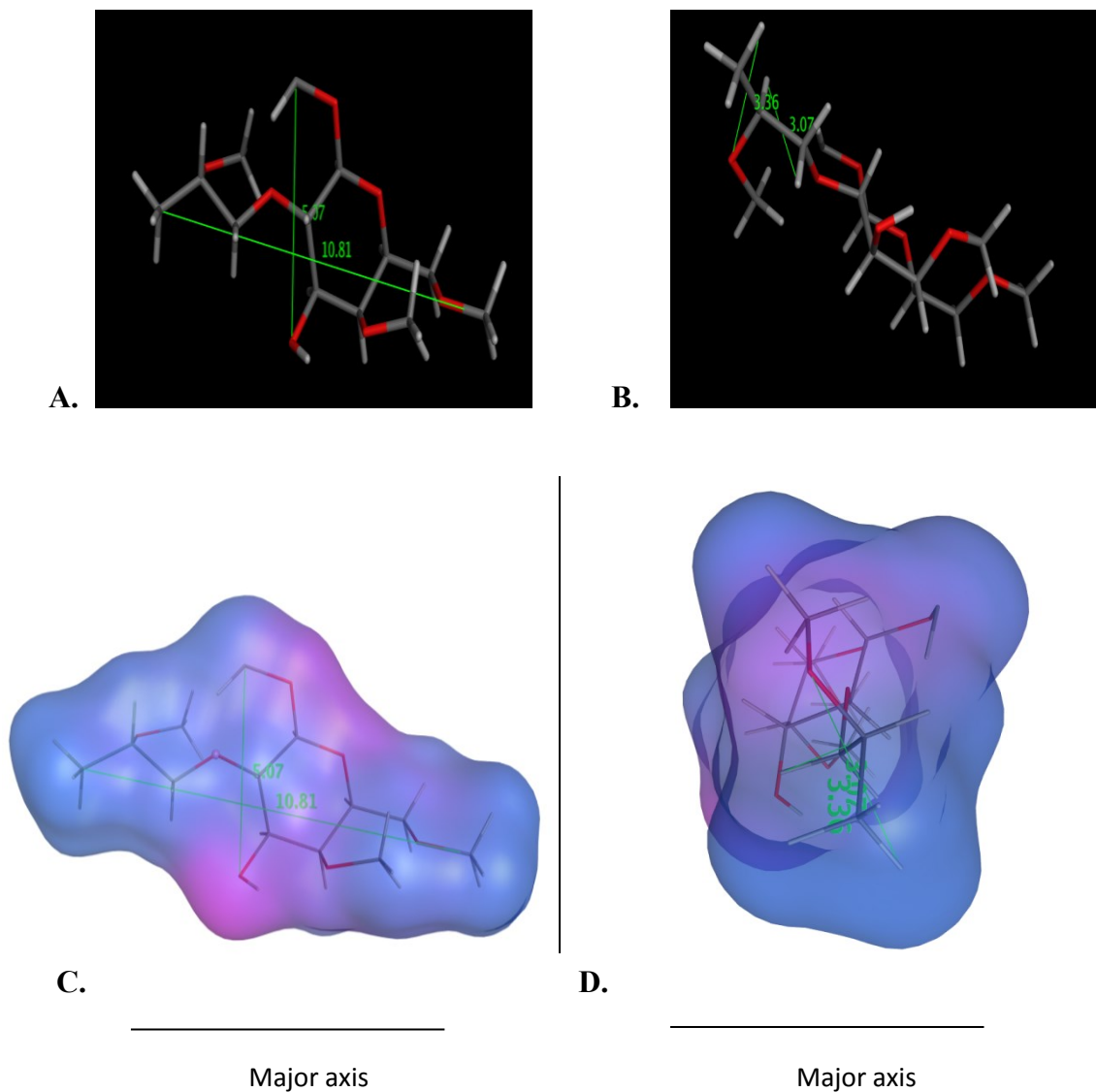


Figure 74: Computation of molecular cross-sectional area for HPMC

A. Measured dimensions (bond length measuring length and breadth) for Orientation 1 of the molecule. **B.** Measured dimensions for orientation 2 of the molecule. **C.** Surface constructed for the molecule in orientation 1. **D.** Surface constructed for the molecule in orientation 2. The surface accounts for the van-der Waals radii of atoms.

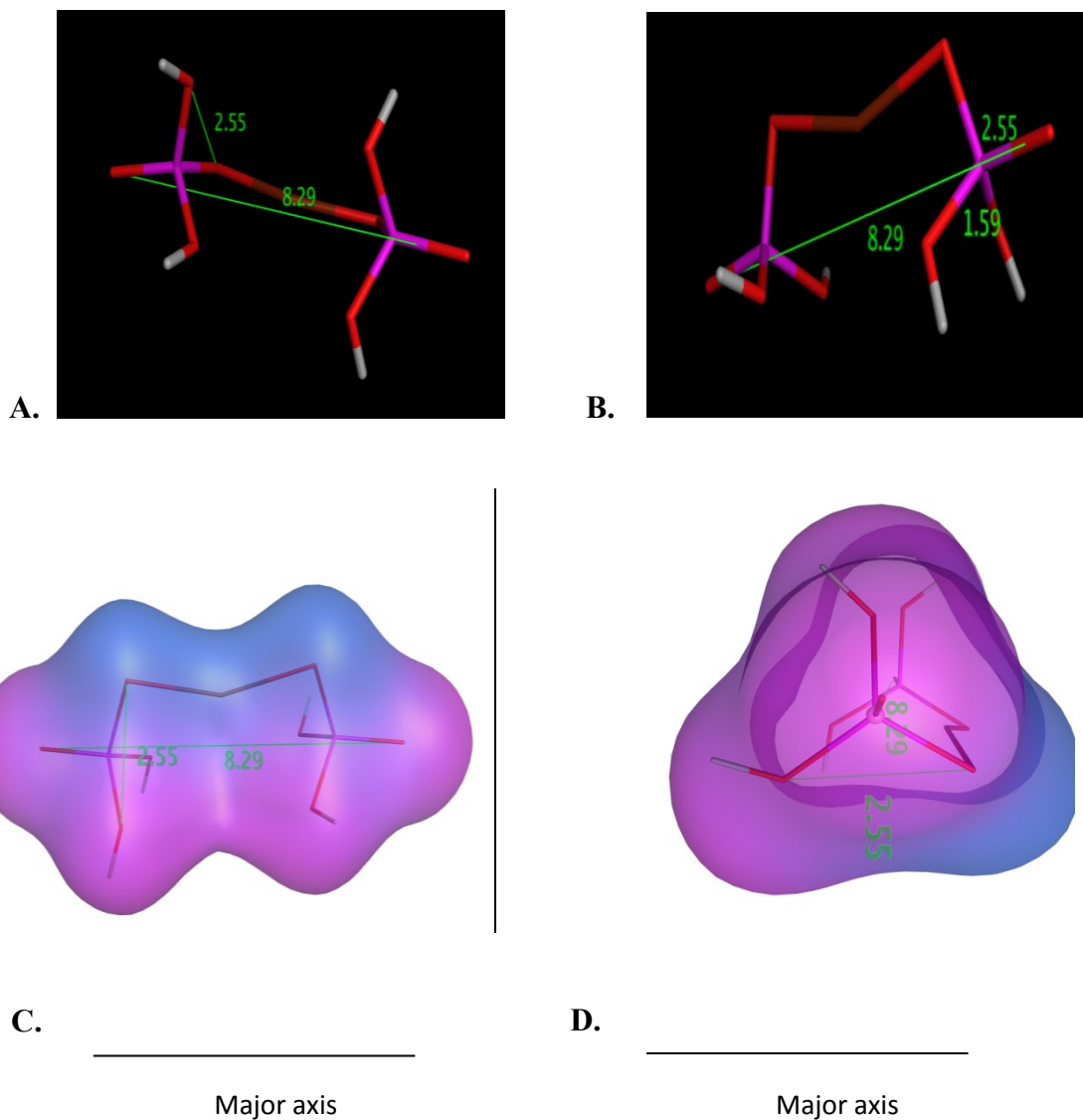


Figure 75: Computation of molecular cross-sectional area for Mono-Tab

A. Measured dimensions (bond length measuring length and breadth) for Orientation 1 of the molecule. **B.** Measured dimensions for orientation 2 of the molecule. **C.** Surface constructed for the molecule in orientation 1. **D.** Surface constructed for the molecule in orientation 2. The surface accounts for the van-der Waals radii of atoms.

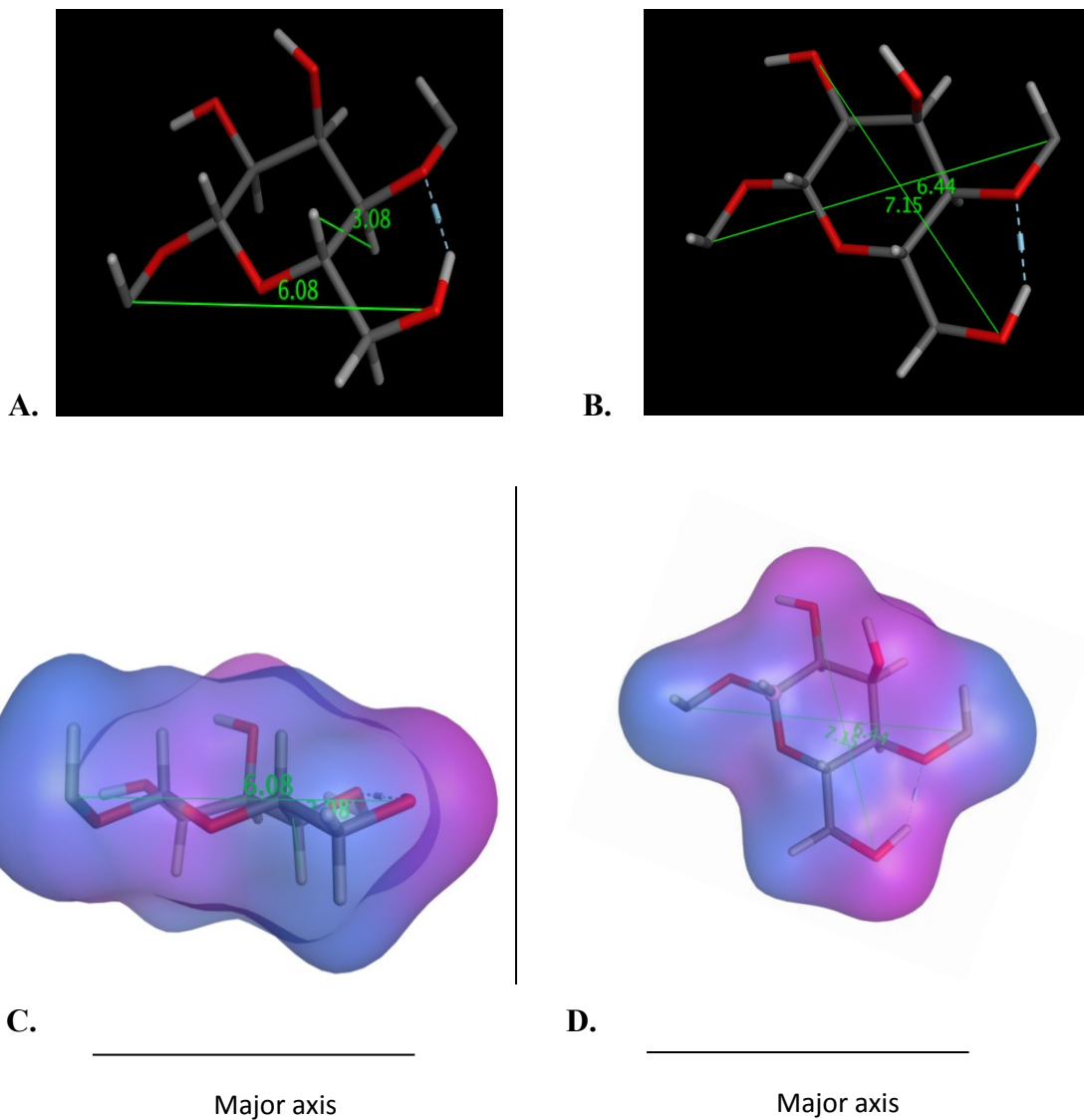


Figure 76: Computation of molecular cross-sectional area for starch

A. Measured dimensions (bond length measuring length and breadth) for Orientation 1 of the molecule. **B.** Measured dimensions for orientation 2 of the molecule. **C.** Surface constructed for the molecule in orientation 1. **D.** Surface constructed for the molecule in orientation 2. The surface accounts for the van-der Waals radii of atoms.

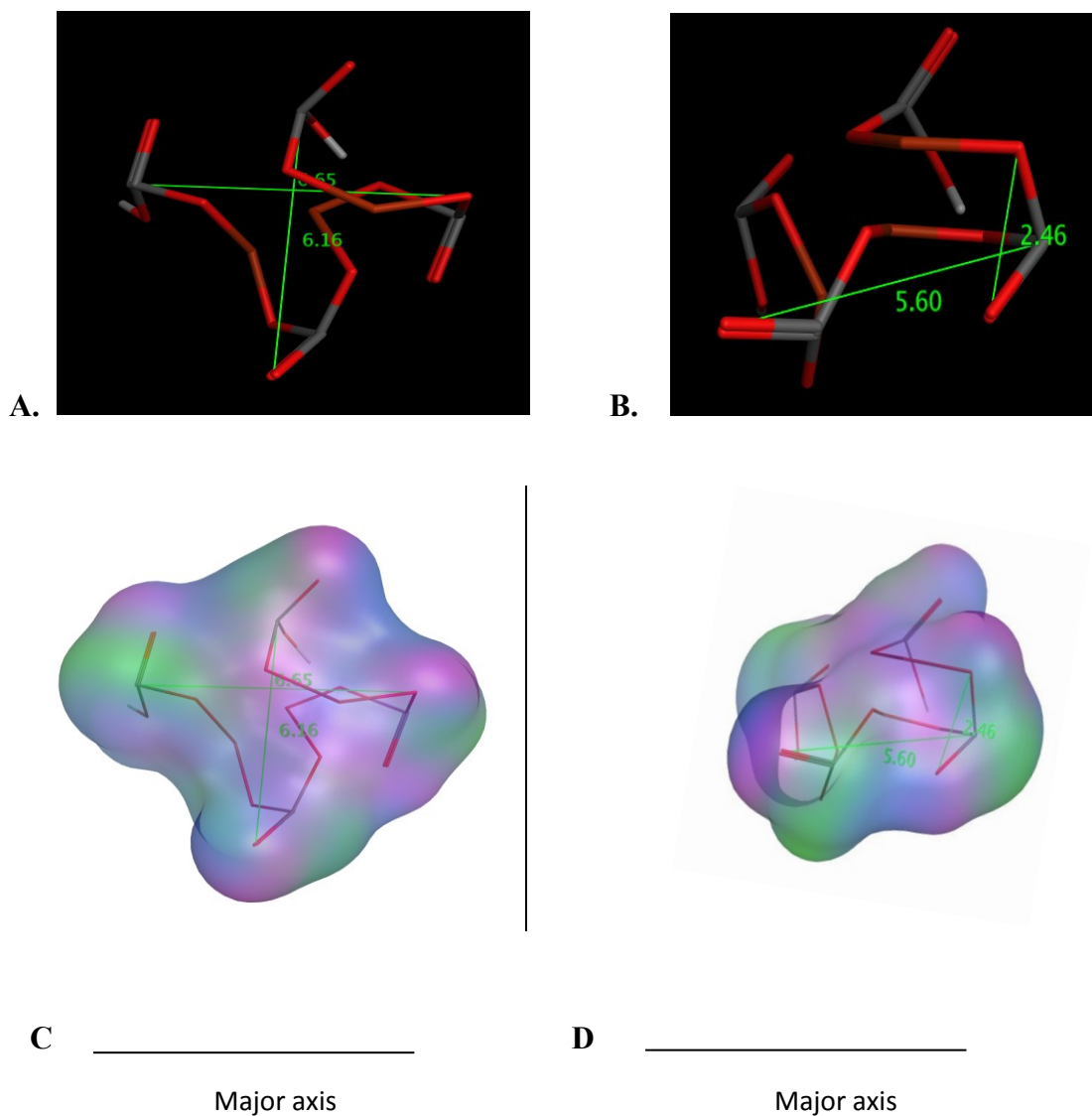


Figure 77: Computation of molecular cross-sectional area for talc

A. Measured dimensions (bond length measuring length and breadth) for Orientation 1 of the molecule. **B.** Measured dimensions for orientation 2 of the molecule. **C.** Surface constructed for the molecule in orientation 1. **D.** Surface constructed for the molecule in orientation 2. The surface accounts for the van-der Waals radii of atoms.

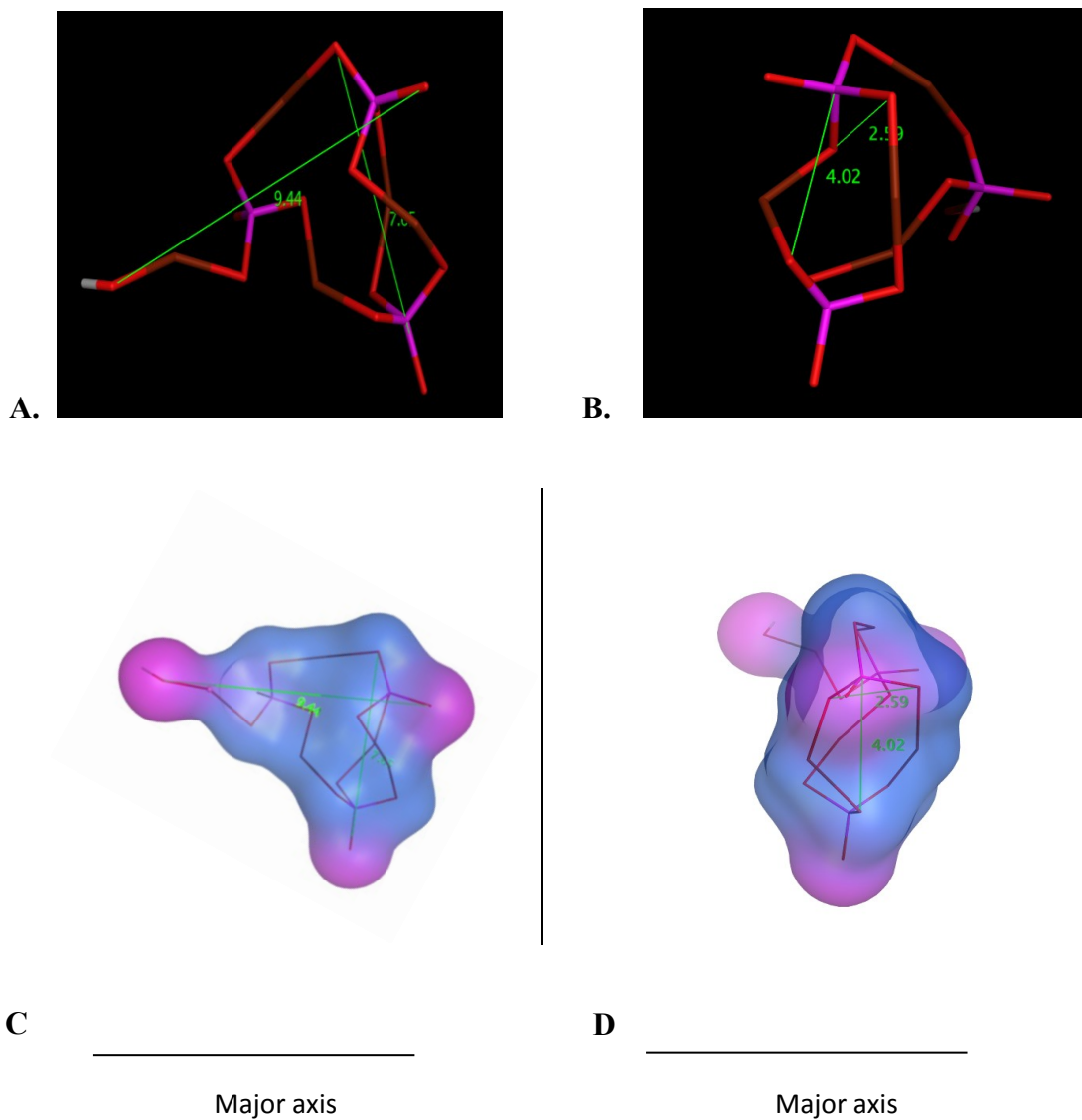


Figure 78: Computation of molecular cross-sectional area for Tri-Tab[®]

A. Measured dimensions (bond length measuring length and breadth) for Orientation 1 of the molecule. **B.** Measured dimensions for orientation 2 of the molecule. **C.** Surface constructed for the molecule in orientation 1. **D.** Surface constructed for the molecule in orientation 2. The surface accounts for the van-der Waals radii of atoms.